Mesonic Chiral Perturbation Theory

Odd Intrinsic Parity Sector

Dissertation
zur Erlangung des Grades
”Doktor der Naturwissenschaften”

am Fachbereich Physik der
Johannes Gutenberg-Universität Mainz

vorgelegt von
Thomas Ebertshäuser
geboren in Bad Ems

Institut für Kernphysik
Johannes Gutenberg-Universität Mainz

2001

“Die moderne Physik ist für Physiker viel zu schwer”.

David Hilbert (1862-1943)

Termin der mündlichen Doktorprüfung: 2002

Contents

Chapter 1

Introduction

According to our present understanding, quantum chromodynamics (QCD) is believed to best describe the strong force, which constitutes, together with the electro-weak and gravitational interactions, the fundamental forces in nature.[1]

The core of any quantum field theory (QFT) is given by its Lagrangian density. In QCD the latter is written in terms of quark and gluon fields and possesses an exact local colour $SU(3)$ as well as an approximate global flavour $SU(3)_L \times SU(3)_R$ symmetry. Looking at the associated hadron spectrum, one immediately discovers that free quark and gluon states seem to be forbidden by nature. We only find pions, nucleons, etc., which are thought to be colour-neutral objects composed of quarks and gluons. This characteristic feature, whose exact physical origin is still unclear, is called *confinement*. Despite our fairly detailed knowledge of the strong interaction, there appears to be no way to perturbatively compute Green's functions at low energies. This failure is due to a very peculiar mechanism QCD does exhibit. The operative QCD coupling constant g becomes extremely large as the interaction energy tends to zero. At high energies, however, the coupling gets weaker and weaker, which is usually referred to as *asymptotic freedom*. The entire behaviour can be illustrated by the following picture. Imagine a group of prisoners whose iron leg chains are all joined together at one link. Staying close to each other, all of them can move more or less freely, but separation beyond a certain distance is blocked by the unbreakable chains. Only towards the case of asymptotic freedom conventional perturbative methods can legitimately be applied.

Fortunately, several approaches have been invented to get us off the hook. Let us just name and characterize a few of them without going into detail:

- Lattice gauge theories furnish non-perturbative numerical (i.e., computer based) solutions of QCD by discretizing space-time [2, 3].
- Different phenomenological models (such as bag, Skyrme, etc.) have been constructed to imitate QCD [4, 5, 6].

[1] The strong and electro-weak interactions can be modelled by a sole sophisticated quantum gauge theory, the so-called Standard Model, where gravitation does not fit in [1].

- The N_c^{-1} expansion method assumes an enlarged colour gauge group, $SU(N_c)$, letting N_c tend to infinity but keeping the product $g^2 N_c$ fixed. The envisaged amplitudes are then analysed in powers of N_c^{-1} [7, 8, 9].

Still another attempt consists in mapping a part of the theory's symmetries, namely the chiral $SU(3)_L \times SU(3)_R$ symmetry, and its realization, i.e., spontaneous symmetry breakdown to $SU(3)_V$, onto a so-called effective Lagrangian density. The latter is written in terms of the asymptotically observed pseudoscalar Goldstone boson fields and describes the low-energy behaviour of QCD. The incorporated interactions vanish in the limit of zero energies and massless u, d, and s quarks. The whole procedure then allows the application of non-conventional perturbation theory. The prefix 'non' is supposed to refer to the fact that one does not expand matrix elements in powers of the QCD coupling constant g, but in powers of (low) external Goldstone boson momenta and (small) quark masses. This method is known as mesonic chiral perturbation theory (mesonic ChPT).[2] A pedagogic introduction into the field may be found in [10, 11] and in the many references mentioned therein.

Since low-energy QCD comprises far more than only symmetries, its full dynamical content is not *a priori* included in ChPT. It has to be parameterized by the weights of all conceivable monomials of the most general effective Lagrangian density consistent with chiral symmetry. These weights or couplings are called low-energy constants (LECs) and their numerical values may be determined experimentally or within specific model calculations. In general, one can find an infinite number of linearly independent monomials and thus an infinite number of LECs. If those terms were all of the same order in the above mentioned low-energy expansion, then ChPT would not have any practical significance. Fortunately, matters are different. With the assistance of chiral counting schemes one can always select a finite subset of relevant structures. Differently speaking, up to the chosen chiral order one is able to compute physical quantities including a finite (hopefully small) number of LECs.

The LECs, which especially incorporate information on virtual effects of heavier particles, are also necessary for a further important purpose. We know from other QFTs that the evaluation of loop graphs involves infinities, which have to be made finite in order to predict measureable quantities.

Theories generating only a finite number of different divergences, which can be cancelled altogether by redefining some of the (finite number of) parameters in the respective Lagrangian density, are called renormalizable.

In the above sense ChPT is non-renormalizable. Including all chiral orders, it contains, at least in principle, an infinite number of different terms. The divergent structures triggered by whatever part of the entire Lagrangian density do not manifest themselves at the same but at a higher chiral level. In other words, we can only cancel singularities by an appropriate redefinition of LECs of higher chiral orders. Therefore, we cannot globally get rid of all infinities of the theory, but we need to absorb divergences up to a certain chiral order.

[2] Baryonic ChPT exists as well but will not be treated in the present thesis.

In the normal or even intrinsic parity sector, this whole procedure was successfully carried out by Gasser and Leutwyler up to next-to-leading order, $O(p^4)$ [12, 13]. The one-loop singularities arising from the leading-order Lagrangian density $\mathcal{L}_2$, which includes 2 LECs, were absorbed by 8 of the 12 parameters of $\mathcal{L}_4$ (numbers are only valid for $SU(3)$). The extension up to next-to-next-to-leading order, $O(p^6)$, was taken up by Bijnens *et al.* [14, 15, 16].

In the anomalous or odd intrinsic parity sector, the one-loop renormalization of the leading-order term, which is the so-called Wess-Zumino-Witten (WZW) term being of chiral order $O(p^4)$, was initiated by several authors [17, 18, 19, 20], but has never been completely accomplished. Besides the fact that these authors used very different notations and conventions which make any comparison rather difficult,[3] only two of them [19, 20] furnished a most general anomalous chiral Lagrangian density of order $O(p^6)$, $\mathcal{L}_{6,\varepsilon}$, which is necessary to absorb the singularities. Both the final set proposed in [19] (49 elements) and the one listed in [20] (30 elements), which mutually disagree with each other, turn out to be incomplete and, in addition to this, to include too many elements. New mathematical strategies and more systematic procedures have been elaborated during the last few years [21, 15] which allow to further eliminate redundant structures as well as to add missing monomials. These supplementary tools were not used by the above groups at the time. Finally, one should clearly emphasize that none of the mentioned authors has ever performed the concluding absorption. The revision and completion of this still open project is the main objective of the present thesis which is organized as follows.

In Chapter 2, the substantial features of QCD, as it is treated today in nuclear physics, are briefly repeated. Mesonic ChPT is then shown to originate as a low-energy approximation to QCD incorporating important principles such as chiral symmetry and spontaneous symmetry breaking.

One of our key issues of the whole thesis is addressed in Chapter 3. We learn how to systematically build up effective actions in general and in particular (for $\mathcal{L}_{6,\varepsilon}$). After getting to know the leading-order terms of the even and odd intrinsic parity sector in its original language (i.e., Gasser and Leutwyler's nomenclature), we switch over to another notation which is more appropriate for our specific purposes.

Chapter 4 and 5 are respectively devoted to the recapitulation of path-integral techniques and the investigation of the so-called saddle-point method which is an indispensable tool for the extraction of the entire one-loop part of whatever QFT.

The above mentioned one-loop renormalization program of the WZW action, which consists in applying the one-loop extraction procedure to the WZW part, compactly isolating the associated singularites, and appropriately absorbing them afterwards, is subject of Chapter 6.

The assignment of LECs (belonging to $\mathcal{L}_{6,\varepsilon}$) to physical reactions in which they are involved appears in Chapter 7. The exact mathematical contributions, which allow

[3] As already mentioned in [18], the chosen approach and the resulting formulae of [17] are evidently not compatible with those of the other three groups. Therefore, [17] will be discarded in what follows.

the (formal) determination of their numerical values, are carried out for a subset of our LECs.

In Chapter 8, three-pseudoscalar photon interactions, and especially the process $\gamma^* + K^\pm \to K^\pm + \pi^0$, are consistently examined up to chiral order $O(p^6)$. The concerned LECs are roughly estimated within a simple model which includes vector mesons as additional degrees of freedom.

Hadronic structure functions which enter the differential cross section of $\gamma^* + K^\pm \to K^\pm + \pi^0$ are numerically determined in Chapter 9. The same is revisited for $\gamma^* + \pi^\pm \to \pi^\pm + \pi^0$.

We close with a short summary of the treated items and an outlook on future projects in Chapter 10.

Last but not least, the reader should certainly not forget to take a look at the many helpful details discussed in the several appendices. As they might have blurred the main stream of the thesis, they are transferred to this final part. For those of you who actually want to work with the presented material these collections may, as always, be of valuable assistance.

Chapter 2

QCD and ChPT

In the present chapter, we repeat the foundations of mesonic ChPT which has proven to be a highly successful method for describing the interactions of the pseudoscalar meson octet ($\pi^+,\pi^-,\pi^0,K^+,K^-,K^0,\bar{K}^0,\eta_8$) at low energies (for recent activities see, e.g., Ref. [22]).

Before pointing out the intimate relation between ChPT and QCD, let us begin by very briefly recalling the basic features of QCD. In the early seventies of the past century QCD was introduced as the $SU(3)_{\text{colour}}$ gauge theory of the strong interaction, including three ($N_c = 3$) different colour types of quarks[1] (namely red, green, and blue ones), eight ($N_c^2 - 1 = 8$) different gluons (being the massless mediators of the strong force), and one universal coupling constant g [23, 24, 25]. As $SU(3)$ is a non-Abelian Lie group, the entire theory 'suffers' from non-linearities, i.e., the gluons may and do interact with each other. Besides the colour, there is another criterion that distinguishes quarks which is called the flavour.

flavour	mass [MeV]	charge [$e > 0$]
u (up)	5	$+\frac{2}{3}$
d (down)	9	$-\frac{1}{3}$
s (strange)	175	$-\frac{1}{3}$
c (charm)	1350	$+\frac{2}{3}$
b (bottom)	5300	$-\frac{1}{3}$
t (top)	176000	$+\frac{2}{3}$

Table 2.1: Quark flavours.

Each flavour species can, of course, carry either of the three colours. Only the latter determine the interaction structure of the theory. The only flavour dependence is hence due to the different quark masses.

[1]The name 'quark' was taken from James Joyce's novel *Finnegan's Wake*. The three quarks are actually Mr. Finn's children and sometimes they represent their father. In terms of QCD Mr. Finn may be considered as the nucleon which does sometimes behave as if it was built up of three quarks.

Looking once more at Table 2.1, one discovers that the first three flavours are very light, while the remaining three are rather heavy in comparison to, say, the ρ meson ($m_\rho = 770$ MeV). The masses m_u, m_d, and m_s are almost vanishing in terms of a typical hadronic scale (e.g., the chiral-symmetry-breaking scale $\Lambda_{\rm ChSB} \approx 4\pi F_0 \approx 1$ GeV). Therefore, it is not too unreasonable to assume that at very low energies only these lightest three need to be considered.[2] Thus, we reset our starting point to the three-flavour QCD Lagrangian density coupled to colour-neutral external fields in the limit of massless u, d, and s quarks:

$$\begin{aligned} \mathcal{L} &= \mathcal{L}^0_{QCD} + \bar{q}\gamma^\mu(v_\mu + \gamma_5 a_\mu)q - \bar{q}(s - i\gamma_5 p)q, \qquad (2.1)\\ \text{with} \quad \mathcal{L}^0_{QCD} &= \sum_{f=u,d,s} (i\bar{q}_{L,f}\gamma^\mu D_\mu q_{L,f} + i\bar{q}_{R,f}\gamma^\mu D_\mu q_{R,f}) - \frac{1}{4}G^a_{\mu\nu}G^{\mu\nu}_a. \end{aligned}$$

The definitions of the left- and right-handed quark field projections are respectively given by

$$q_L = \frac{1}{2}(1-\gamma_5)q, \qquad q_R = \frac{1}{2}(1+\gamma_5)q. \qquad (2.2)$$

The gluon field strength tensor is defined as

$$G^a_{\mu\nu} = \partial_\mu A^a_\nu - \partial_\nu A^a_\mu - g f_{abc} A^b_\mu A^c_\nu, \qquad (2.3)$$

where f_{abc} are the totally anti-symmetric structure constants of $SU(3)$ (see Appendix D). The vector, axial-vector, scalar, and pseudoscalar source fields can be expanded in terms of the eight standard Gell-Mann matrices $\lambda^1, \cdots, \lambda^8$ and the identity matrix (N.B.: $\lambda^0 = \sqrt{2/3}\, 1_{3\times 3}$),

$$v_\mu = \sum_{a=1}^{8} \frac{\lambda^a}{2} v^a_\mu, \quad a_\mu = \sum_{a=1}^{8} \frac{\lambda^a}{2} a^a_\mu, \quad s = \sum_{a=0}^{8} \frac{\lambda^a}{2} s^a, \quad p = \sum_{a=0}^{8} \frac{\lambda^a}{2} p^a. \qquad (2.4)$$

As one can easily see, the above Lagrangian density (2.1) remains invariant under $q_L \to V_L(x) q_L$ and $q_R \to V_R(x) q_R$, provided the external fields transform as

$$\begin{aligned} v_\mu + a_\mu &\to V_R(v_\mu + a_\mu)V_R^\dagger + iV_R\partial_\mu V_R^\dagger,\\ v_\mu - a_\mu &\to V_L(v_\mu - a_\mu)V_L^\dagger + iV_L\partial_\mu V_L^\dagger,\\ s + ip &\to V_R(s+ip)V_L^\dagger,\\ s - ip &\to V_L(s-ip)V_R^\dagger, \qquad (2.5) \end{aligned}$$

where $(V_L, V_R) \in SU(3)_L \times SU(3)_R$. Furthermore, QCD seems to undergo spontaneous symmetry breaking to $SU(3)_V$ (also referred to as hidden symmetry). The reader

[2] The stronger restriction to u and d quarks is obviously even more justified, but here we want to deal with the more general three-flavour case. Everything that follows can, at least formally, be worked out for n flavours and later specified to $n = 2$ or 3.

should be aware of the fact that there is neither any hint in the QCD Lagrangian density nor any rigorous proof that this mechanism does really happen in nature. One evidence is the existence of the Goldstone boson octet. The absence of parity doublets in the hadron spectrum and current algebra predictions are further hints.

Let us pause for a moment and review. According to Goldstone's theorem [26, 27, 28], each broken generator, i.e., each generator which does not annihilate the vacuum, gives rise to a massless Goldstone boson whose properties are tightly connected to the generator in question.

In the present case, one expects eight pseudoscalar Goldstone bosons transforming as an octet under $SU(3)_V$ with vanishing interactions in the limit of zero energies. These Goldstone bosons are identified with the low-energy pseudoscalar octet, where the finite masses of the physical multiplet result from an explicit symmetry breaking due to the finite u, d, and s quark masses in the underlying QCD Lagrangian.

Low-energy QCD is hence strictly governed by the Lie group $SU(3)_L \times SU(3)_R$ broken down to $SU(3)_V$ and so is the behaviour of the Goldstone bosons. As already mentioned in Chapter 1, the crucial idea behind ChPT is to find the most general theory, i.e., the most general effective Lagrangian density that is written in terms of the observed Goldstone bosons, fulfilling the required symmetry.

The decisive interface between QCD and ChPT is then given via their generating functionals which are supposed to yield the same Green's functions at low energies

$$\begin{aligned} \exp\left(iZ(v_\mu, a_\mu, s, p)\right) &= \int \mathcal{D}q\mathcal{D}\bar{q}\mathcal{D}A_\mu^a \exp\left(i\int dx \mathcal{L}(q, \bar{q}, A_\mu^a, v_\mu, a_\mu, s, p)\right) \\ &\stackrel{!}{=} \int \mathcal{D}U \exp\left(i\int dx \mathcal{L}_{\text{eff}}(U, v_\mu, a_\mu, s, p)\right). \end{aligned} \tag{2.6}$$

The entire concept of generating functionals will be introduced and illuminated in Chapter 4.[3]

The different monomials of the most general Lagrangian can be classified and organized according to their chiral order. Our ordering scheme (which is not unique) basically makes use of a combined derivative ($\rightarrow$ momentum) and squared meson mass expansion. As the following chapter will show in more detail, in the mesonic sector the involved structures are all of chiral order $O(p^{2n})$, where $n \in \{1, 2, \cdots\}$ must be satisfied. For example, $\mathcal{L}_2$ is meant to include all parts of order $O(p^2)$. Those can either consist of a two-derivative or of a simple squared mass term. At this order, ChPT essentially coincides with Current Algebra.

The final point to discuss is the systematic treatment of physical matrix elements. This is furnished by Weinberg's power counting scheme [29], that we want to quote and illustrate without proving it.

[3]The integration measure dx indicated in (2.6) is the standard four-dimensional Minkowski measure. Only in Chapter 8, within the framework of dimensional regularization, we shall use the more rigorous notation d^4x.

Let us consider an arbitrary Feynman diagram of our effective theory. Rescaling all external meson momenta and their masses simultaneously, the invariant amplitude shows the following characteristic behaviour

$$\begin{aligned} \mathcal{M}(tp, t^2M^2) &= t^D \mathcal{M}(p, M^2) \\ \text{with} \quad D &= 2 + \sum_{n=1}^{\infty} 2(n-1)N_{2n} + 2N_L. \end{aligned} \tag{2.7}$$

Here, N_{2n} represents the number of vertices originating from $\mathcal{L}_{2n}$ and N_L the number of loops, respectively. At low energies, diagrams with small D values, i.e., $D \in \{2,4\}$, dominate the matrix element. Loop diagrams are always somehow suppressed. Observe that the rescaling of masses, being mathematically performable, cannot be realized in experiments. Nevertheless, it simulates the fact that Goldstone boson masses do vanish in the chiral limit.

Let us close with an example. Suppose we want to consistently calculate a matrix element up to $O(p^4)$. Then we have to consider all relevant tree-level diagrams with at most one vertex from $\mathcal{L}_4$ and an arbitrary number of vertices from $\mathcal{L}_2$ and all necessary one-loop diagrams with vertices from $\mathcal{L}_2$.

Chapter 3

How to build effective actions in mesonic ChPT

3.1 Fundamental strategy

As ChPT is an effective field theory modelling the low-energy behaviour of QCD, one needs to find the most general $SU(n)_L \times SU(n)_R$ invariant Lagrangian density describing the dynamics of the n^2-1 Goldstone bosons.[1] Whatever chiral order one may consider, the effective Lagrangian has to be constructed in terms of some so-called basic building blocks as well as their adjoints and covariant derivatives. These basic building blocks are:

1. The $SU(n)$ matrix U collecting the Goldstone boson fields in the conventional way

$$U = \exp\left(i\frac{\phi}{F_0}\right) , \tag{3.1}$$

$$\text{with} \quad \phi = \begin{pmatrix} \pi^0+\frac{1}{\sqrt{3}}\eta_8 & \sqrt{2}\pi^+ & \sqrt{2}K^+ \\ \sqrt{2}\pi^- & -\pi^0+\frac{1}{\sqrt{3}}\eta_8 & \sqrt{2}K^0 \\ \sqrt{2}K^- & \sqrt{2}\bar{K}^0 & -\frac{2}{\sqrt{3}}\eta_8 \end{pmatrix} \quad \text{in the } n=3 \text{ case} ,$$

   transforming under the chiral group as

$$U \to V_R U V_L^\dagger \quad \text{with} \quad (V_L, V_R) \in SU(n)_L \times SU(n)_R , \tag{3.2}$$

   and having the covariant derivative obeying the same transformation rule

$$D_\mu U = \partial_\mu U - iR_\mu U + iUL_\mu , \; D_\mu U \to V_R D_\mu U V_L^\dagger . \tag{3.3}$$

[1] The following investigations first treat the general n-flavour case and specify to $n=3$ and 2 afterwards.

2. The external Lorentz-vector fields $L_\mu := v_\mu - a_\mu$ and $R_\mu := v_\mu + a_\mu$ transforming as

$$I_\mu \;\rightarrow\; V_I I_\mu V_I^\dagger + i V_I \partial_\mu V_I^\dagger \quad \text{with } I \in \{L,R\}\ , \tag{3.4}$$

and composing the field strength tensors

$$F^I_{\mu\nu} := \partial_\mu I_\nu - \partial_\nu I_\mu - i[I_\mu, I_\nu]\ ,\ F^I_{\mu\nu} \rightarrow\ \ V_I F^I_{\mu\nu} V_I^\dagger\ . \tag{3.5}$$

3. The external Lorentz-scalar field χ being defined by and tranforming as

$$\chi := 2B_0(s+ip)\ ,\ \chi \rightarrow V_R \chi V_L^\dagger\ ,\ \text{respectively.} \tag{3.6}$$

Quark mass terms can be included here by setting $s = \mathrm{diag}(m_u, m_d, m_s)$.

The chiral order of our building blocks is supposed to be

$$U \leftrightarrow O(p^0), \quad D_\mu U \leftrightarrow O(p), \quad F^{L/R}_{\mu\nu},\, \chi \leftrightarrow O(p^2), \quad \dots\ ,$$

where the dots mean to indicate covariant derivatives of the former expressions (N.B.: each derivative increases the chiral order of a block by one). Here, we work in the framework of ordinary ChPT, where the quark mass term is counted as $O(p^2)$, or, in other words, matrix elements are treated at a fixed ratio m_{quark}/p^2 [12]. For an overview of a different organization procedure we refer the reader to Ref. [22, contribution by J. Stern: *Light Quark Masses and Condensates in QCD*].

Requiring the total Lagrangian density to be a real Lorentz scalar (fulfilling in addition chiral, C, P, and T invariance), we finally have to take traces $\langle \dots \rangle$ of strings of several basic blocks and contract all indices with metric tensors $g_{\mu\nu}$ or with one totally anti-symmetrical epsilon tensor $\varepsilon_{\mu\nu\alpha\beta}$. The whole procedure implies

$$\mathcal{L} = \sum_{n \in \mathbf{N}} \mathcal{L}_{2n}. \tag{3.7}$$

Although the blocks introduced above may represent the most natural choice of basic ingredients, their technical applicability is rather limited. For the construction of the most general Lagrangians of order p^2 and p^4 one might get along well enough, but for higher orders it turns out to be more convenient to switch over to some different, more systematical, definition of blocks. Those are shown in one of the next sections.

3.1.1 Leading orders in the even intrinsic parity sector

At lowest order, $O(p^2)$, there are only two linearly independent monomials available

$$\mathcal{L}_2 = \frac{F_0^2}{4}\langle D_\mu U (D^\mu U)^\dagger \rangle + \frac{F_0^2}{4}\langle \chi U^\dagger + U \chi^\dagger \rangle. \tag{3.8}$$

The occuring LECs are given by the pion decay constant $F_0 = 92.4$ MeV and B_0, being hidden in χ, which is related to the scalar quark condensate $\langle 0|\bar{q}q|0\rangle$.

At next-to-leading order, $O(p^4)$, the most general chiral Lagrangian density consists of 12 monomials [13]

$$\begin{aligned}
\mathcal{L}_4 &= L_1 \langle D_\mu U (D^\mu U)^\dagger \rangle^2 \\
&+ L_2 \langle D_\mu U (D_\nu U)^\dagger \rangle \langle D^\mu U (D^\nu U)^\dagger \rangle \\
&+ L_3 \langle D_\mu U (D^\mu U)^\dagger D_\nu U (D^\nu U)^\dagger \rangle \\
&+ L_4 \langle D_\mu U (D^\mu U)^\dagger \rangle \langle \chi U^\dagger + U \chi^\dagger \rangle \\
&+ L_5 \langle D_\mu U (D^\mu U)^\dagger (\chi U^\dagger + U \chi^\dagger) \rangle \\
&+ L_6 \langle \chi U^\dagger + U \chi^\dagger \rangle^2 \\
&+ L_7 \langle \chi U^\dagger - U \chi^\dagger \rangle^2 \\
&+ L_8 \langle U \chi^\dagger U \chi^\dagger + \chi U^\dagger \chi U^\dagger \rangle \\
&- L_9 \, i \langle F_{\mu\nu}^R D^\mu U (D^\nu U)^\dagger + F_{\mu\nu}^L (D^\mu U)^\dagger D^\nu U \rangle \\
&+ L_{10} \langle U F_{\mu\nu}^L U^\dagger F_R^{\mu\nu} \rangle \\
\\
&+ H_1 \langle F_{\mu\nu}^R F_R^{\mu\nu} + F_{\mu\nu}^L F_L^{\mu\nu} \rangle \\
&+ H_2 \langle \chi \chi^\dagger \rangle . \qquad (3.9)
\end{aligned}$$

The latter two do not include any Goldstone boson fields at all. They provide purely external contributions which are of secondary interest.

3.1.2 Leading order in the odd intrinsic parity sector

Both, $\mathcal{L}_2$ and $\mathcal{L}_4$, turn out to possess a quite peculiar property. Let us therefore have a look at the transformation behaviour of our ingredients under intrinsic parity P (i.e., normal P neglecting the transformation part of space-time x itself)

$$\begin{aligned}
& U \leftrightarrow U^\dagger \; (\Leftrightarrow \phi \leftrightarrow -\phi), \\
& \chi \leftrightarrow \chi^\dagger, \; L_\mu \leftrightarrow R^\mu, \; F_{\mu\nu}^L \leftrightarrow F_R^{\mu\nu}, \\
& \varepsilon_{\mu\nu\alpha\beta} \leftrightarrow -\varepsilon^{\mu\nu\alpha\beta}. \qquad (3.10)
\end{aligned}$$

With the restriction to the special cases of e.m. reactions ($R_\mu = L_\mu = -eA_\mu Q$ and $\chi = \chi^\dagger$) or pure QCD ($R_\mu = L_\mu = 0$ and $\chi = \chi^\dagger$), we can see that the intrinsic parity transformation is equivalent to replacing ϕ by $-\phi$ and ε by $-\varepsilon$. Since our monomials M are all parity invariant, structures without [with] an ε tensor will expose the property $M(\phi) = M(-\phi)$ $[M(\phi) = -M(-\phi)]$. The former [latter], which exclusively induce e.m. or pure QCD processes with an even [odd] number of Goldstone bosons, are called *normal* [*anomalous*] or of *even* [*odd*] *intrinsic parity*.

As a consequence, reactions such as $\pi^0 \to \gamma\gamma$ or $K^+K^- \to \pi^+\pi^-\pi^0$, which are of course allowed by QCD, cannot be described by Gasser and Leutwyler's most general Lagrangian densities $\mathcal{L}_2$ or $\mathcal{L}_4$. To remove this contradiction one has to look out for terms of odd intrinsic parity.

According to the Veltman-Sutherland theorem [30, 31, 32], one had expected to have no p^4 contribution at all to reactions of the above mentioned type, but explicit computations of the π^0 decay (including quark loops) revealed this assumption to be wrong [33, 34, 35]. This mismatching between symmetry predictions and direct calculations has been referred to as the non-Abelian anomaly[2] ever since. That is the reason why the odd intrinsic parity sector is also called anomalous.[3]

Wess and Zumino [36] were the first to write down an effective anomalous action obtained by integration of the anomaly consistency condition. Their action could not be given in a closed manner, i.e., using the U block. Up to order $O(p^4)$ there is no way to construct conventional chirally invariant monomials including an ε tensor. Witten [37] succeeded in writing down a five-dimensional action of order $O(p^4)$

$$\begin{aligned} S_{WZW} = & - \frac{iN_c}{240\pi^2}\int_D d^5x\,\varepsilon^{ijklm}\langle \mathcal{U}_i^L\mathcal{U}_j^L\mathcal{U}_k^L\mathcal{U}_l^L\mathcal{U}_m^L\rangle \\ & - \frac{iN_c}{48\pi^2}\int d^4x\,\varepsilon^{\mu\nu\alpha\beta}\langle Z_{\mu\nu\alpha\beta}\rangle \end{aligned} \tag{3.11}$$

parameterizing the non-Abelian anomaly. Here, D is a five-dimensional disc whose four-dimensional boundary is supposed to be conventional Minkowski space-time, and $\mathcal{U}_i^L$ and $\mathcal{U}_i^R$ are defined via $\mathcal{U}_i^L = U^\dagger\frac{\partial U}{\partial x^i}$ and $\mathcal{U}_i^R = U\frac{\partial U^\dagger}{\partial x^i}$, respectively. Furthermore, note that $\varepsilon_{01234} = \varepsilon_{0123} = 1$.

The second term in (3.11), which has to be added when considering external fields, includes

$$\begin{aligned} Z_{\mu\nu\alpha\beta} = & + \frac{1}{2}\,UL_\mu U^\dagger R_\nu U L_\alpha U^\dagger R_\beta \\ & + UL_\mu L_\nu L_\alpha U^\dagger R_\beta - U^\dagger R_\mu R_\nu R_\alpha U L_\beta \\ & + i\,U\partial_\mu L_\nu L_\alpha U^\dagger R_\beta - i\,U^\dagger\partial_\mu R_\nu R_\alpha U L_\beta \\ & + i\,\partial_\mu R_\nu U L_\alpha U^\dagger R_\beta - i\,\partial_\mu L_\nu U^\dagger R_\alpha U L_\beta \\ & - i\,\mathcal{U}_\mu^L L_\nu U^\dagger R_\alpha U L_\beta + i\,\mathcal{U}_\mu^R R_\nu U L_\alpha U^\dagger R_\beta \\ & - i\,\mathcal{U}_\mu^L L_\nu L_\alpha L_\beta + i\,\mathcal{U}_\mu^R R_\nu R_\alpha R_\beta \\ & + \mathcal{U}_\mu^L U^\dagger\partial_\nu R_\alpha U L_\beta - \mathcal{U}_\mu^R U\partial_\nu L_\alpha U^\dagger R_\beta \\ & - \mathcal{U}_\mu^L\mathcal{U}_\nu^L U^\dagger R_\alpha U L_\beta + \mathcal{U}_\mu^R\mathcal{U}_\nu^R U L_\alpha U^\dagger R_\beta \end{aligned}$$

[2] A different point of view: as, e.g., Gasser points out in his lecture notes [11], in the language of QCD generating functionals, one finds $Z(v_\mu, a_\mu, s, p)$ to split into a piece which is invariant under the chiral group $SU(n)_L \times SU(n)_R$ and another which is not. Only the WZW term mimics the latter part.

[3] Although the chirally invariant ε structures of order p^6 and higher have nothing to do with the anomaly at all.

$$
\begin{aligned}
&+ \quad \mathcal{U}^L_\mu L_\nu \partial_\alpha L_\beta - \mathcal{U}^R_\mu R_\nu \partial_\alpha R_\beta \\
&+ \quad \mathcal{U}^L_\mu \partial_\nu L_\alpha L_\beta - \mathcal{U}^R_\mu \partial_\nu R_\alpha R_\beta \\
&+ \quad \frac{1}{2}\, \mathcal{U}^L_\mu L_\nu \mathcal{U}^L_\alpha L_\beta - \frac{1}{2}\, \mathcal{U}^R_\mu R_\nu \mathcal{U}^R_\alpha R_\beta \\
&- \quad i\, \mathcal{U}^L_\mu \mathcal{U}^L_\nu \mathcal{U}^L_\alpha L_\beta + i\, \mathcal{U}^R_\mu \mathcal{U}^R_\nu \mathcal{U}^R_\alpha R_\beta . \qquad (3.12)
\end{aligned}
$$

At this stage it is worth stressing two important facts. First of all, Eq. (3.11) does not lead to any new free parameters, but simply contains the integer number N_c. Second, when computing physical reactions, i.e., going over to fields ϕ in (3.11), the arising five-dimensional structures can always be converted into four-dimensional ones via the Stokes theorem (for manifolds).

Other people used different, mathematically more refined, methods to reproduce the above formulae (see, e.g., [38, 39, 40]). Actually, there are quite many physical examples that exhibit *WZW* like terms. An 'introductory' overview over the entire field including its interpretation in terms of differential geometry (especially in the language of principal fibre bundles) can be found in Ref. [41]. However, for our current needs this sophisticated and powerful (in plain English, *complicated*) machinery is indeed dispensable. Nevertheless, sometimes we will come across one notion or another (such as chiral connection) which obviously stems from this underlying framework.

To complete this account, note that the $SU(2)$ version of Eq. (3.11) completely vanishes in case one allows no or just e.m. external fields.[4] In sharp contrast to that, the $SU(3)$ theory does not exhibit this peculiarity. While the latter agrees with the non-existence of any hadronic reactions including only pions, e.m. processes such as $\gamma + \pi^\pm \to \pi^\pm + \pi^0$ are allowed. It may therefore be asked: how can this kind of reaction be computed within the framework of $SU(2)$ ChPT at order $O(p^4)$? It turns out that one needs to extend the chiral group $SU(2)_L \times SU(2)_R$ in order to solve the above problem. The extension for arbitrary flavour number n will be introduced in Section 3.2.8.

[4] This is due to trace relations to be outlined in one of the next sections.

3.2 The most general anomalous chiral action at order $O(p^6)$

The ChPT action functional, which is (apart from the special case of the WZW term) the four-dimensional space-time integral over some chirally invariant Lagrangian denstiy, generates at any given chiral order a finite-dimensional real vector space. The finite dimension is due to the fact that our basic building blocks can only be multiplied together in a finite number of different manners. Unfortunately, there seems to be neither a way to predict this dimension beforehand nor a general algorithm to decide whether a couple of given terms are linearly independent or not. That is the reason why it is almost impossible to tell if a set of structures actually represents a basis, i.e., a linearly independent generating system, of the above mentioned vector space.

To our knowledge even Gasser and Leutwyler have never formally proved their $\mathcal{L}_4$ to provide a basis. It is without any doubt a generating system and countless calculations seem to confirm that the terms are independent.

Fearing and Scherer were the first to systematically write down the most general Lagrangian density of chiral order $O(p^6)$, both for the normal ($\rightarrow$ 111 $SU(3)$ terms) and anomalous ($\rightarrow$ 32 $SU(3)$ terms) sector [21]. Although their sets are also most likely to be generating systems, the normal sector was later shown to include redundant structures [15].

For the epsilon sector, we present a reduced and slightly modified list of 24 $SU(n)$, 23 $SU(3)$, and 5 $SU(2)$ terms,[5] whose derivation is tightly linked to Fearing and Scherer's method. Taking into account all different (chirally invariant) basic building blocks available, we start out by writing down all possible anomalous structures fulfilling invariance under P and C, hermiticity, and chiral order p^6. We then work out and introduce all mechanisms generating relations among those terms of the Lagrangian we are aware of.

One final observation: as the present PhD thesis is supposed to primarily investigate the anomalous sector of mesonic ChPT, we only mention the following statement without going into detail. We also carefully revisited the normal sector at chiral order p^6. The latter happens to include a very huge number (about 110 for the general n-flavour case) of final structures which renders the entire analysis quite complex. Although our number does agree with [15], we would rather choose a somewhat different final set, which includes less monomials when sending all external fields to zero, i.e., dealing with pure QCD. In addition to that, we want to stress that, as far as we can see, their claim of linearly independence is not based on any mathematical fundament. The enormous amount of terms, or LECs, prevents one from being absolutely sure.

[5] Additional terms will be introduced due to the extension of the chiral group at the end of this chapter.

3.2.1 Modified basic building blocks and strategy

In Ref. [21] a systematic construction of chiral Lagrangian densities was developed starting from structures of the type

$$[A]_\pm := \frac{1}{2}(AU^\dagger \pm UA^\dagger), \tag{3.13}$$

where A is supposed to transform under the chiral group as $A \to V_R A V_L^\dagger$. The entire approach may be improved considerably by using a modified kind of basic building blocks

$$(A)_\pm := 2u^\dagger [A]_\pm u, \tag{3.14}$$

which has already been used in a slightly different form by several authors (see, e.g., [20, 15]). Note that $(A)_\pm$ obeys the transformation rule $(A)_\pm \to V(A)_\pm V^\dagger$, where $V = \sqrt{V_R U V_L^\dagger}^{-1} V_R \sqrt{U}$ is the so-called compensator, and u is defined via $u^2 = U$. The covariant derivative

$$\nabla_\mu (A)_\pm := \partial_\mu (A)_\pm + [\Gamma_\mu, (A)_\pm] \quad \text{(N.B.: } \nabla_\mu (A)_\pm \to V \nabla_\mu (A)_\pm V^\dagger) \tag{3.15}$$

induced by the chiral connection $\Gamma_\mu = \frac{1}{2}\left[u^\dagger, \partial_\mu u\right] - \frac{i}{2} u^\dagger R_\mu u - \frac{i}{2} u L_\mu u^\dagger$ provides a key element for an easier and more efficient application of the total-derivative procedure, which is to be outlined in more detail shortly.

Since we always have to take single or multiple traces to obtain Lagrangian density monomials, our final results will only differ by a number compared to the former structures

$$\langle (A_1)_\pm \ldots (A_m)_\pm \rangle = 2^m \langle [A_1]_\pm \ldots [A_m]_\pm \rangle. \tag{3.16}$$

Let us illustrate this fact by looking at the leading-order non-anomalous Lagrangian density

$$\mathcal{L}_2 = -\frac{F_0^2}{16}\langle (D_\mu U)_- (D^\mu U)_- \rangle + \frac{F_0^2}{4}\langle (\chi)_+ \rangle = -\frac{F_0^2}{4}\langle [D_\mu U]_- [D^\mu U]_- \rangle + \frac{F_0^2}{2}\langle [\chi]_+ \rangle.$$

As pointed out in [21], it is sufficient to restrict oneself to $[D^m U]_-, [D^n G]_+, [D^n H]_+$, and $[D^n \chi]_\pm$ (with $m \in \mathbf{N}$ and $n \in \mathbf{N_0}$). So, we simply have to substitute for those ingredients the new blocks $(D^m U)_-, (D^n G)_+, (D^n H)_+$, and $(D^n \chi)_\pm$. Here we use the definition $G^{\mu\nu} := F_R^{\mu\nu} U + U F_L^{\mu\nu}$ and $H^{\mu\nu} := F_R^{\mu\nu} U - U F_L^{\mu\nu}$, where $F_{L/R}^{\mu\nu}$ are evidently the field strength tensors belonging to the corresponding external fields R_μ and L_μ. The χ block was introduced in (3.6) and is related to the scalar quark condensate $\langle 0|\bar{q}q|0\rangle$.

To simplify the comparision with the previously mentioned other groups, we give a translation prescription in the following table.

our notation	Ref. [21]	Ref. [15]	Ref. [20]
$(\chi)_\pm$	$2u^\dagger[\chi]_\pm u$	$\chi_\pm$	$2M^\pm$
$(D_\mu U)_-$	$2u^\dagger[D_\mu U]_- u$	$-2iu_\mu$	$4\Delta_\mu$
$(G^{\mu\nu})_+$	$2u^\dagger[G^{\mu\nu}]_+ u$	$2f_+^{\mu\nu}$	$-2iF^{+\mu\nu}$
$(H^{\mu\nu})_+$	$2u^\dagger[H^{\mu\nu}]_+ u$	$-2f_-^{\mu\nu}$	$2iF^{-\mu\nu}$

Table 3.1: Translation prescription.

The so-called hierarchy strategy of [21] has proven to be extremely fruitful. Collecting $(D^n G_{\mu\nu})_+, (D^n H_{\mu\nu})_+$, and $(D^n\chi)_\pm$ for a moment in one symbol $(D^n\chi_{\mu\nu})_\pm$, one immediately finds that all possible terms at $O(p^6)$ can either include no, one, two, or three $(D^n\chi_{\mu\nu})_\pm$ blocks which naturally defines four distinct sectors or levels to be considered. We say: the more $(D^n\chi_{\mu\nu})_\pm$ blocks are included in one monomial, the lower its level. Once all terms one can think of (at each level) are listed, one tries to generate relations to eliminate as many structures as possible. We always try to get rid of terms as high in the hierarchy as possible. After setting all external fields equal to zero, then the number of remaining terms will be minimal. There is no need to proceed in the above way, but it seems to be the most natural to us.

Before explaining the mentioned improvements in more detail, let us pause and have a word on the symmetry of multiple covariant derivatives. It turns out to be more appropriate not to assume the multiple covariant derivatives to be symmetrized from the very beginning. We implement the relations among unsymmetrized structures noting that just one general (i.e., non-contracted) index combination is actually independent. For double derivatives this statement reads

$$(D_\mu D_\nu A)_\pm = (D_\nu D_\mu A)_\pm + \frac{i}{4}[(A)_\pm, (G_{\mu\nu})_+] - \frac{i}{4}\{(A)_\mp, (H_{\mu\nu})_+\}. \tag{3.17}$$

Although there would not be any disadvantage in keeping these unsymmetrized monomials in our final set (N.B.: $(D_\mu D_\nu U)_-$ will be the only to be kept), for aesthetical reasons we replace them by symmetrized ones making use of the formula

$$(D_\mu D_\nu U)^s_- := \frac{1}{2}(\{D_\mu, D_\nu\}U)_- = (D_\mu D_\nu U)_- + \frac{i}{2}(H_{\mu\nu})_+. \tag{3.18}$$

We are now ready to initiate the construction procedure. First of all, we write down all conceivable (we find 74, see Table A.1) anomalous structures (satisfying P and C invariance, hermiticity, and chiral order p^6) in terms of our chirally invariant basic building blocks. We then collect as many relations as possible which follow from any of the mechanisms we are aware of. Those are:

1. Partial integration,

2. Equation-of-motion argument,

3. Epsilon relations,

4. Bianchi identities,

5. Trace relations.

The explicit non-redundant relations are listed in App. B. There is no unique way in kicking dependent monomials out. We basically follow the example of [21], i.e., in addition to the hierarchy approach we always try to get rid of multiple-derivative terms, especially of the type $(D^2U)_-$. However, by treating a highly non-trivial problem there is no guarantee that another approach might not happen to lead to a smaller final number. Yet we have not found an alternative way giving rise to further reductions.

3.2.2 Partial integration (total-derivative argument)

Recalling the fact that a total derivative in the Lagrangian density does not change the equation of motion, we can generate relations of the following type

$$\begin{aligned} & \partial_\mu\langle (A_1)_\pm \dots (A_m)_\pm\rangle + \overbrace{\langle [\Gamma_\mu, (A_1)_\pm \dots (A_m)_\pm]\rangle}^{0} \overset{(3.15)}{=} \langle \nabla_\mu [(A_1)_\pm \dots (A_m)_\pm]\rangle \\ = \;& \langle \nabla_\mu (A_1)_\pm \dots (A_m)_\pm\rangle + \dots + \langle (A_1)_\pm \dots \nabla_\mu (A_m)_\pm\rangle . \end{aligned} \tag{3.19}$$

This derivative-shifting procedure is also valid for multiple traces. The enormous advantage of our new basic building blocks stems from the relatively simple connection between the covariant derivative ∇_μ outside the block brackets and the covariant derivative D_μ inside

$$\nabla_\mu (A)_\pm \;=\; (D_\mu A)_\pm - \frac{1}{4}\{(D_\mu U)_-, (A)_\mp\}. \tag{3.20}$$

The importance of (3.20) can hardly be overestimated because it helps to avoid extremely tedious algebraic manipulations one had to perform in the old framework.[6]

Note that some relations of Appendix B might neglect contributions from lower levels. Since we always try to find the most general Lagrangian density at each level, in almost all cases those lower terms do not need to be known explicitly.

3.2.3 Equation-of-motion argument (EOM terms)

Table A.1 contains a couple of monomials exhibiting the block $(D_\lambda D^\lambda U)_-$. These terms, which are called EOM terms in what follows, can actually be related to terms lower down in our hierarchy plus an additional one to be transformed away by a suitable field transformation. A detailed discussion of this subject can be found in Ref. [42].

[6] A combination of shifting derivatives back and forth and interchanging indices of multiple derivatives is sometimes referred to as index exchange.

The basic idea is to perform a field transformation on the Goldstone boson fields induced by an appropriate traceless Hermitian matrix-valued generator S:

$$U \to U' = \exp(iS)U. \tag{3.21}$$

We know that transformations of this kind do not affect measurable quantities such as the S matrix [43].

For our concerns, one can be convinced that one just has to perform the replacement

$$(D_\lambda D^\lambda U)_- \quad = \quad (\chi)_- - \frac{1}{N_f}\langle(\chi)_-\rangle 1_{N_f\times N_f} \tag{3.22}$$

in order to eliminate the EOM structures.

3.2.4 Epsilon relations

In the anomalous sector the so-called epsilon relations provide another important tool to link and hence eliminate structures. As shown in Ref. [21], all conceivable epsilon relations stem from the fundamental equation

$$g^{\mu\nu}\varepsilon^{\alpha\beta\gamma\delta} - g^{\mu\alpha}\varepsilon^{\nu\beta\gamma\delta} - g^{\mu\beta}\varepsilon^{\alpha\nu\gamma\delta} - g^{\mu\gamma}\varepsilon^{\alpha\beta\nu\delta} - g^{\mu\delta}\varepsilon^{\alpha\beta\gamma\nu} = 0, \tag{3.23}$$

which is sometimes referred to as Schouten's identity.

The left-hand side of the above equation represents a tensor which is totally anti-symmetric in its five latter indices ($\nu\alpha\beta\gamma\delta$). Since all Lorentz indices run from 0 to 3, at least two of the above mentioned indices have to have equal values (for whatever combination of index values), which makes the entire tensor vanish.

Contracting (3.23) with an arbitrary tensor $Q_{\mu\nu\alpha\beta\gamma\delta}$ in all possible manners yields six different equations

$$\begin{aligned}
(Q_\mu{}^\mu{}_{\alpha\beta\gamma\delta} - Q_{\mu\alpha}{}^\mu{}_{\beta\gamma\delta} + Q_{\mu\alpha\beta}{}^\mu{}_{\gamma\delta} - Q_{\mu\alpha\beta\gamma}{}^\mu{}_\delta + Q_{\mu\alpha\beta\gamma\delta}{}^\mu)\varepsilon^{\alpha\beta\gamma\delta} &= 0,\\
(Q^\mu{}_{\mu\alpha\beta\gamma\delta} - Q_{\alpha\mu}{}^\mu{}_{\beta\gamma\delta} + Q_{\alpha\mu\beta}{}^\mu{}_{\gamma\delta} - Q_{\alpha\mu\beta\gamma}{}^\mu{}_\delta + Q_{\alpha\mu\beta\gamma\delta}{}^\mu)\varepsilon^{\alpha\beta\gamma\delta} &= 0,\\
(Q^\mu{}_{\alpha\mu\beta\gamma\delta} - Q_\alpha{}^\mu{}_{\mu\beta\gamma\delta} + Q_{\alpha\beta\mu}{}^\mu{}_{\gamma\delta} - Q_{\alpha\beta\mu\gamma}{}^\mu{}_\delta + Q_{\alpha\beta\mu\gamma\delta}{}^\mu)\varepsilon^{\alpha\beta\gamma\delta} &= 0,\\
(Q^\mu{}_{\alpha\beta\mu\gamma\delta} - Q_\alpha{}^\mu{}_{\beta\mu\gamma\delta} + Q_{\alpha\beta}{}^\mu{}_{\mu\gamma\delta} - Q_{\alpha\beta\gamma\mu}{}^\mu{}_\delta + Q_{\alpha\beta\gamma\mu\delta}{}^\mu)\varepsilon^{\alpha\beta\gamma\delta} &= 0,\\
(Q^\mu{}_{\alpha\beta\gamma\mu\delta} - Q_\alpha{}^\mu{}_{\beta\gamma\mu\delta} + Q_{\alpha\beta}{}^\mu{}_{\gamma\mu\delta} - Q_{\alpha\beta\gamma}{}^\mu{}_{\mu_\delta} + Q_{\alpha\beta\gamma\delta\mu}{}^\mu)\varepsilon^{\alpha\beta\gamma\delta} &= 0,\\
(Q^\mu{}_{\alpha\beta\gamma\delta\mu} - Q_\alpha{}^\mu{}_{\beta\gamma\delta\mu} + Q_{\alpha\beta}{}^\mu{}_{\gamma\delta\mu} - Q_{\alpha\beta\gamma}{}^\mu{}_{\delta\mu} + Q_{\alpha\beta\gamma\delta}{}^\mu{}_\mu)\varepsilon^{\alpha\beta\gamma\delta} &= 0,
\end{aligned} \tag{3.24}$$

where the last one can be expressed in terms of the former five and is thus linearly dependent.

For Q we choose single or multiple traces over strings of our basic building blocks.

3.2.5 Bianchi identities

As a consequence of the Jacobi identity

$$[A,[B,C]]+[B,[C,A]]+[C,[A,B]]=0 \tag{3.25}$$

certain combinations of covariant derivatives of the field strength tensors are not linearly independent. According to Eq. (18) of Ref. [21], the covariant derivative is defined as

$$D_\mu F^R_{\nu\rho} = \partial_\mu F^R_{\nu\rho} - i[R_\mu, F^R_{\nu\rho}]. \tag{3.26}$$

Now consider the linear combination

$$\begin{aligned} D_\mu F^R_{\nu\rho} + D_\nu F^R_{\rho\mu} + D_\rho F^R_{\mu\nu} &= \sum_{c.p.\{\mu,\nu,\rho\}} D_\mu F^R_{\nu\rho} = \sum_{c.p.\{\mu,\nu,\rho\}} (\partial_\mu F^R_{\nu\rho} - i[R_\mu, F^R_{\nu\rho}]) \\ &= \sum_{c.p.\{\mu,\nu,\rho\}} \Big(\partial_\mu\partial_\nu R_\rho - \partial_\mu\partial_\rho R_\nu - i[\partial_\mu R_\nu, R_\rho] \\ &- i[R_\nu, \partial_\mu R_\rho] - i[R_\mu, \partial_\nu R_\rho - \partial_\rho R_\nu] - [R_\mu,[R_\nu,R_\rho]] \Big) \\ &= 0, \end{aligned} \tag{3.27}$$

where use of Schwarz' theorem, relabelling of indices, and the Jacobi identity, Eq. (3.25), has been made. Repeating the same arguments for the independent field strength tensor $F^L_{\mu\nu}$, the two resulting constraints can be summarized as

$$\sum_{c.p.\{\mu,\nu,\rho\}} D_\mu F^{L/R}_{\nu\rho} = 0, \tag{3.28}$$

which is referred to as the Bianchi identities (see, e.g., Refs. [44, 45]). Equation (3.28) does not require that $F^{R/L}_{\mu\nu}$ satisfy any equations of motion. In terms of our building blocks $(D_\mu U)_-$, $(G_{\mu\nu})_+$, and $(H_{\mu\nu})_+$ the Bianchi identities read

$$\sum_{c.p.\{\mu,\nu,\rho\}} (D_\mu G_{\nu\rho})_+ = -\frac{1}{4} \sum_{c.p.\{\mu,\nu,\rho\}} [(D_\mu U)_-, (H_{\nu\rho})_+], \tag{3.29}$$

$$\sum_{c.p.\{\mu,\nu,\rho\}} (D_\mu H_{\nu\rho})_+ = -\frac{1}{4} \sum_{c.p.\{\mu,\nu,\rho\}} [(D_\mu U)_-, (G_{\nu\rho})_+]. \tag{3.30}$$

We stress that in Ref. [21] each term (in the old notation, though) of the sum on the left-hand side of Eqs. (3.29) and (3.30) was treated as an independent element.

3.2.6 Trace relations

As all the structures one can think of either involve single or multiple traces, one is particularly interested in finding relations between those traces. We know from the

Cayley-Hamilton theorem that any $n \times n$ matrix A solves its associated characteristical polynomial χ_A. For $n = 2$ this statement reads

$$\begin{aligned} 0 &= \chi_A(A) = A^2 - \langle A \rangle A + \det(A) 1, \\ \Leftrightarrow \quad 0 &= \chi_A(A) = A^2 - \langle A \rangle A + \frac{1}{2}(\langle A \rangle^2 - \langle A^2 \rangle) 1. \end{aligned} \tag{3.31}$$

Setting $A = A_1 + A_2$ in (3.31) and making use of $\chi_{A_1}(A_1) = 0 = \chi_{A_2}(A_2)$ one ends up with the matrix equation

$$F_2(A_1, A_2) = \{A_1, A_2\} - \langle A_1 \rangle A_2 - \langle A_2 \rangle A_1 + \langle A_1 \rangle \langle A_2 \rangle 1 - \langle A_1 A_2 \rangle 1 = 0 \tag{3.32}$$

which is the central piece of information needed to derive trace relations. The analogous $n = 3$ equation is slightly more complex

$$\begin{aligned} F_3(A_1, A_2, A_3) &= A_1\{A_2, A_3\} + A_2\{A_3, A_1\} + A_3\{A_1, A_2\} \\ &- \langle A_1 \rangle \{A_2, A_3\} - \langle A_2 \rangle \{A_3, A_1\} - \langle A_3 \rangle \{A_1, A_2\} \\ &+ \langle A_1 \rangle \langle A_2 \rangle A_3 + \langle A_2 \rangle \langle A_3 \rangle A_1 + \langle A_3 \rangle \langle A_1 \rangle A_2 \\ &- \langle A_1 A_2 \rangle A_3 - \langle A_3 A_1 \rangle A_2 - \langle A_2 A_3 \rangle A_1 \\ &- \langle A_1 A_2 A_3 \rangle 1 - \langle A_1 A_3 A_2 \rangle 1 \\ &+ \langle A_1 A_2 \rangle \langle A_3 \rangle 1 + \langle A_3 A_1 \rangle \langle A_2 \rangle 1 + \langle A_2 A_3 \rangle \langle A_1 \rangle 1 \\ &- \langle A_1 \rangle \langle A_2 \rangle \langle A_3 \rangle 1 = 0. \end{aligned} \tag{3.33}$$

We can now derive trace relations by simply multiplying (3.32) or (3.33) with another arbitrary matrix of adequate dimension and finally taking the trace of the whole construction, i.e.,

$$\begin{aligned} 0 &= \langle F_2(A_1, A_2) A_3 \rangle, \\ 0 &= \langle F_3(A_1, A_2, A_3) A_4 \rangle. \end{aligned} \tag{3.34}$$

Note that A_i may be any $n \times n$ matrix, even a string of our basic building blocks. Although we have never come across a trace relation that could not be obtained in the manner explained above, we are not aware of a general proof showing that any kind of trace relation must be related to the Caley-Hamilton theorem.

Eq. (3.34) actually includes all $SU(3)$ formulae derived in the appendix of Ref. [21] and provides additional ones, e.g., we get one $SU(3)$ in the epsilon sector while Ref. [21] did not have any.

3.2.7 Final sets

After having implemented all relations we could find, our resulting sets read:

LECs	#	$SU(n)$	$SU(3)$	$SU(2)$
3	69	$i\,\langle(\chi)_+\{(G_{\mu\nu})_+(H_{\alpha\beta})_+ - \text{rev}\}\rangle\varepsilon^{\mu\nu\alpha\beta}$	$\times$	$\times$
8	70	$i\,\langle(\chi)_-(G_{\mu\nu})_+(G_{\alpha\beta})_+\rangle\varepsilon^{\mu\nu\alpha\beta}$	$\times$	$\times$
9	73	$i\,\langle(\chi)_-\rangle\langle(G_{\mu\nu})_+(G_{\alpha\beta})_+\rangle\varepsilon^{\mu\nu\alpha\beta}$	$\times$	—
19	37	$i\,\langle(D^\lambda G_{\lambda\mu})_+\{(G_{\nu\alpha})_+(D_\beta U)_- + \text{rev}\}\rangle\varepsilon^{\mu\nu\alpha\beta}$	$\times$	—
1	54	$\langle(\chi)_+\{(H_{\mu\nu})_+(D_\alpha U)_-(D_\beta U)_- + \text{rev}\}\rangle\varepsilon^{\mu\nu\alpha\beta}$	$\times$	$\times$
2	68	$\langle(\chi)_+(D_\mu U)_-\rangle\langle(D_\nu U)_-(H_{\alpha\beta})_+\rangle\varepsilon^{\mu\nu\alpha\beta}$	$\times$	—
5	53	$\langle(\chi)_-\{(G_{\mu\nu})_+(D_\alpha U)_-(D_\beta U)_- - \text{rev}\}\rangle\varepsilon^{\mu\nu\alpha\beta}$	$\times$	—
6	61	$\langle(\chi)_-(D_\mu U)_-(G_{\nu\alpha})_+(D_\beta U)_-\rangle\varepsilon^{\mu\nu\alpha\beta}$	$\times$	$\times$
7	67	$\langle(\chi)_-\rangle\langle(G_{\mu\nu})_+(D_\alpha U)_-(D_\beta U)_-\rangle\varepsilon^{\mu\nu\alpha\beta}$	$\times$	—
13	12^s	$\langle(G_{\lambda\mu})_+\{(D^\lambda D_\nu U)^s_-(D_\alpha U)_-(D_\beta U)_- - \text{rev}\}\rangle\varepsilon^{\mu\nu\alpha\beta}$	$\times$	—
14	13^s	$\langle(G_{\mu\nu})_+\{(D_\lambda D_\alpha U)^s_-(D^\lambda U)_-(D_\beta U)_- - \text{rev}\}\rangle\varepsilon^{\mu\nu\alpha\beta}$	$\times$	—
10	71	$i\,\langle(\chi)_-(H_{\mu\nu})_+(H_{\alpha\beta})_+\rangle\varepsilon^{\mu\nu\alpha\beta}$	$\times$	$\times$
11	74	$i\,\langle(\chi)_-\rangle\langle(H_{\mu\nu})_+(H_{\alpha\beta})_+\rangle\varepsilon^{\mu\nu\alpha\beta}$	$\times$	—
20	43	$i\,\langle(D^\lambda H_{\lambda\mu})_+\{(H_{\nu\alpha})_+(D_\beta U)_- + \text{rev}\}\rangle\varepsilon^{\mu\nu\alpha\beta}$	$\times$	—
21	58	$i\,\langle(G_{\mu\nu})_+\{(H_{\lambda\alpha})_+(D^\lambda U)_-(D_\beta U)_- - \text{rev}\}\rangle\varepsilon^{\mu\nu\alpha\beta}$	$\times$	—
22	59	$i\,\langle(G_{\mu\nu})_+\{(H_{\lambda\alpha})_+(D_\beta U)_-(D^\lambda U)_- - \text{rev}\}\rangle\varepsilon^{\mu\nu\alpha\beta}$	$\times$	—
23	60	$i\,\langle(G_{\mu\nu})_+\{(H_{\alpha\beta})_+(D_\lambda U)_-(D^\lambda U)_- - \text{rev}\}\rangle\varepsilon^{\mu\nu\alpha\beta}$	$\times$	—
24	63	$i\,\langle(G_{\lambda\mu})_+(D_\nu U)_-(H^\lambda{}_\alpha)_+(D_\beta U)_-\rangle\varepsilon^{\mu\nu\alpha\beta}$	$\times$	—
4	4	$i\,\langle(\chi)_-(D_\mu U)_-(D_\nu U)_-(D_\alpha U)_-(D_\beta U)_-\rangle\varepsilon^{\mu\nu\alpha\beta}$	$\times$	—
12	2^s	$i\,\langle(D_\lambda D_\mu U)^s_-\{(D^\lambda U)_-(D_\nu U)_-(D_\alpha U)_-(D_\beta U)_- + \text{rev}\}\rangle\varepsilon^{\mu\nu\alpha\beta}$	$\times$	—
15	24	$\langle(H_{\lambda\mu})_+\{(D^\lambda U)_-(D_\nu U)_-(D_\alpha U)_-(D_\beta U)_- + \text{rev}\}\rangle\varepsilon^{\mu\nu\alpha\beta}$	—	—
16	26	$\langle(H_{\mu\nu})_+\{(D_\lambda U)_-(D^\lambda U)_-(D_\alpha U)_-(D_\beta U)_- + \text{rev}\}\rangle\varepsilon^{\mu\nu\alpha\beta}$	$\times$	—
17	31	$\langle(H_{\mu\nu})_+\{(D_\lambda U)_-(D_\alpha U)_- + \text{rev}\}\rangle\langle(D^\lambda U)_-(D_\beta U)_-\rangle\varepsilon^{\mu\nu\alpha\beta}$	$\times$	—
18	30	$\langle(H_{\mu\nu})_+(D_\alpha U)_-\rangle\langle(D_\beta U)_-(D_\lambda U)_-(D^\lambda U)_-\rangle\varepsilon^{\mu\nu\alpha\beta}$	$\times$	—

Table 3.2: The final $SU(n)$ set. Trace relations lead to the corresponding $SU(3)$ and $SU(2)$ sets.

For a better understanding of the above table let us add some helpful comments:

- As one cannot be absolutely sure whether the remaining structures are linearly independent or not, we avoid talking about a basis set.
- The first column is meant to label the associated LECs $\mathbf{L_i^{6,\varepsilon}}$, while the second refers to the number assigned to each monomial in our initial list (compare with App. A).

- While the superscript s indicates the symmetrized version of a term, the abbreviation 'rev' stands for 'reversed order'.

- A new ordering scheme has been introduced to group structures according to their leading-order expansion in terms of Goldstone boson and external fields (more details will be presented in Chapter 7).

In summary, we have found 24 final $SU(n)$, 23 $SU(3)$, and 5 $SU(2)$ elements. Our sets are considerably smaller than those proposed by [19] (49 $SU(3)$ elements) or [20] (30 $SU(3)$ elements), which are both incomplete and redundant. The 32 anomalous $SU(3)$ terms listed in [21] have been slightly modified and reduced thanks to a more efficient application of partial integration, implementation of Bianchi identities, and additional trace relations.

3.2.8 Extension of the chiral group

LECs	#	additional structures
$2'$	$26'$	$i\, v^{(s)}_{\mu\nu}\langle(\chi)_-(G_{\alpha\beta})_+\rangle\varepsilon^{\mu\nu\alpha\beta}$
$3'$	$30'$	$i\, v^{(s)}_{\mu\nu}v^{(s)}_{\alpha\beta}\langle(\chi)_-\rangle\varepsilon^{\mu\nu\alpha\beta}$
$5'$	$13'$	$i\, v^{(s)}_{\mu\nu}\langle(D^\lambda G_{\lambda\alpha})_+(D_\beta U)_-\rangle\varepsilon^{\mu\nu\alpha\beta}$
$6'$	$7'$	$i\, \partial^\lambda v^{(s)}_{\lambda\mu}\langle(G_{\nu\alpha})_+(D_\beta U)_-\rangle\varepsilon^{\mu\nu\alpha\beta}$
$1'$	$25'$	$v^{(s)}_{\mu\nu}\langle(\chi)_-(D_\alpha U)_-(D_\beta U)_-\rangle\varepsilon^{\mu\nu\alpha\beta}$
$4'$	$1'$	$\partial^\lambda v^{(s)}_{\lambda\mu}\langle(D_\nu U)_-(D_\alpha U)_-(D_\beta U)_-\rangle\varepsilon^{\mu\nu\alpha\beta}$
$7'$	$22'$	$i\, v^{(s)}_{\lambda\mu}\langle(H^\lambda{}_\nu)_+(D_\alpha U)_-(D_\beta U)_-\rangle\varepsilon^{\mu\nu\alpha\beta}$
$8'$	$29'$	$v^{(s)}_{\mu\nu}\langle(G_{\lambda\alpha})_+(H^\lambda{}_\beta)_+\rangle\varepsilon^{\mu\nu\alpha\beta}$

Table 3.3: Final set of additional structures valid for arbitrary n.

So far we have presented the most general anomalous $SU(n)_L \times SU(n)_R$ invariant Lagrangian density (respecting external fields v_μ, a_μ, s, and p) at chiral order p^6 from which one can extract the $SU(2)$ or $SU(3)$ version by applying the respective trace relations. Since $(G_{\mu\nu})_+$ and $(H_{\mu\nu})_+$ are both supposed to be traceless and the $SU(2)$ quark charge matrix $Q = \mathrm{diag}(\frac{2}{3}, -\frac{1}{3})$ is not, even the special case of electromagnetism ($L_\mu = R_\mu = -eA_\mu Q$) is not fully included in the general $SU(2)$ formulae. As Q happens to be traceless in $SU(3)$, there is no such problem. If we want to do away with this apparent weakness, we need to extend the chiral group to $SU(n)_L \times SU(n)_R \times U(1)_V$. For $n = 2$ the e.m. interaction is then fully included by setting $L_\mu = R_\mu = -\frac{e}{2}A_\mu\tau_3$ and $v^{(s)}_\mu = -\frac{e}{2}A_\mu$, where $v^{(s)}_\mu$ is the $U(1)_V$ gauge field [10]. Equivalently, one might argue that the traceless fields L_μ and R_μ have to be replaced by non-traceless ones of the

form $\tilde{L}_\mu = L_\mu + \frac{1}{3} v_\mu^{(s)} 1_{n\times n}$ and $\tilde{R}_\mu = R_\mu + \frac{1}{3} v_\mu^{(s)} 1_{n\times n}$, respectively.[7] This way, the $SU(2)$ WZW term gets the additional pieces discussed at the end of Section 3.1.2.

The extension basically comes down to the fact that we get one more independent elementary building block of chiral order p^2, namely the field strength tensor $v_{\mu\nu}^{(s)} = \partial_\mu v_\nu^{(s)} - \partial_\nu v_\mu^{(s)}$. Again, we write down all (30) anomalous p^6 structures including at least one $v_{\mu\nu}^{(s)}$ (see Tab. A.2). Observe that at lower orders there is no way to construct such terms. We then use the mechanisms of the previous sections to eliminate as many of the additional monomials as possible. Since trace relations do not induce reductions in this field, our result is valid for any n, although we are primarily interested in $n = 2$ at this stage. While all explicit relations can be found in App. B, the final set has already been shown above.

[7] The factor $\frac{1}{3}$ has to be introduced to match the Lagrangian of [10].

Chapter 4

Path-integral quantization, generating functionals, and Green's functions

As Steven Weinberg points out in his textbooks on QFT [45], any physical theory combining, or as he actually says 'reconciling', the ideas of special relativity and quantum mechanics will look like a QFT at sufficiently low (today accessible) energies. That is the reason why QED or QCD, which might fundamentally not be field theories, are still treated that way — and needless to add, very successfully.

The recipes for setting up a QFT are basically canonical quantization and the path-integral formalism (PIF). Although, due to its elegance and power, the latter has become quite fashionable during the last 30 years or so, it still seems less established among many physicists than the former, sometimes referred to as a pedestrian approach.

But why do we, in the present thesis, need to bother with path-integral quantization? Besides the general interest or the intellectual challenge there is one specific point regarding our purposes which requires the PIF. As mentioned in the introduction, we want to extract the entire one-loop part of a QFT triggered by a certain Lagrangian density. This can only be accomplished with the assistance of the PIF. Of course, that is just one somehow tiny particular aspect of a huge and advanced field we will never be able to cover in its entirety.

We could have totally omitted the present chapter by beginning the following one, 'As we all know, the one-loop contribution of a QFT is given by ...' pretending everybody knew where the result came from. However, that is definitely not the adequate way a Ph.D. thesis should address one of its key issues. On the other hand, we clearly cannot go back to the very foundations of path-integrals and rederive step by step every single formula we need to deal with. Therefore, this chapter is intended to provide a compromise between a textbook which carefully goes through mathematical details and a paper which only quotes so-called well-established results.

Assuming at least a minimum acquaintance with the PIF, we first give a list of its

fundamental notions and then work out some specific aspects which are of particular importance to us. Differently speaking, we mean to offer the reader a somewhat condensed summary of textbook material and, above all, a feeling for the framework in order to guide him or her more or less safely through the jungle of formulae to come in the following chapters.

Let us start with some general introductary comments. In many cases the procedure of canonical quantization (i.e., roughly speaking, the replacement of fields by operators and of Poisson brackets by commutators) is rather cumbersome. For more complicated theories, like non-Abelian gauge theories or general relativity, canonical quantization is almost not applicable. What one would like to have is a formalism which naturally generates all Feynman graphs in their final Lorentz-invariant form departing from the respective Lagrangian density. This requirement is nicely fulfilled by the PIF.

Before coming to the physical core of the PIF, some historical information might be of interest. Feynman, inspired by a somewhat unclear note by Dirac, was the first to present path-integral techniques in non-relativistic quantum mechanics [46]. He tried to find a method which would allow starting out with the Lagrangian instead of the Hamiltonian. Years later, the idea was rediscovered, when Faddeev, Popov [47], and De Witt [48] pointed out how to apply the PIF to non-Abelian gauge theories and general relativity. Those techniques then became an indispensable tool, when 't Hooft [49] used the PIF for the derivation of Feynman rules of gauge theories with spontaneous symmetry breaking.

Last but not least, we do not want to suppress the fact that from a pedagogic point of view the PIF also exhibits one serious drawback which canonical quantization does not. The unitarity of the S matrix is somehow blurred and not obvious at all. Therefore, both formalisms should be used complementarily to obtain full insight.

4.1 Fundamental notions

In what follows we collect and also shortly explain the most fundamental notions of the PIF (for one scalar field with Lagrangian density $\mathcal{L}$). A more or less elementary introduction into the subject may be found in [50, 51, 52, 53, 54, 55, 44, 45, 56]. Most of these references start with conventional quantum mechanics before going over to quantum field theory.

For completeness we want to state the following (mathematically quite subtle) remark without paying attention to it in the remainder of this chapter. In order to make sure that all path-integrals do converge properly, their strict definition should be given in terms of Euclidian quantities (i.e., allow time to become complex and then set $\mathbf{C} \ni t = -i\tau, \tau \in \mathbf{R}$). The physical interpretation requires the transition (via analytical continuation) to Minkowski space, though.

- **Not necessarily connected Green's functions (n-point functions) in co-ordinate space**:

We start out by recalling the equivalent definitions of Green's functions, first given in the canonical language, where $\hat{\Phi}$ are usual Heisenberg operators, and afterwards in terms of the PIF:

$$\begin{aligned} G^{(n)}(x_1,\cdots,x_n) &= \langle 0|T(\hat{\Phi}(x_1)\cdots\hat{\Phi}(x_n))|0\rangle \\ &\propto \int \mathcal{D}\Phi\, \Phi(x_1)\cdots\Phi(x_n)\exp\left(\frac{i}{\hbar}\int dx\mathcal{L}\right). \end{aligned} \tag{4.1}$$

In order to avoid confusion, let us review the difference between a Feynman diagram and a Green's function. The former is a graphical one-to-one transcription of a certain mathematical expression contributing to the S matrix where all external legs are imperatively on the mass shell. The latter concept is a slightly modified extension. In contrast to Feynman graphs, the external lines of Green's functions are always off the mass shell and in addition to that they carry the corresponding propagator instead of the wave function.

- **Not necessarily connected Green's functions in momentum space**:
  Fourier transformation of (4.1) with *a priori* implementation of conservation of momentum leads to

$$\begin{aligned} & G^{(n)}(p_1,\cdots,p_n)\left(\frac{\hbar}{2\pi}\right)^4\delta(p_1+\cdots+p_n) \\ = & \int dx_1\cdots\int dx_n \exp\left(\frac{i}{\hbar}(p_1\cdot x_1+\cdots+p_n\cdot x_n)\right) G^{(n)}(x_1,\cdots,x_n). \end{aligned} \tag{4.2}$$

- **The generating functional W (for not necessarily connected n-point functions):**
  Whatever the states of a given system may look like, everybody should agree that there is a state of minimum energy (vacuum state). We now investigate the transition amplitude (vacuum at $t=-\infty$ to vacuum at $t=\infty$) of our system in the presence of arbitrary external forces:

$$W[J] = \langle 0|0\rangle_J = \frac{\int \mathcal{D}\Phi \exp\left(\frac{i}{\hbar}\int dx\,(\mathcal{L}+J\Phi)\right)}{\int \mathcal{D}\Phi\exp\left(\frac{i}{\hbar}\int dx\mathcal{L}\right)}. \tag{4.3}$$

In other words, we allow ourselves to manipulate the system at whatever time and look how it responds. Observe that the normalization condition $W[0]=1$ has been implemented. $W[J]$ includes all information about the considered QFT in terms of its Green's functions which can be extracted via functional derivation:

$$\begin{aligned} & W[J] = \sum_{n=0}^{\infty}\int dx_1\cdots\int dx_n \frac{1}{n!}\left(\frac{i}{\hbar}\right)^n J(x_1)\cdots J(x_n)G^{(n)}(x_1,\cdots,x_n) \\ & \Leftrightarrow\ G^{(n)}(x_1,\cdots,x_n) = \left(\frac{\hbar}{i}\right)^n\left(\frac{\delta^n W[J]}{\delta J(x_1)\cdots\delta J(x_n)}\right)_{J=0}. \end{aligned} \tag{4.4}$$

More on the functional calculus can be found in Appendix C.

- **The generating functional Z (for connected n-point functions):**
  The above functional W does not *per se* exclude graphs which contain several particle clusters being far away from each other in space-time. In order to get rid of these irrelevant contributions, we restrict ourselves to the *connected* parts for which we can write down a new generating functional

$$\begin{aligned} W[J] &= \exp\left(\frac{i}{\hbar}Z[J]\right) \Leftrightarrow \\ \frac{i}{\hbar}Z[J] &= \sum_{n=0}^{\infty}\int dx_1\cdots\int dx_n\frac{1}{n!}\left(\frac{i}{\hbar}\right)^n J(x_1)\cdots J(x_n)G_c^{(n)}(x_1,\cdots,x_n) \end{aligned} \tag{4.5}$$

  and associated Green's functions

$$G_c^{(n)}(x_1,\cdots,x_n) = \left(\frac{\hbar}{i}\right)^{n-1}\left(\frac{\delta^n Z[J]}{\delta J(x_1)\cdots\delta J(x_n)}\right)_{J=0}. \tag{4.6}$$

- **The effective action and amputated 1PI Green's functions:**
  The so-called effective action is obtained via Legendre transforming Z. As we show in more detail later, Green's functions associated with this new generating functional (named *proper vertices*) turn out to be 1PI[1] and do not possess any external legs at all. Therefore, they are usually referred to as *amputated*.

  We sketch the Legendre transformation

$$\begin{aligned} &\Phi_{cl}[J,x] := \frac{\delta Z[J]}{\delta J(x)} \quad \text{and} \quad \Gamma[\Phi_{cl}] := Z[J] - \int dx J(x)\Phi_{cl}[J,x] \\ &\Rightarrow \frac{\delta\Gamma[\Phi_{cl}]}{\delta\Phi_{cl}(x)} = -J[\Phi_{cl},x]. \end{aligned} \tag{4.7}$$

  In complete analogy to the preceding cases, we find the effective action with the corresponding proper verices:

$$\begin{aligned} \Gamma[\Phi_{cl}] &= \sum_{n=0}^{\infty}\int dx_1\cdots\int dx_n\frac{1}{n!}\Phi_{cl}(x_1)\cdots\Phi_{cl}(x_n)\Gamma^{(n)}(x_1,\cdots,x_n), \\ \Gamma^{(n)}(x_1,\cdots,x_n) &= \left(\frac{\delta\Gamma[\Phi_{cl}]}{\delta\Phi_{cl}(x_1)\cdots\delta\Phi_{cl}(x_n)}\right)_{\Phi_{cl}=0}. \end{aligned} \tag{4.8}$$

[1] One-particle irreducible (1PI) diagrams cannot be disconnected by simply cutting through any one internal line.

4.2 Scalar quantum field with self-interaction

More light is shed on the whole formalism by considering the following simple but instructive example.

- **Lagrangian density**:

$$\begin{aligned} &\mathcal{L} = \mathcal{L}_0 + \mathcal{L}_{int} \quad \text{falls into} \\ &\mathcal{L}_0 = \frac{1}{2}\partial_\mu\Phi\partial^\mu\Phi - \frac{m^2}{2}\Phi^2 \quad \text{and} \quad \mathcal{L}_{int} = -V(\Phi) = -\frac{\lambda}{4!}\Phi^4. \end{aligned} \tag{4.9}$$

- **Free theory and Feynman propagator:**
  The so-called free theory (i.e., $\mathcal{L} = \mathcal{L}_0$) can be solved by performing a generalized Gauss-type integral. Therefore, let us quickly remind the reader of a standard result for positive definite $n \times n$ matrices A and arbitrary n-dimensional vectors b, namely

$$\int d^n x \exp\left(-\frac{1}{2}x^T A x - b^T y\right) = \sqrt{\frac{(2\pi)^n}{\det(A)}} \exp\left(\frac{1}{2}b^T A^{-1} b\right), \tag{4.10}$$

  which also includes the usual Gauss formula ($n = 1$)

$$\int dx \exp\left(-ax^2\right) = \sqrt{\frac{\pi}{a}}.$$

  Extending Eq. (4.10) to infinite dimensions, we can easily compute

$$\begin{aligned} W_0[J] &= \frac{\int \mathcal{D}\Phi \exp\left(\frac{i}{\hbar}\int dx\,(\mathcal{L}_0 + J\Phi)\right)}{\int \mathcal{D}\Phi \exp\left(\frac{i}{\hbar}\int dx \mathcal{L}_0\right)} \\ &= \exp\left(-\frac{i}{2\hbar}\int dx' \int dx J(x')\Delta(x',x)J(x)\right) \\ &\text{with} \quad A(x)\Delta(x,x') := (\Box_x + m^2)\Delta(x,x') = -\delta(x-x'), \end{aligned}$$

  from which we immediately obtain

$$Z_0[J] = -\frac{1}{2}\int dx' \int dx J(x')\Delta(x',x)J(x). \tag{4.11}$$

- **Non-vanishing interaction (Φ^4 theory)**:
  Even for the simple case of the Φ^4 theory there appears to be no way to obtain a closed result. The only thing we can actually carry out are Gaussian integrals. Therefore, we need to develop a perturbation series involving those integrals:[2]

$$W[J] = \frac{\int \mathcal{D}\Phi \exp\left(\frac{i}{\hbar}\int dx\,(\mathcal{L}_0 + \mathcal{L}_{int} + J\Phi)\right)}{\int \mathcal{D}\Phi \exp\left(\frac{i}{\hbar}\int dx\,(\mathcal{L}_0 + \mathcal{L}_{int})\right)}$$

[2] Divergences and their cancellation are ignored at this stage of our discussion.

$$
\begin{aligned}
&= \exp\left(-\frac{i}{\hbar}\int dy V\left(\frac{\hbar}{i}\frac{\delta}{\delta J(y)}\right)\right)\frac{\int \mathcal{D}\Phi \exp\left(\frac{i}{\hbar}\int dx\left(\mathcal{L}_0+J\Phi\right)\right)}{\int \mathcal{D}\Phi \exp\left(\frac{i}{\hbar}\int dx \mathcal{L}\right)} \\
&= \mathcal{C}\exp\left(-\frac{i}{\hbar}\int dy V\left(\frac{\hbar}{i}\frac{\delta}{\delta J(y)}\right)\right) W_0[J] \qquad (4.12)
\end{aligned}
$$

$$
\text{with} \quad \mathcal{C} = \frac{\int \mathcal{D}\Phi \exp\left(\frac{i}{\hbar}\int dx \mathcal{L}_0\right)}{\int \mathcal{D}\Phi \exp\left(\frac{i}{\hbar}\int dx \mathcal{L}\right)} .
$$

We have just derived a formally very compact expression for the generating functional $W[J]$. Yet we do not know how to actually extract Green's functions in an efficient manner. We illustrate two different algorithms, 'spitting out' all n-point functions of the theory, in a moment.

The first one is based on the following nice trick [53]:

$$
\begin{aligned}
& F\left(\frac{\delta}{\delta\Phi(z)}\right)\left[G(\Phi(x))\exp\left(\frac{i}{\hbar}\int dy J(y)\Phi(y)\right)\right] \\
= \; & F\left(\frac{\delta}{\delta\Phi(z)}\right)\left[G\left(\frac{\hbar}{i}\frac{\delta}{\delta J(x)}\right)\exp\left(\frac{i}{\hbar}\int dy J(y)\Phi(y)\right)\right] \\
= \; & G\left(\frac{\hbar}{i}\frac{\delta}{\delta J(x)}\right) F\left(\frac{\delta}{\delta\Phi(z)}\right)\exp\left(\frac{i}{\hbar}\int dy J(y)\Phi(y)\right) \\
= \; & G\left(\frac{\hbar}{i}\frac{\delta}{\delta J(x)}\right)\left[F\left(\frac{i}{\hbar}J(z)\right)\exp\left(\frac{i}{\hbar}\int dy J(y)\Phi(y)\right)\right]. \qquad (4.13)
\end{aligned}
$$

Setting Φ to zero, the above equation finally reads

$$
\begin{aligned}
& \left\{F\left(\frac{\delta}{\delta\Phi(z)}\right)\left[G(\Phi(x))\exp\left(\frac{i}{\hbar}\int dy J(y)\Phi(y)\right)\right]\right\}_{\Phi=0} \\
= \; & G\left(\frac{\hbar}{i}\frac{\delta}{\delta J(x)}\right) F\left(\frac{i}{\hbar}J(z)\right). \qquad (4.14)
\end{aligned}
$$

Now, we can use (4.14) to rewrite (4.12):

$$
\begin{aligned}
W[J] &= \mathcal{C}\left\{\exp\left(-\frac{\hbar}{2i}\int dx' \int dx \frac{\delta}{\delta\Phi(x')}\Delta(x',x)\frac{\delta}{\delta\Phi(x)}\right)\right. \\
&\times \left.\exp\left(-\frac{i}{\hbar}\int dy\left(V\left(\Phi(y)\right)-J(y)\Phi(y)\right)\right)\right\}_{\Phi=0} \\
&= \mathcal{C}\sum_{n=0}^{\infty}\int dy_1\cdots\int dy_n \frac{1}{n!}\left(\frac{i}{\hbar}\right)^n J(y_1)\cdots J(y_n) \\
&\times \left\{\exp\left(-\frac{\hbar}{2i}\int dx' \int dx \frac{\delta}{\delta\Phi(x')}\Delta(x',x)\frac{\delta}{\delta\Phi(x)}\right)\right. \\
&\times \left.\Phi(y_1)\cdots\Phi(y_n)\exp\left(-\frac{i}{\hbar}\int dy V\left(\Phi(y)\right)\right)\right\}_{\Phi=0}
\end{aligned}
$$

$$
\begin{aligned}
=: \quad & \mathcal{C}\sum_{n=0}^{\infty}\int dy_1\cdots\int dy_n\frac{1}{n!}\left(\frac{i}{\hbar}\right)^n J(y_1)\cdots J(y_n) \\
\times \quad & \left\langle \Phi(y_1)\cdots\Phi(y_n)\exp\left(-\frac{i}{\hbar}\int dy V\left(\Phi(y)\right)\right)\right\rangle_0 . \qquad (4.15)
\end{aligned}
$$

Without calculating any functional derivative, the Green's functions can be read off as

$$
G^{(n)}(y_1,\cdots,y_n) = \mathcal{C}\left\langle \Phi(y_1)\cdots\Phi(y_n)\exp\left(-\frac{i}{\hbar}\int dy V\left(\Phi(y)\right)\right)\right\rangle_0 . \quad (4.16)
$$

In order to efficiently handle the just defined $\langle\cdots\rangle_0$-bracket, observe that

$$
\begin{aligned}
\langle\Phi(y_1)\Phi(y_2)\rangle_0 &= i\hbar\Delta(y_1-y_2), \\
\langle\Phi(y_1)\Phi(y_2)\Phi(y_3)\Phi(y_4)\rangle_0 &= (i\hbar)^2\Delta(y_1-y_2)\Delta(y_3-y_4) \\
&+ (i\hbar)^2\Delta(y_1-y_2)\Delta(y_3-y_4) \\
&+ (i\hbar)^2\Delta(y_1-y_2)\Delta(y_3-y_4), \\
&\vdots \\
\text{and} \qquad \langle\Phi(y_1)\cdots\Phi(y_{2n+1})\rangle_0 &= 0 \quad \forall\, n\in\mathbf{N}_0. \qquad (4.17)
\end{aligned}
$$

For the free case, both $\mathcal{C}$ and the exp-function in (4.16) turn one and we only get the rather uninteresting $2n$-point functions indicated in (4.17).

A more exciting result is found when looking at the interacting case. The 2-point function turns out to yield

$$
\begin{aligned}
G^{(2)}(y_1,y_2) &= \mathcal{C}\left\langle \Phi(y_1)\Phi(y_2)\exp\left(-\frac{i}{\hbar}\int dy V\left(\Phi(y)\right)\right)\right\rangle_0 \\
&= \mathcal{C}\langle\Phi(y_1)\Phi(y_2)\rangle_0 \\
&- \mathcal{C}\frac{i\lambda}{4!\hbar}\int dx\left\langle\Phi(y_1)\Phi(y_2)\Phi^4(x)\right\rangle_0 \\
&- \frac{\mathcal{C}}{2}\frac{\lambda^2}{4!^2\hbar^2}\int dx\int dx'\left\langle\Phi(y_1)\Phi(y_2)\Phi^4(x)\Phi^4(x')\right\rangle_0 \\
&+ O(\lambda^3), \qquad (4.18)
\end{aligned}
$$

which does correspond to the five 2-point diagrams depicted in Fig. 4.1. The detailed translation prescription of how to assign mathematical terms to graphical constituents and vice versa is given within our second approach. The remaining $2n$-point functions may be computed analogously. According to the last line in (4.17), one finds all $(2n+1)$-point functions to vanish. Without proof we want to mention that the normalization constant $\mathcal{C}$ is responsible for kicking disconnected vacuum parts out.

The second strategy consists in simply expanding both exp-functions in (4.12) and combining the respective terms with each other. $W[J]$ can then explicitly be written as an infinite sum of contributions from which the Green's functions are obtained by functional derivation. Below, we translate every single mathematical part of our formula into a diagrammatic element (conventions analogous to Rivers [55]). This way, any graph of the theory (including the lowest-order ones shown in Fig. 4.1) gushes from our algorithm (with its correct symmetry factor in front) by stringing the diagrammatic constituents together according to

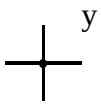

$$W[J] = \mathcal{C}\exp\left(\frac{1}{4!}\int dy\,\overbrace{-i\lambda}\left(\frac{\hbar}{i}\frac{\delta}{\delta J(y)}\right)^4\right) \times \exp\left(\frac{1}{2}\int dx\,\underbrace{\frac{i}{\hbar}J(x)}\int dx'\,\underbrace{\frac{i}{\hbar}J(x')}\,\underbrace{\hbar\Delta(x-x')}\right).$$

Rule : integrate over vertices and sources, respectively!

N.B.: $\frac{\hbar}{i}\frac{\delta}{\delta J(y)}\int dx\int dx'$  $= 2\int dx$ 

- **Connection between $\hbar$ and loops**

  In the next chapter we want to show how to compactly extract the entire one-loop part (and nothing else) of whatever QFT. Of course, we shall only be treating our familiar Φ^4 theory in detail. To this end, we need to carefully prepare ourselves and establish a connection between the number of loops contained in a n-point function and the power of $\hbar$. Let us start by collecting some helpful topological input:

$$\begin{aligned} E &: \text{number of external lines,} \\ I &: \text{number of internal lines,} \\ M &: \text{number of vertices,} \\ m &: \text{power of vertex (} m\text{=4 for } \Phi^4 \text{ theory),} \\ L &: \text{number of loops.} \end{aligned} \tag{4.19}$$

  With some effort one can see that the following general relations hold for connected Green's functions:

$$\begin{aligned} mM &= E + 2I, \\ I - M &= L - 1. \end{aligned} \tag{4.20}$$

  We are now ready to prove, or let us better say, illustrate, the following statement (for our specific example):
  On the level of the generating functional $Z[J]$ there is an one-to-one correspondence between the (relative) number of $\hbar$ and the number of loops.

  The above relation can be elucidated with either of our two previously discussed strategies. Let us begin with the first one and repeat Eq. (4.15),

$$\begin{aligned} W[J] &= \mathcal{C} \sum_{E=0}^{\infty} \int dy_1 \cdots \int dy_E \frac{1}{E!} \left(\frac{i}{\hbar}\right)^E J(y_1) \cdots J(y_E) \\ &\times \left\langle \Phi(y_1) \cdots \Phi(y_E) \exp\left(-\frac{i}{\hbar} \int dy V(\Phi(y))\right) \right\rangle_0 , \end{aligned}$$

  tacitly assuming to discard disconnected parts. We find $\hbar$ contributions to originate from four different 'sources'.[3] As our statement refers to the generating functional $Z[J]$, we have to include one global $\hbar$. The remaining have to be added according to the above formula (always keeping (4.17) in mind). Putting everything together, we finally get

$$\underbrace{\hbar}_{Z[J]} \overbrace{\hbar^{-E}}^{\text{ext. lines}} \underbrace{\hbar^{E+I}}_{\text{propagators}} \overbrace{\hbar^{-M}}^{\text{vertices}} = \hbar^{1+I-M} = \hbar^L . \tag{4.21}$$

[3] We do not need to care about the $\hbar$ dependence of $\mathcal{C}$. That is the reason why we speak about the relative number of $\hbar$.

Within our second strategy,

$$\begin{aligned} W[J] &= C\exp\left(-\frac{i}{\hbar}\int dyV\left(\frac{\hbar}{i}\frac{\delta}{\delta J(y)}\right)\right) \\ &\times \exp\left(-\frac{i}{2\hbar}\int dx\int dx' J(x')\Delta(x',x)J(x)\right), \end{aligned}$$

we may proceed in a similar manner. Remembering that the first exp-function produces the vertices and the second one the propagators, we end up with

$$\underbrace{\hbar}_{Z[J]}\overbrace{\hbar^{(m-1)M}}^{\text{vertices}}\underbrace{\hbar^{-(E+I)}}_{\text{propagators}} = \hbar^{1+I-M} = \hbar^{L}, \tag{4.22}$$

which coincides, as expected, with Eq. (4.21).

Vacuum graphs:

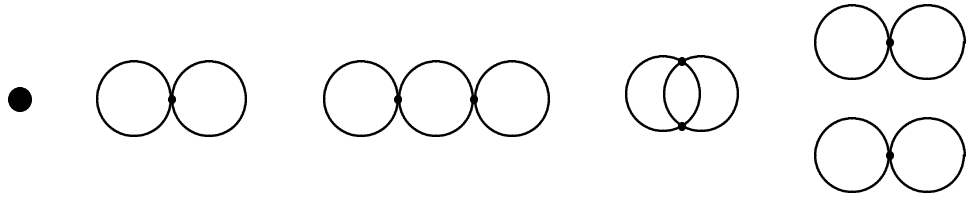

2-point function:

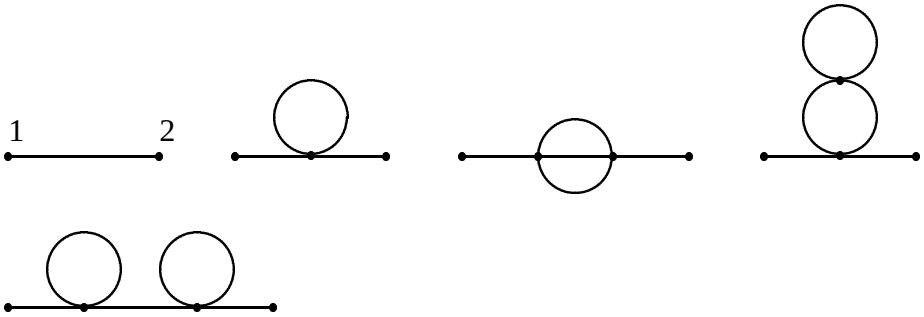

4-point function:

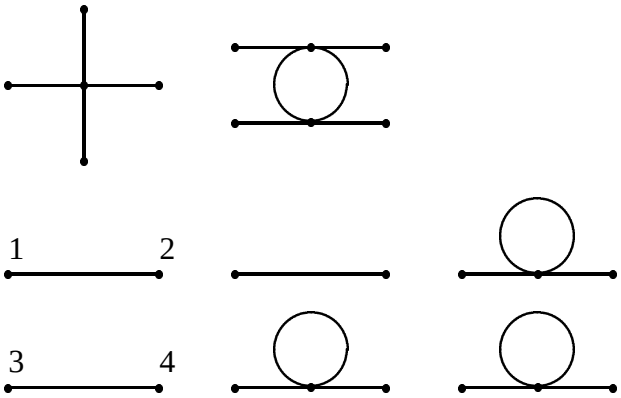

+ Perm.

(Higher **2n-point functions** omitted)

Figure 4.1: Diagrammatic representation of Φ^4 theory Green's functions (without symmetry factors) up to order $O(\lambda^2)$. The above ordering respects the following priority scheme: 1PI $>$ 1PR $>$ disconnected.

Chapter 5

The saddle-point method

After having familiarized ourselves with the main results of the PIF, we can now draw our attention on another aspect which is tightly linked with our envisaged one-loop extraction. So far we have got to know two different procedures which both generate all n-point functions of the theory in a somehow disordered manner. What we would like to have is a prescription to tell us how to elegantly filter out all one-loop graphs. This wish is fulfilled by the so-called saddle-point method. The present chapter is mainly inspired by Ramon's textbook [54].

5.1 An introductory example in one dimension

Let us have a closer look at the following type of integral:

$$I = \int_{-\infty}^{\infty} dx \exp\Big(-f(x)\Big). \tag{5.1}$$

The function f is supposed to be convex around its minimum x_0. The associated Taylor expansion then clearly reads

$$f(x) = f(x_0) + \frac{f''(x_0)}{2}(x-x_0)^2 + \cdots . \tag{5.2}$$

If the function's minimum is sharp enough, then the integral may be approximated in the following way

$$\begin{aligned} I &\approx \exp\Big(-f(x_0)\Big) \int_{-\infty}^{\infty} dx \exp\left(-\frac{f''(x_0)}{2}(x-x_0)^2\right) \\ &= \exp\Big(-f(x_0)\Big) \int_{-\infty}^{\infty} dy \exp\left(-\frac{f''(x_0)}{2}y^2\right), \end{aligned} \tag{5.3}$$

where translational invariance has been used in the last line. This way we have successfully reduced our initial integral to a Gaussian which we perfectly know how to carry out. However, it is not prohibited to take more terms of the Taylor series into account. We will later see how to manage this kind of situation.

5.2 Analogous proceeding for the Φ^4 theory

For a QFT we can (formally) copy the above procedure whose major outcome is a nice separation of tree and loop contributions. To see this, we first want to recall the initial field-theoretical integral

$$\begin{aligned} W[J] &= \frac{\int \mathcal{D}\Phi \exp\left(\frac{i}{\hbar}T[\Phi,J]\right)}{\int \mathcal{D}\Phi \exp\left(\frac{i}{\hbar}T[\Phi,0]\right)}, \qquad (5.4)\\ \text{where} \quad T[\Phi,J] &= S[\Phi] + \int dx J(x)\Phi(x) \\ &= \int dx \left(\Phi(x)\frac{-A(x)}{2}\Phi(x) - \frac{\lambda}{4!}\Phi^4(x) + J(x)\Phi(x)\right). \end{aligned}$$

In this case the Taylor expansion is, of course, a functional one:

$$\begin{aligned} T[\Phi,J] &= \sum_{n=0}^{\infty} \int dy_1 \cdots \int dy_n \frac{1}{n!} \frac{\delta^n T[\Phi_0,J]}{\delta\Phi(y_1)\cdots\delta\Phi(y_n)} \\ &\times \underbrace{(\Phi(y_1)-\Phi_0(y_1))}_{\Phi'(y_1)} \cdots \underbrace{(\Phi(y_n)-\Phi_0(y_n))}_{\Phi'(y_n)}. \qquad (5.5) \end{aligned}$$

We now need to compute all functional derivatives and, in particular, determine the minimum:

$$\begin{aligned} \frac{\delta T[\Phi,J]}{\delta\Phi(y_1)} &= -A(y_1)\Phi(y_1) - \frac{\lambda}{6}\Phi^3(y_1) + J(y_1) \\ \frac{\delta T[\Phi_0,J]}{\delta\Phi(y_1)} \stackrel{!}{=} 0 \quad \text{(min.!)} &\Leftrightarrow A(y_1)\Phi_0(y_1) + \frac{\lambda}{6}\Phi_0^3(y_1) = J(y_1) \\ &\Leftrightarrow \text{in short terms:} \quad \left(\frac{\delta S}{\delta\Phi}\right)_{\Phi_0} = -J, \\ \frac{\delta^2 T[\Phi,J]}{\delta\Phi(y_1)\delta\Phi(y_2)} &= -\left(A(y_1) + \frac{\lambda}{2}\Phi^2(y_1)\right)\delta(y_1-y_2), \\ \frac{\delta^3 T[\Phi,J]}{\delta\Phi(y_1)\cdots\delta\Phi(y_3)} &= -\lambda\Phi(y_1)\delta(y_1-y_2)\delta(y_1-y_3), \\ \frac{\delta^4 T[\Phi,J]}{\delta\Phi(y_1)\cdots\delta\Phi(y_4)} &= -\lambda\delta(y_1-y_2)\delta(y_1-y_3)\delta(y_1-y_4), \\ \frac{\delta^n T[\Phi,J]}{\delta\Phi(y_1)\cdots\delta\Phi(y_n)} &= 0 \quad \forall\, n = 5,6,\cdots. \end{aligned}$$

Putting all pieces together, we end up with the Taylor series

$$\begin{aligned} T[\Phi,J] &= T[\Phi_0,J] - \frac{1}{2}\int dy \Phi'(y)\left(A(y) + \frac{\lambda}{2}\Phi_0^2(y)\right)\Phi'(y) \\ &- \frac{\lambda}{6}\int dy \Phi_0(y)\Phi'^3(y) - \frac{\lambda}{24}\int dy \Phi'^4(y). \qquad (5.6) \end{aligned}$$

5.2.1 Leading-order approximation

Now, we want to spend some time on showing the leading-order approximation to our field-theoretical integral to provide all tree (non-loop) diagrams. Restricting ourselves to the very first term of (5.6), there is nothing left to integrate over in (5.4) and we simply get[1]

$$\begin{aligned} W[J] &\approx \frac{\exp\left(\frac{i}{\hbar}T[\Phi_0,J]\right)}{\int \mathcal{D}\Phi \exp\left(\frac{i}{\hbar}T[\Phi,0]\right)} \\ \Leftrightarrow \quad Z[J] &\approx -\int dx \left(\Phi_0(x)\frac{A(x)}{2}\Phi_0(x)+\frac{\lambda}{4!}\Phi_0^4(x)\right)+\int dx J(x)\Phi_0(x) \\ &= \int dx \left(\frac{1}{2}J(x)\Phi_0(x)+\frac{\lambda}{24}\Phi_0^4(x)\right). \end{aligned} \tag{5.7}$$

We have just learned that the minimal Φ_0 is related to the source J. Since we want to determine Green's functions, Φ_0 must be expressed in terms of J. Unfortunately, $\Phi_0[J,x)$ cannot be given in an analytically closed form. Therefore, one must assume the expansion

$$\Phi_0(x) \quad =: \quad \Phi_{(0)}(x)+\lambda\Phi_{(1)}(x)+\lambda^2\Phi_{(2)}(x)+\cdots \tag{5.8}$$

and solve

$$\begin{aligned} J(x) &= A(x)\left(\Phi_{(0)}(x)+\lambda\Phi_{(1)}(x)+\lambda^2\Phi_{(2)}(x)+\cdots\right) \\ &+ \frac{\lambda}{6}\left(\Phi_{(0)}(x)+\lambda\Phi_{(1)}(x)+\lambda^2\Phi_{(2)}(x)+\cdots\right)^3 \end{aligned} \tag{5.9}$$

perturbatively. Comparison then yields

$$\begin{aligned} &(i) && A(x)\Phi_{(0)}(x)=J(x), \\ &(ii) && \lambda\left(A(x)\Phi_{(1)}(x)+\frac{1}{6}\Phi_{(0)}^3(x)\right)=0, \\ &(iii) && \lambda^2\left(A(x)\Phi_{(2)}(x)+\frac{1}{2}\Phi_{(0)}^2(x)\Phi_{(1)}(x)\right)=0, \\ &\vdots \\ &\text{ad } (i) && \Phi_{(0)}(x)=-\int dy\Delta(x-y)J(y), \\ &\text{ad } (ii) && \lambda\Phi_{(1)}(x)=\frac{\lambda}{6}\int dy\Delta(x-y)\Phi_{(0)}^3(y) \\ & && =-\frac{\lambda}{6}\int dy\int dy_1\cdots\int dy_3 \end{aligned}$$

[1] Since Φ_0 represents the classical solution to our field theory, the present leading-order approximation is also referred to as classical.

$$\times \Delta(x-y)\Delta(y-y_1)\cdots\Delta(y-y_3)J(y_1)\cdots J(y_3),$$

ad (iii)
$$\lambda^2\Phi_{(2)}(x) = \frac{\lambda^2}{2}\int dy\Delta(x-y)\Phi^2_{(0)}(y)\Phi_{(1)}(y)$$
$$= -\frac{\lambda^2}{12}\int dy\int dy_1\int dy_2\int dz\int dz_1\cdots\int dz_3$$
$$\times \Delta(x-y)\Delta(y-y_1)\Delta(y-y_2)\Delta(y-z)\Delta(z-z_1)\cdots\Delta(z-z_3)$$
$$\times J(y_1)J(y_2)J(z_1)\cdots J(z_3),$$

$$\vdots$$

The individual terms of (5.8) can thus be represented graphically (neglecting symmetry factors) as shown in Fig. 5.1.

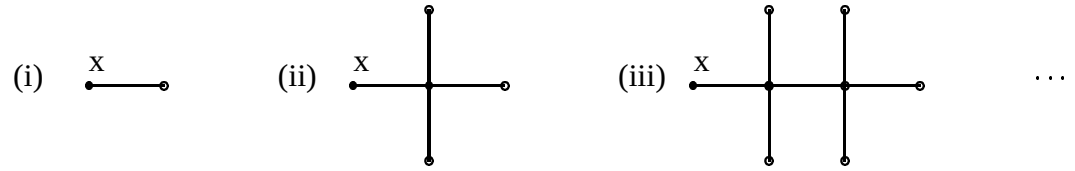

Figure 5.1: Diagrammatical transcription of expansion (5.8) without symmetry factors. The full and open circles indicate the conventional space-time dependence of Φ_0 and its functional dependence on the sources, respectively.

At this point, we can already make out that there is no way to construct any loop diagrams. However, we carry on and use the above result to explicitly show the generating functional $Z[J]$ to become

$$Z[J] \approx -\frac{1}{2}\int dx\int dy\Delta(x-y)J(x)J(y)$$
$$-\frac{\lambda}{24}\int dx\int dy\int dy_1\cdots\int dy_3$$
$$\times \Delta(x-y)\Delta(y-y_1)\cdots\Delta(y-y_3)J(x)J(y_1)\cdots J(y_3)$$
$$-\frac{\lambda^2}{72}\int dx\int dy\int dy_1\int dy_2\int dz\int dz_1\cdots\int dz_3$$
$$\times \Delta(x-y)\Delta(y-y_1)\Delta(y-y_2)\Delta(y-z)\Delta(z-z_1)\cdots\Delta(z-z_3)$$
$$\times J(x)J(y_1)J(y_2)J(z_1)\cdots J(z_3)$$
$$+O(\lambda^3), \tag{5.10}$$

from which the two lowest connected Green's functions can easily be identified:

$$G_c^{(2)}(x_1,x_2) = i\hbar\Delta(x_1-x_2),$$
$$G_c^{(4)}(x_1,\cdots,x_4) = \int dy\frac{-i\lambda}{\hbar}[i\hbar\Delta(y-x_1)]\cdots[i\hbar\Delta(y-x_4)]. \tag{5.11}$$

Hence, we find our claim to just have tree graphs fully confirmed.

For completeness, we want to finish by identifying the 1PI ones. An arbitrary tree Green's function $G_c^{(E)}(x_1,\cdots,x_E)$ obeys the topological relations, quoted in (4.20),

$$I = \frac{E}{2} - 2, \qquad M = \frac{E}{2} - 1. \tag{5.12}$$

In other words, for our tree diagrams both the number of internal lines I and vertices M are fully determined, once the number of external legs E is given. The above relations especially imply that for $M = 2$ or $O(\lambda^2)$ (and beyond) no 1PI graphs will occur anymore. Therefore, the 1PI part of Z comes down to

$$Z_{1PI}[\Phi_{(0)}] \approx \frac{1}{2}\int dx \Phi_{(0)}(x) A(x) \Phi_{(0)}(x) - \frac{\lambda}{24}\Phi_{(0)}^4(x), \tag{5.13}$$

which has got a slightly different functional form in comparison to the associated effective action as we can see in a second. Rushing through the main steps of the procedure,

$$\begin{aligned}
Z[J] &\overset{\text{(tree)}}{=} T[\Phi_0, J] = S[\Phi_0] + \int dx J(x)\Phi_0(x), \\
\Phi_{cl}(y) &:= \frac{\delta Z[J]}{\delta J(y)} \\
&= \int dx \underbrace{\frac{\delta S[\Phi_0]}{\delta \Phi_0(x)}}_{-J(x)} \frac{\delta \Phi_0(x)}{\delta J(y)} + \Phi_0(y) + \int dx J(x) \frac{\delta \Phi_0(x)}{\delta J(y)} = \Phi_0(y), \\
\Gamma[\Phi_{cl}] &= \Gamma[\Phi_0] = Z[J] - \int dx J(x)\Phi_0(x) \\
&= S[\Phi_0] + \int dx J(x)\Phi_0(x) - \int dx J(x)\Phi_0(x) = S[\Phi_0] = S[\Phi_{cl}],
\end{aligned}$$

we finally arrive at the effective action

$$\Gamma[\Phi_{cl}] = -\int dx \left(\Phi_{cl}(x) \frac{A(x)}{2} \Phi_{cl}(x) + \frac{\lambda}{4!}\Phi_{cl}^4(x) \right) \tag{5.14}$$

and the two lowest proper vertices

$$\begin{aligned}
\Gamma^{(2)}(x_1,x_2) &= -A(x_1)\delta(x_1 - x_2), \\
\Gamma^{(4)}(x_1,\cdots,x_4) &= -\lambda\delta(x_1 - x_2)\delta(x_1 - x_3)\delta(x_1 - x_4).
\end{aligned} \tag{5.15}$$

It is interesting to note how they are linked with the corresponding connected Green's functions:

$$\begin{aligned}
G_c^{(2)}(x_1,x_2) &= \hbar \left(\Gamma^{(2)}(x_1,x_2) \right)^{-1}, \\
G_c^{(4)}(x_1,\cdots,x_4) &= \frac{i}{\hbar} \int dx_1' \cdots \int dx_4' G_c^{(2)}(x_1,x_1') \cdots G_c^{(2)}(x_4,x_4') \Gamma^{(4)}(x_1',\cdots,x_4').
\end{aligned} \tag{5.16}$$

Inspecting the last line in (5.16), we can, after all, understand why the proper vertices are referred to as amputated.

5.2.2 Next-to-leading-order approximation

After this fairly detailed discussion we are ready to examine one-loop contributions. We look at them from two completely different perspectives. Taking also the second term of (5.6) into account, we obtain

$$\begin{aligned} W[J] &\approx \mathcal{K}\int \mathcal{D}\Phi' \exp\left(-\frac{i}{2\hbar}\int dy\Phi'(y)\overbrace{\left(A(y)+\frac{\lambda}{2}\Phi_0^2(y)\right)}^{B(y,\Phi_0)}\Phi'(y)\right) \\ &\propto \mathcal{K}\int \mathcal{D}\Phi'' \exp\left(-\frac{i}{2}\int dy\Phi''(y)B(y,\Phi_0)\Phi''(y)\right) \qquad (5.17) \\ \text{with} \quad \mathcal{K} &:= \frac{\exp\left(\frac{i}{\hbar}T[\Phi_0,J]\right)}{\int \mathcal{D}\Phi \exp\left(\frac{i}{\hbar}T[\Phi,0]\right)}\,. \end{aligned}$$

In the second line we have rescaled the functional variable according to the prescription $\Phi'' := \hbar^{-\frac{1}{2}}\Phi'$, which makes the $\hbar$ disappear in the above exp-function. The coefficient in front is changed as well (what has been taken into account by replacing the $=$ by the $\propto$ sign).

The remaining integral is a Gaussian and can, within our first approach, at least formally be solved. With the well-known identity $\det(B) = \exp\langle\ln(B)\rangle$ one comes to

$$\begin{aligned} W[J] &\approx \frac{\exp\left(\frac{i}{\hbar}T[\Phi_0,J] - \frac{1}{2}\langle \ln B(y,\Phi_0)\delta(y-y')\rangle\right)}{\int \mathcal{D}\Phi \exp\left(\frac{i}{\hbar}T[\Phi,0]\right)} \\ \Leftrightarrow \quad Z[J] &\approx \underbrace{T[\Phi_0,J]}_{\text{tree}} + \underbrace{\frac{\hbar}{2}\langle \ln B(y,\Phi_0)\delta(y-y')\rangle}_{\text{1-loop}}\,. \qquad (5.18) \end{aligned}$$

Since the first term was shown to only include tree graphs, thanks to our loop-$\hbar$ connection argument of section 4.2 we can now be sure the second term to comprise one-loop contributions and nothing else. Actually, a generalized version of this latter term is used within the framework of ChPT later in the present thesis.

The second approach is a perturbative one which explicitly substantiates the above statement. We proceed in analogy to our second strategy of the previous chapter (again, we only consider connected contributions). We find

$$\begin{aligned} &\int \mathcal{D}\Phi' \exp\left(-\frac{i}{2\hbar}\int dy\Phi'(y)\left(A(y)+\frac{\lambda}{2}\Phi_0^2(y)\right)\Phi'(y)\right) \\ = &\left\{\exp\left(-\frac{i\lambda}{4\hbar}\int dx\Phi_0^2(x)\left(\frac{\hbar}{i}\frac{\delta}{\delta j(x)}\right)^2\right)\right. \\ \times &\left.\int \mathcal{D}\Phi' \exp\left(\frac{i}{\hbar}\int dy\left(\Phi'(y)\frac{-A(y)}{2}\Phi'(y)+j(x)\Phi'(y)\right)\right)\right\}_{j=0} \end{aligned}$$

$$
\begin{aligned}
&= \mathcal{N}\left\{\exp\left(-\frac{i\lambda}{4\hbar}\int dx\Phi_0^2(x)\left(\frac{\hbar}{i}\frac{\delta}{\delta j(x)}\right)^2\right)\right.\\
&\times \left.\exp\left(-\frac{i}{2\hbar}\int dy\int dy' j(y)\Delta(y-y')j(y')\right)\right\}_{j=0}. \qquad (5.19)
\end{aligned}
$$

As it stands, the last expression exclusively includes vacuum graphs. At *each* vertex they possess two (out of four) incoming lines that are generated by a new source Φ_0 ($\odot$). Such graphs neither exhibit (explicit) external legs nor regular sources. Keeping in mind that $\odot$ only contains tree contributions, one can be persuaded that all graphs do exactly have one loop. Since we are particularly interested in 1PI graphs, we simply have to replace Φ_0 by $\Phi_{(0)}$, see (5.8), due to the fact that higher contributions represent 1PR tree structures.

The construction prescription is thus the following: Connected vacuum graphs (see Fig. 4.1) have to be cut into pieces, in a way that, at each vertex, we get two (free) lines which have to be attached to a source $\odot$. This is illustrated in the below figure.

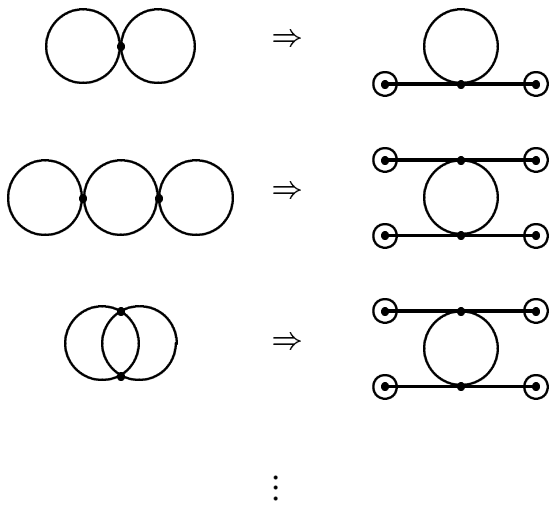

Figure 5.2: The next-to-leading-order term is shown to just include one-loop parts by graphical means.

5.2.3 Next-to-next-to-leading-order approximation

We have seen that the second term in (5.18) collects one-loop contributions and nothing else. Nevertheless, we do not know yet if there are additional one-loop parts in the higher terms. That is exactly what we want to check out in the following. Going

another step further in the Taylor series, the integral we need to carry out can then be rewritten as

$$\begin{aligned} W[J] &\approx \mathcal{K}\int \mathcal{D}\Phi' \exp\left(-\frac{i}{2\hbar}\int dy\Phi'(y)\left(A(y)+\frac{\lambda}{2}\Phi_0^2(y)\right)\Phi'(y)\right) \\ &\times \exp\left(-\frac{i\lambda}{6\hbar}\int dz\Phi_0(z)\Phi'^3(z)\right) \\ &= \mathcal{K}\left\{\exp\left(-\frac{i\lambda}{6\hbar}\int dx\Phi_0(x)\left(\frac{\hbar}{i}\frac{\delta}{\delta j(x)}\right)^3\right)\right. \\ &\times \left.\int \mathcal{D}\Phi' \exp\left(\frac{i}{\hbar}\int dy\left(\Phi'(y)\frac{-B(y)}{2}\Phi'(y)+j(x)\Phi'(y)\right)\right)\right\}_{j=0} \\ &= \mathcal{K}\left\{\exp\left(-\frac{i\lambda}{6\hbar}\int dx\Phi_0(x)\left(\frac{\hbar}{i}\frac{\delta}{\delta j(x)}\right)^3\right)\right. \\ &\times \left.\exp\left(-\frac{i}{2\hbar}\int dy\int dy' j(y)\tilde{\Delta}(y-y')j(y')\right)\right\}_{j=0} \end{aligned} \tag{5.20}$$

and interpreted in our conventional manner. In (5.20), $\tilde{\Delta}$ represents a modified propagator. The remaining structure of the theory does not change. This time we need to cut connected vacuum graphs into pieces, in a way that only one line per vertex is freed and then attached to $\odot$.

In order to gain deeper insight into things, let us expand the first exp-function and look at the individual terms one after the other. Since the very first term has already been considered within the next-to-leading-order approximation, we pass to the second one

$$0 = -\frac{i\lambda\mathcal{K}}{6\hbar}\left\{\int dx\Phi_0(x)\left(\frac{\hbar}{i}\frac{\delta}{\delta j(x)}\right)^3 \exp\left(-\frac{i}{2\hbar}\int dy\int dy' j(y)\tilde{\Delta}(y-y')j(y')\right)\right\}_{j=0} \tag{5.21}$$

which vanishes, as the above construction cannot be applied to one-vertex structures. The third term does not vanish

$$\begin{aligned} 0 &\neq \frac{\lambda^2\mathcal{K}}{72\hbar^2}\left\{\int dx\Phi_0(x)\left(\frac{\hbar}{i}\frac{\delta}{\delta j(x)}\right)^3\int dx'\Phi_0(x')\left(\frac{\hbar}{i}\frac{\delta}{\delta j(x')}\right)^3\right. \\ &\times \left.\exp\left(-\frac{i}{2\hbar}\int dy\int dy' j(y)\tilde{\Delta}(y-y')j(y')\right)\right\}_{j=0} \\ &\propto \frac{\lambda^2\mathcal{K}\hbar}{72}\left\{\int dx\Phi_0(x)\left(\frac{\hbar}{i}\frac{\delta}{\delta j(x)}\right)^3\int dx'\Phi_0(x')\left(\frac{\hbar}{i}\frac{\delta}{\delta j(x')}\right)^3\right. \\ &\times \left.\exp\left(-\frac{i}{2}\int dy\int dy' j(y)\tilde{\Delta}(y-y')j(y')\right)\right\}_{j=0}. \end{aligned} \tag{5.22}$$

Here, after rescaling the fields as we did before, two-loop contributions can be read off thanks to our $\hbar$ counting scheme. If we went ahead like this, we would find the next term to be vanishing, the next-to-next non-vanishing ($\hbar^2$) and so forth. This evidently says that $\frac{\delta^3 T[\Phi_0,J]}{(\delta\Phi)^3}$ leads to loop contributions with $L \geq 2$ and not only $L = 2$ as one might have naively expected.

We are now ready to explicitly construct the lowest 2-loop graphs (see Fig. 5.3). We must keep in mind that the following diagrams do not include the conventional propagators. Nevertheless, those new propagators cannot lead to additional loop structures. Differences show up in the tree structure, though.

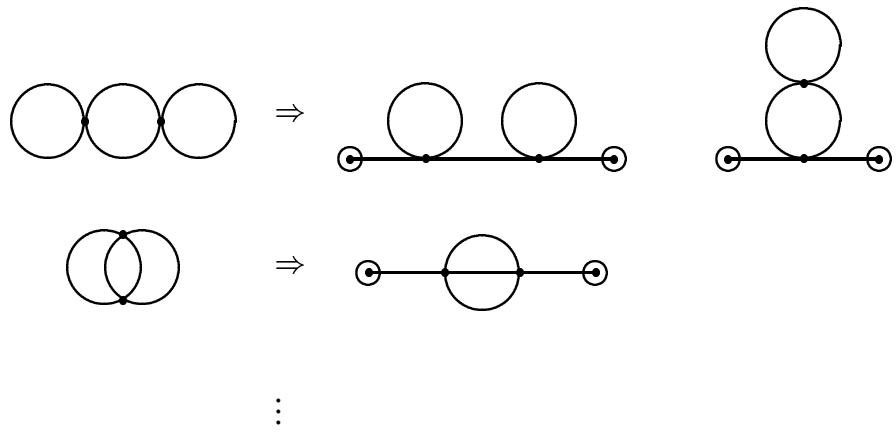

Figure 5.3: Graphical construction of two-loop diagrams.

All in all, we have clearly seen that the saddle-point method is especially adopted to the extraction of the one-loop part.

5.3 More on the effective action and proper vertices

In Chapter 4 we claimed that all amputated 1PI graphs are included in the effective action and nothing more. We are finally in a position to prove this statement by using the saddle-point method. Here is a sketch of the proof:

- Start out with $\Gamma[\Phi]$ instead of $S[\Phi]$ and apply the previously introduced saddle-point method.
- Again, determine the minimum:

$$\left(\frac{\delta T_\Gamma[\Phi,J]}{\delta\Phi(x)}\right)_{\Phi_0^\Gamma} \stackrel{!}{=} 0$$

$$\Leftrightarrow \quad \left(\frac{\delta\Gamma[\Phi]}{\delta\Phi(x)}\right)_{\Phi_0^\Gamma} = -J(x) \quad \Leftrightarrow \quad \Phi_0^\Gamma \text{ is simply } \Phi_{cl}. \tag{5.23}$$

N.B.: $\Gamma[\Phi]$ evidently provides the quantum-corrected field equations.

- Consider tree level:

$$\begin{aligned} \overbrace{Z_\Gamma^{(0)}[J]}^{\text{connected tree part }(\Gamma)} &\overset{(5.7)}{=} T_\Gamma[\Phi_{cl},J] = \Gamma[\Phi_{cl}] + \int dx J(x)\Phi_{cl}(x) \\ &\overset{(4.7)}{=} Z[J] - \int dx J(x)\Phi_{cl}(x) + \int dx J(x)\Phi_{cl}(x) \\ &= \underbrace{Z[J]}_{\text{entire connected part }(S)}. \end{aligned} \tag{5.24}$$

  The above result states that all connected diagrams of our initial S theory can be expressed in terms of connected tree graphs which do include propagators and generic vertices of the Γ theory. Differently speaking, each $2n$-point function on the right-hand side has got a unique partner on the left-hand side, which implies that our Γ theory cannot create any non-vanishing $(2n+1)$-point functions as well.

- Determine the Feynman propagator of the Γ theory:

$$\begin{aligned} \Gamma[\Phi_{cl}] &= -\frac{1}{2}\int dx \Phi_{cl}(x) A^\Gamma(x)\Phi_{cl}(x) + \cdots \\ \Rightarrow \quad \Gamma^{(2)}(x_1,x_2) &= \left(\frac{\delta^2\Gamma[\Phi_{cl}]}{\delta\Phi_{cl}(x_1)\delta\Phi_{cl}(x_2)}\right)_{\Phi_{cl}=0} = -A^\Gamma(x_1)\delta(x_1-x_2) \\ \text{and} \quad \Delta^\Gamma &= \left(-A^\Gamma\right)^{-1} = {\Gamma^{(2)}}^{-1}. \end{aligned} \tag{5.25}$$

  According to Eq. (5.24), Δ^Γ has to be the full propagator of the S theory ($G_c^{(2)} = i\hbar\Delta^\Gamma$).

- Next, investigate the (remaining) proper vertices:
  As indicated at the beginning of the preceding chapter, see Eq. (4.8), the proper vertices are the Green's functions associated to the effective action. Furthermore, the very Eq. (4.8) tells us that they are the generic vertices of the Γ theory considered above. Those can be extracted by amputating all propagators Δ^Γ from any 1PI tree diagram. Although the 1PI tree graphs do not exactly coincide with the 1PI ones of the S theory, their amputated versions do. Hence, we finally see our initial claim to be verified.

Chapter 6

One-loop renormalization of the Wess-Zumino-Witten action

As already mentioned in the introduction, within the framework of ChPT, infinities arising from loop calculations can only be absorbed order by order. Our intention is to fully renormalize, once and for all, the odd intrinsic parity p^6 Lagrangian density established in Chapter 3. According to Weinberg's power counting scheme, the only possible divergences can come from one-loop graphs which involve exactly one WZW vertex and an arbitrary number of $\mathcal{L}_2$ vertices. In other words, we perform the one-loop renormalization of the WZW action.

The entire renormalization procedure can in general be subdivided into three major steps:

1. Extraction of the respective one-loop contribution using the saddle-point method.
2. Compact isolation of arising one-loop singularities by application of dimensional regularization (or operator regularization, see [19]) within the formalism of the heat kernel technique.
3. Absorption of the isolated infinite structures by redefinition of the low-energy constants of the most general Lagrangian at higher-order level.

The points 1. and 2. described above have already been carried out by several authors [17, 18, 19, 20] using totally different conventions and notations. The last step has never been accomplished, though.

6.1 The saddle-point evaluation in ChPT

In Chapter 5 we learned how to (exclusively) extract the one-loop part of a rather simple QFT, namely the Φ^4 theory which just involves one field species and one interaction term. However, the whole saddle-point procedure, and especially its final result

$$Z_{\text{1-loop}} = \frac{i}{2}\ln(\det D), \tag{6.1}$$

can be extended to whatever (mesonic) QFT possessing the Lagrangian density $\mathcal{L}$ and the generating functional

$$\exp(iZ) \propto \int \mathcal{D}U \exp\left(i\int dx \mathcal{L}(U)\right). \tag{6.2}$$

Here, the variable U already alludes to our chiral field matrix (but at this stage it can still be considered as a general field variable).

Although (6.1) represents a nicely compact formula, its real content is rather hidden than revealed. Therefore, we need to have a closer look at the detailed structure of the above operator D.

Let us begin with some preliminary investigations. As one knows from linear algebra, any complex $n\times n$ matrix can uniquely be expanded in terms of $\lambda^0 := \sqrt{\frac{2}{n}}1_{n\times n}$ and the conventional n^2-1 $SU(n)$ generators λ^a

$$A(x) = \sum_{a=0}^{n^2-1} A^a(x)\lambda^a, \tag{6.3}$$

with $A^a(x) \in \mathbf{C}$ for any fixed $x \in \mathbf{M}$ and $a \in \{0,\cdots,n^2-1\}$. A standard scalar product is provided by the following definition

$$(A,B) = \frac{1}{2}\int dx \langle A^\dagger(x)B(x)\rangle = \sum_{a=0}^{n^2-1}\int dx A^{a*}(x)B^a(x), \tag{6.4}$$

where we have made use of the relation $\langle\lambda^a\lambda^b\rangle = 2\delta^{ab}$.

We are now ready to roughly retrace the saddle-point procedure in ChPT. Instead of performing explicit functional derivatives, we parameterize our $SU(n)$ field matrix $U(x)$ around the classical solution $\bar{U}(x)$ (which is the minimum field configuration) in an appropriate (non-uniquely determined) manner

$$U(x) = u(x)\exp\left(i\xi(x)\right)u(x). \tag{6.5}$$

Here, $u^2(x) = \bar{U}(x)$ must hold and $\xi(x)$ has to be a traceless Hermitian matrix

$$\xi(x) = \sum_{a=1}^{n^2-1}\xi^a(x)\lambda^a, \tag{6.6}$$

with $\xi^a(x) \in \mathbf{R}$ for any fixed $x \in \mathbf{M}$ and $a \in \{1, \cdots, n^2-1\}$.

In what follows we omit denoting any explicit x dependence. Furthermore, in contrast to (6.4) all indices a or b are meant to take values in $\{1, \ldots, n^2-1\}$ and have to be summed over when appearing twice according to Einstein's convention.

Without proof we quote the result that under certain circumstances, which are fulfilled in ChPT, Eq. (6.2) may be rewritten as

$$\begin{aligned} \exp(iZ) &\overset{\text{1-loop}}{\propto} \int \mathcal{D}\xi \exp\left(-\tfrac{iF_0^2}{2}(\xi, D\xi)\right) \\ &= \int \mathcal{D}\xi \exp\left(-\tfrac{iF_0^2}{2}\int dx \xi^a D^{ab} \xi^b\right). \end{aligned} \tag{6.7}$$

The elliptic operator D of the type

$$\begin{aligned} D &= d^\mu d_\mu + \hat{\sigma}, \\ \text{with} \qquad d_\mu \xi &= \partial_\mu \xi + \left[\Gamma_\mu, \xi\right], \end{aligned} \tag{6.8}$$

is supposed to be positive, unbounded, and self-adjoint, and has the spectral decomposition $\{\phi_n; \lambda_n\}$. The matrices ϕ_n form a complete system of eigenfunctions and λ_n represent the associated positive eigenvalues.

Obviously, the anti-Hermitian Γ_μ and the positive Hermitian $\hat{\sigma}$ are the very objects which contain all one-loop information of the specific theory (which is itself defined by its action or Lagrangian density).

In non-matrix terms the same operator looks like

$$\begin{aligned} D^{ab}\xi^b &= d^\mu d_\mu \xi^a + \hat{\sigma}^{ab}\xi^b \\ d_\mu \xi^a &= \partial_\mu \xi^a + \hat{\Gamma}_\mu^{ab}\xi^b \end{aligned} \tag{6.9}$$

and $\hat{\Gamma}_\mu^{ab}$ leads to the natural definition

$$\hat{\Gamma}_{\mu\nu}^{ab} = \partial_\mu \hat{\Gamma}_\nu^{ab} - \partial_\nu \hat{\Gamma}_\mu^{ab} + \left[\hat{\Gamma}_\mu, \hat{\Gamma}_\nu\right]^{ab}. \tag{6.10}$$

To put this section's content in a nutshell, the one-loop part of our considered QFT and therefore step 1. of the renormalization procedure will be under control as soon as we manage to determine the corresponding objects Γ_μ and $\hat{\sigma}$.

6.2 The heat kernel technique

The so-called heat kernel approach is a very sophisticated mathematical method which is native to the theory of positive unbounded self-adjoint elliptic operators on compact Riemannian manifolds [57, 50]. As often in theoretical physics we only try to understand the main features of the mechanism without paying too much attention to refined details mathematicians would probably consider primordial to look at. In other words,

for our concerns the heat kernel technique represents a powerful tool helping us to answer physically interesting questions (i.e., in our actual situation, to elegantly isolate all one-loop divergences). Therefore, we content ourselves with a somewhat sketchy presentation of its derivation.

First of all, we define the zeta function for our operator given in (6.8)

$$\zeta_D(s) := \sum_n \lambda_n^{-s}, \quad s \in \mathbf{R}, \tag{6.11}$$

which obviously solely depends on D via its eigenvalues λ_n.

One can then relate the associated one-loop part to the zeta function

$$\frac{i}{2}\ln(\det D) = -\frac{i}{2}\frac{d}{ds}\zeta_D(0), \tag{6.12}$$

where $\det D$ may formally be regarded as the product of all eigenvalues.

The next thing to do is the introduction of the so-called heat kernel

$$\langle x|\exp(-\tau D)|y\rangle = \sum_n \exp(-\tau\lambda_n)\phi_n(x)\phi_n^\dagger(y), \tag{6.13}$$

which obeys the heat equation

$$D_x\langle x|\exp(-\tau D)|y\rangle = -\frac{\partial}{\partial\tau}\langle x|\exp(-\tau D)|y\rangle. \tag{6.14}$$

The last two expressions are written in a suitable $|x\rangle$ basis representation, where $|x\rangle$ has nothing to do with the space-time degree of freedom.

In considering the trace of (6.13)

$$\int dx\Big\langle \langle x|\exp(-\tau D)|x\rangle\Big\rangle = \sum_n \exp(-\tau\lambda_n), \tag{6.15}$$

one may now connect the zeta function to the heat kernel

$$\Gamma(s)\zeta_D(s) = \int_0^\infty d\tau\tau^{s-1}\int dx\Big\langle \langle x|\exp(-\tau D)|x\rangle\Big\rangle. \tag{6.16}$$

If we knew the exact form of the heat kernel, we could easily compute the zeta function and all the rest. So let us try to determine the needed heat kernel.

The straightest way to get things going consists in solving the heat equation induced by the D'Alembertian, which turns out to be the dominant part at short distances, in general d dimensions ($\rightarrow$ dimensional regularization)

$$\langle x|\exp(-\tau\partial^2)|y\rangle = \frac{i}{(4\pi\tau)^{\frac{d}{2}}}\exp\left(\frac{(x-y)^2}{4\tau}\right). \tag{6.17}$$

We then make a separation ansatz to find the solution for the entire operator D

$$\begin{aligned}\langle x|\exp(-\tau D)|y\rangle &= \langle x|\exp(-\tau\partial^2)|y\rangle H(x|\tau|y)\\ &= \langle x|\exp(-\tau\partial^2)|y\rangle \sum_{n=0}^{\infty}\tau^n H_n(x|y)\end{aligned} \tag{6.18}$$

satisfying the constraint $H(x|0|x)=0$ (or equivalently $H_0(x|x)=0$).[1]

With the above ansatz we succeed in deriving the differential equation

$$0=\frac{\partial}{\partial\tau}H(x|\tau|y)+\frac{z}{\tau}dH(x|\tau|y)+(dd+\hat{\sigma})H(x|\tau|y) \tag{6.19}$$

from which every single $H_n(x|y)$ function can be determined recursively.

Careful analysis yields a splitting of the entire integral into an infinite and a finite part

$$\begin{aligned}\zeta_D(s) &= \frac{1}{\Gamma(s)}\int_0^1 d\tau\tau^{s-1}\int dx\Big\langle\langle x|\exp(-\tau D)|y\rangle\Big\rangle + \text{ finite part}\\ &= \frac{i}{(4\pi)^{\frac{d}{2}}\Gamma(s)}\sum_{n=0}^{\infty}\int_0^1 d\tau\tau^{s-1-\frac{d}{2}+n}\int dx\langle H_n(x|x)\rangle + \text{ finite part.}\end{aligned} \tag{6.20}$$

In perfoming the necessary differentiation (we essentially need to make use of the identities $\frac{d}{ds}\frac{1}{\Gamma(0)}=1$ and $\frac{1}{\Gamma(0)}=0$) we manage to isolate and identify the wanted singularities

$$-\frac{i}{2}\frac{d}{ds}\zeta_D(0)=-\frac{\int dx}{(4\pi)^{\frac{d}{2}}}\sum_{n=0}^{\infty}\frac{1}{d-2n}\langle H_n(x|x)\rangle + \text{ finite part.} \tag{6.21}$$

Since Minkowski space-time corresponds to dimension $d=4$, there is just one singular term to be kept in Eq. (6.21), namely the one including $H_2(x|x)$ which must be worked out recursively. Putting all links of our argumentation chain, Eq. (6.1), Eq. (6.12), Eq. (6.21), together, we finally obtain the the heat kernel master formula

$$Z_{\text{1-loop}}^{(\text{sing})}=-\frac{\int dx}{16\pi^2(d-4)}\langle\tfrac{1}{12}\hat{\Gamma}_{\mu\nu}\hat{\Gamma}^{\mu\nu}+\tfrac{1}{2}\hat{\sigma}^2\rangle, \tag{6.22}$$

which is the very means to successfully carry out step 2. As expected, the divergences are expressed in terms of $\hat{\Gamma}_{\mu}^{ab}$ and $\hat{\sigma}^{ab}$ (the above trace is referred to the indices a and b) since these objects include all information on the one-loop structure of the theory.

[1]The somewhat confusing notation for the matrix $H(x|\tau|y)$, which was introduced in the mathematical articles indicated, simply means $H(x,y,\tau)$.

6.2.1 Exemplary illustration for the Φ^4 theory

In Chapter 5 we studied the Φ^4 theory in some detail but left singularity and renormalization problems completely aside. We are now in a position to give a compact concluding answer to these questions (at least at the one-loop level) and illustrate the application of the heat kernel mechanism in a very simple case.[2]

Recalling the saddle-point approximation of the associated action

$$S^{(2)}_{\Phi^4}[\Phi'] = \int dy\, \Phi'(y) \left(\partial_\mu \partial^\mu + m^2 + \frac{\lambda}{2}\Phi_0^2(y) \right) \Phi'(y), \tag{6.23}$$

one easily identifies the non-vanishing part of the corresponding operator D to yield

$$\hat{\sigma} = m^2 + \frac{\lambda}{2}\Phi_0^2(y). \tag{6.24}$$

In considering this, the divergent structures thus turn out to be

$$\begin{aligned} Z^{(\text{sing})}_{\text{1-loop}} &= -\frac{\int dx}{16\pi^2(d-4)}\, \frac{1}{2}\hat{\sigma}^2 \\ &= -\frac{\int dx}{16\pi^2(d-4)} \Big(\frac{m^4}{2} + \frac{\lambda m^2}{2}\Phi_0^2(x) + \frac{\lambda^2}{8}\Phi_0^4(x) \Big) \end{aligned} \tag{6.25}$$

in complete accordance with the well-known textbook results (see [44]). The first term does not involve any field and can, of course, be dropped.

6.3 Application to $\mathcal{L}_2$

The major task we are facing is the determination of $\hat{\Gamma}^{ab}_\mu$ and $\hat{\sigma}^{ab}$ for our specific case. Since we have to include both $\mathcal{L}_2$ and the WZW action, let us recapitulate what Gasser and Leutwyler [12, 13] carried out for the former part. This way we get a first idea of how the whole procedure is supposed to work and, in addition to that, we can shortly recall their notation and convention to which we shall stick (as [20] did).

The main objects we are dealing with are collected below:

$$\begin{aligned} \Gamma_\mu &= \frac{1}{2}\left[u^\dagger, \partial_\mu u\right] - \frac{i}{2}u^\dagger R_\mu u - \frac{i}{2}u L_\mu u^\dagger, \\ \Delta_\mu &= \frac{1}{2}u^\dagger D_\mu \bar{U} u^\dagger = -\frac{1}{2}u D_\mu \bar{U}^\dagger u, \\ F^\pm_{\mu\nu} &= iu(F^L_{\mu\nu} \pm \bar{U}^\dagger F^R_{\mu\nu}\bar{U})u^\dagger, \\ \Gamma_{\mu\nu} &= -\left[\Delta_\mu, \Delta_\nu\right] - \frac{1}{2}F^+_{\mu\nu}. \end{aligned} \tag{6.26}$$

[2] The heat kernel technique works for both renormalizable and non-renormalizable theories.

The action can now be expanded according to our prescription

$$S_2^{(2)}[\xi] = -\frac{F_0^2}{2}\int dx \xi^a D^{ab}\xi^b \tag{6.27}$$

and after a lot of straightforward algebra (basically, one has to systematically insert (6.5) and expand the exp-function containing ξ) the needed quantities turn out to read

$$\begin{aligned} \hat{\Gamma}_\mu^{ab} &= -\frac{1}{2}\langle[\lambda^a,\lambda^b]\Gamma_\mu\rangle \\ \text{and} \qquad \hat{\sigma}^{ab} &= \frac{1}{2}\langle[\lambda^a,\Delta_\mu][\lambda^b,\Delta^\mu]\rangle + \frac{1}{4}\langle\{\lambda^a,\lambda^b\}\sigma\rangle, \end{aligned} \tag{6.28}$$

where the matrix σ is defined via

$$\sigma = \frac{u\chi^\dagger u + u^\dagger\chi u^\dagger}{2}\,. \tag{6.29}$$

If we were to renormalize the LECs of $\mathcal{L}_4$ (this was done in [12, 13]), we could isolate the respective one-loop singularities straight away by using the heat kernel result (6.22) of the previous section. Of course, the resulting singularities must be rewritten in terms of the $\mathcal{L}_4$ monomials before perfoming step 3. The final absorption consists in a redefinition of the concerned LECs according to the rule (based on DR)

$$\begin{aligned} L_i &= L_i^r + \Gamma_i\lambda \quad \text{(analogous for } H_i\text{)}, \\ \lambda &= \frac{\mu^{d-4}}{(4\pi)^2}\Big\{\frac{1}{d-4} - \frac{1}{2}\Big(\ln(4\pi) + \Gamma'(1) + 1\Big)\Big\} = \frac{\mu^{d-4}}{(4\pi)^2}\frac{R}{2}. \end{aligned} \tag{6.30}$$

6.4 Extension to the WZW action

Our actual case to be revisited and completed is more complicated. Nevertheless, the described strategy does not differ at all. Basically, we have to work out extended quantities $\hat{\Gamma}'^{ab}_{\mu\nu}$ and $\hat{\sigma}'^{ab}$ which include WZW as well as $\mathcal{L}_2$ contributions.

Extremely tedious calculations yield a first important result

$$\begin{aligned} S_{WZW}^{(2)}[\xi] = -\frac{iN_c\varepsilon^{\mu\nu\alpha\beta}}{48\pi^2}\int dx \quad \Big\langle \quad & (\xi d_\mu\xi - d_\mu\xi\xi)\{\Gamma_{\nu\alpha},\Delta_\beta\} \\ + \quad & (\xi\Delta_\mu d_\nu\xi - d_\nu\xi\Delta_\mu\xi)(\Gamma_{\alpha\beta} - 2\Delta_\alpha\Delta_\beta) \\ - \quad & \frac{1}{8}\xi^2[\Gamma_{\mu\nu} - 2\Delta_\mu\Delta_\nu, F^-_{\alpha\beta}] \\ - \quad & \frac{1}{2}\xi\Delta_\mu\xi\{F^-_{\nu\alpha},\Delta_\beta\} \quad \Big\rangle, \end{aligned} \tag{6.31}$$

which can, with some effort, be shown to read

$$S_{WZW}^{(2)}[\xi] = -\frac{F_0^2}{2}\int dx \Big\{\hat{\Gamma}^{\mu\ ab}_{WZW}(\xi^a d_\mu\xi^b - \xi^b d_\mu\xi^a) + \xi^a\hat{\sigma}^{ab}_{WZW}\xi^b\Big\}; \tag{6.32}$$

with the ingredients

$$\begin{aligned}
\hat{\Gamma}^{\mu\,ab}_{WZW} &= \frac{iN_c\varepsilon^{\mu\nu\alpha\beta}}{48\pi^2F_0^2}\langle[\lambda^a,\lambda^b]X_{\nu\alpha\beta}-(\lambda^a\Delta_\nu\lambda^b-\lambda^b\Delta_\nu\lambda^a)Y_{\alpha\beta}\rangle,\\
\hat{\sigma}^{ab}_{WZW} &= \frac{-iN_c\varepsilon^{\mu\nu\alpha\beta}}{384\pi^2F_0^2}\langle\{\lambda^a,\lambda^b\}[Y_{\mu\nu},F^-_{\alpha\beta}]+4(\lambda^a\Delta_\mu\lambda^b+\lambda^b\Delta_\mu\lambda^a)\{F^-_{\nu\alpha},\Delta_\beta\}\rangle,\\
X_{\nu\alpha\beta} &= -\frac{1}{2}\{F^+_{\nu\alpha},\Delta_\beta\}-4\Delta_\nu\Delta_\alpha\Delta_\beta,\\
Y_{\alpha\beta} &= -\frac{1}{2}F^+_{\alpha\beta}-4\Delta_\alpha\Delta_\beta.
\end{aligned}\tag{6.33}$$

Here, one should note that the algebraic stucture in (6.32) is somewhat different from the one in (6.27). This is no contradiction because the combined action only has to structurally agree with (6.27) in order to match the heat kernel formula and it does as we can see in a moment.

We first define two new (generalized) quantities

$$\begin{aligned}
d'_\mu\xi^a &:= \partial_\mu\xi^a+\overbrace{(\hat{\Gamma}^{ab}_\mu+\hat{\Gamma}^{ab}_{WZW\,\mu})}^{\hat{\Gamma}'^{ab}_\mu}\xi^b\\
\text{and}\quad \hat{\sigma}'^{ab} &:= \hat{\sigma}^{ab}+\hat{\sigma}^{ab}_{WZW}.
\end{aligned}\tag{6.34}$$

Again, $\hat{\Gamma}'_{\mu\nu}$ is related to $\hat{\Gamma}'_\mu$ via (6.10)

$$\begin{aligned}
\hat{\Gamma}'_{\mu\nu} &= \partial_\mu\hat{\Gamma}'_\nu-\partial_\nu\hat{\Gamma}'_\mu+\left[\hat{\Gamma}'_\mu,\hat{\Gamma}'_\nu\right]\\
&= \hat{\Gamma}_{\mu\nu}+\hat{\Gamma}^{WZW}_{\mu\nu}+\left[\hat{\Gamma}_\mu,\hat{\Gamma}^{WZW}_\nu\right]+\left[\hat{\Gamma}^{WZW}_\mu,\hat{\Gamma}_\nu\right]\;=\\
O(p^2): &\quad \hat{\Gamma}_{\mu\nu}\\
O(p^4): &+ \partial_\mu\hat{\Gamma}^{WZW}_\nu-\partial_\nu\hat{\Gamma}^{WZW}_\mu+\left[\hat{\Gamma}_\mu,\hat{\Gamma}^{WZW}_\nu\right]+\left[\hat{\Gamma}^{WZW}_\mu,\hat{\Gamma}_\nu\right]\\
O(p^6): &+ \left[\hat{\Gamma}^{WZW}_\mu,\hat{\Gamma}^{WZW}_\nu\right]
\end{aligned}\tag{6.35}$$

and evidently contains terms of different chiral order. Putting all pieces together, one finally ends up with

$$\begin{aligned}
S^{(2)}_2[\xi]+S^{(2)}_{WZW}[\xi] &- \frac{F_0^2}{2}\int dx\xi^a\hat{\Gamma}^{\mu\,ab}_{WZW}\hat{\Gamma}^{bc}_{WZW\,\mu}\xi^c\\
&= -\frac{F_0^2}{2}\int dx\left\{\xi^a d'^\mu d'_\mu\xi^a+\xi^a\hat{\sigma}'^{ab}\xi^b\right\}.
\end{aligned}\tag{6.36}$$

The second line of (6.36) exhibits the exact structure we have been looking for. The first line, however, includes one 'spoiling' term, namely the last one, whose effect on our concerns can be discussed away due to chiral power counting. In complete analogy to the former examples, our new operator leads to one-loop singularities of the general type

$$Z^{(\text{sing})}_{\text{1-loop}}=-\frac{\int dx}{16\pi^2(d-4)}\langle\tfrac{1}{12}\hat{\Gamma}'_{\mu\nu}\hat{\Gamma}'^{\mu\nu}+\tfrac{1}{2}\hat{\sigma}'^2\rangle,\tag{6.37}$$

which comprises as well contributions possessing different chiral orders. At $O(p^6)$, which is the level we are interested in, the divergent part turns out to read

$$\begin{aligned} Z_{\text{1-loop}}^{(\text{sing})} &\overset{O(p^6)}{=} -\frac{\int dx}{16\pi^2(d-4)}\langle \tfrac{1}{6}\hat{\Gamma}_{\mu\nu}\check{\Gamma}^{\mu\nu}_{WZW} + \hat{\sigma}\hat{\sigma}_{WZW}\rangle \qquad (6.38)\\ \text{with}\quad \check{\Gamma}^{\mu\nu}_{WZW} &= \partial^\mu\hat{\Gamma}^\nu_{WZW} - \partial^\nu\hat{\Gamma}^\mu_{WZW} + \left[\hat{\Gamma}^\mu, \hat{\Gamma}^\nu_{WZW}\right] + \left[\hat{\Gamma}^\mu_{WZW}, \hat{\Gamma}^\nu\right]. \end{aligned}$$

Inserting the necessary expressions, one obtains

$$\begin{aligned} \int dx \langle \tfrac{1}{6}\hat{\Gamma}_{\mu\nu}\check{\Gamma}^{\mu\nu}_{WZW}\rangle &= \frac{iN_c\varepsilon^{\mu\nu\alpha\beta}}{96\pi^2F_0^2}\int dx\Big(-\frac{8N_f}{3}\Big)\ \times \\ &\left\langle \left([d^\lambda\Delta_\lambda,\Delta_\mu] + [\Delta_\lambda, d^\lambda\Delta_\mu] + \frac{i}{4}(D^\lambda G_{\lambda\mu})_+\right)\{\Gamma_{\nu\alpha},\Delta_\beta\}\right\rangle \qquad (6.39) \end{aligned}$$

and

$$\begin{aligned} \int dx\langle\hat{\sigma}\hat{\sigma}_{WZW}\rangle &= \frac{iN_c\varepsilon^{\mu\nu\alpha\beta}}{96\pi^2F_0^2}\int dx\ \times \\ &\Big\{\ \frac{N_f^2-4}{4N_f}\langle\sigma[F^+_{\mu\nu},F^-_{\alpha\beta}]\rangle - \frac{4-2N_f^2}{N_f}\langle\sigma[\Delta_\mu\Delta_\nu,F^-_{\alpha\beta}]\rangle - 4\langle\sigma\Delta_\mu\rangle\langle\Delta_\nu F^-_{\alpha\beta}\rangle \\ &-\ \frac{N_f}{2}\langle\Delta_\lambda\Delta^\lambda[F^+_{\mu\nu},F^-_{\alpha\beta}]\rangle - 4N_f\langle\Delta_\lambda\Delta^\lambda[\Delta_\mu\Delta_\nu,F^-_{\alpha\beta}]\rangle \\ &+\ 8\langle\Delta_\lambda\Delta^\lambda\Delta_\mu\rangle\langle\Delta_\nu F^-_{\alpha\beta}\rangle - 8\langle\Delta_\lambda\Delta_\mu\rangle\langle\{\Delta^\lambda,\Delta_\nu\}F^-_{\alpha\beta}\rangle\ \Big\}. \qquad (6.40) \end{aligned}$$

The above results agree with [20] as well as with [18][3] and [19]. Since the latter groups used totally different conventions, the agreement is not obvious at first glance. In addition to that, one should re-stress that all outcoming terms are chirally invariant and four-dimensional.[4] There is no need for additional WZW like structures. The non-Abelian chiral anomaly is fully saturated by the WZW part itself.

The just isolated infinite $O(p^6)$ structures shown in Eq. (6.39) and (6.40) have to be translated into our language in order to conclude the renormalization procedure. Transcribing block by block according to Table 3.1, we find

$$\begin{aligned} Z_{\text{1-loop}}^{(\text{sing})} &\overset{O(p^6)}{=} -\frac{\int dx}{16\pi^2(d-4)}\frac{N_c\varepsilon^{\mu\nu\alpha\beta}}{96\pi^2F_0^2}\quad\Big\{ \\ &+\quad \frac{N_f}{96}\quad i\,\langle[(D^\lambda D_\lambda U)_-,(D_\mu U)_-](D_\nu U)_-(D_\alpha U)_-(D_\beta U)_-\rangle \\ &+\quad \frac{N_f}{96}\quad i\,\langle[(D_\lambda U)_-,(D^\lambda D_\mu U)_-](D_\nu U)_-(D_\alpha U)_-(D_\beta U)_-\rangle \end{aligned}$$

[3] While [18] provides the correct formulae, the commonly quoted review article [58] is full of misprints.

[4] The block $(D^\lambda G_{\lambda\mu})_+$ does not match the above nomenclature. Our very convention has been anticipated for notational simplicity.

$$
\begin{aligned}
&- \quad \frac{N_f}{24} \quad \langle (D^\lambda G_{\lambda\mu})_+ (D_\nu U)_- (D_\alpha U)_- (D_\beta U)_- \rangle \\
&- \quad \frac{N_f}{96} \quad \langle [(D^\lambda D_\lambda U)_-, (D_\mu U)_-] \{ (G_{\nu\alpha})_+, (D_\beta U)_- \} \rangle \\
&- \quad \frac{N_f}{96} \quad \langle [(D_\lambda U)_-, (D^\lambda D_\mu U)_-] \{ (G_{\nu\alpha})_+, (D_\beta U)_- \} \rangle \\
&- \quad \frac{N_f}{24} \quad i \, \langle (D^\lambda G_{\lambda\mu})_+ \{ (G_{\nu\alpha})_+, (D_\beta U)_- \} \rangle \\
&+ \quad \frac{N_f^2 - 4}{32 N_f} \quad i \langle (\chi)_+ [(G_{\mu\nu})_+, (H_{\alpha\beta})_+] \rangle \\
&+ \quad \frac{N_f^2 - 2}{32 N_f} \quad \langle (\chi)_+ [(D_\mu U)_- (D_\nu U)_-, (H_{\alpha\beta})_+] \rangle \\
&- \quad \frac{1}{16} \quad \langle (\chi)_+ (D_\mu U)_- \rangle \langle (D_\nu U)_- (H_{\alpha\beta})_+ \rangle \\
&- \quad \frac{N_f}{128} \quad i \, \langle (D_\lambda U)_- (D^\lambda U)_- [(G_{\mu\nu})_+, (H_{\alpha\beta})_+] \rangle \\
&- \quad \frac{N_f}{128} \quad \langle (D_\lambda U)_- (D^\lambda U)_- [(D_\mu U)_- (D_\nu U)_-, (H_{\alpha\beta})_+] \rangle \\
&+ \quad \frac{1}{64} \quad \langle (D_\lambda U)_- (D^\lambda U)_- (D_\mu U)_- \rangle \langle (D_\nu U)_- (H_{\alpha\beta})_+ \rangle \\
&- \quad \frac{1}{64} \quad \langle (D_\lambda U)_- (D_\mu U)_- \rangle \langle \{ (D^\lambda U)_-, (D_\nu U)_- \} (H_{\alpha\beta})_+ \rangle \quad \Big\}.
\end{aligned}
\tag{6.41}
$$

The first five expressions cannot be identified in terms of our 24 monomials straight away (compare with Table 3.2). EOM replacement and symmetrization of $(D_\mu D_\nu U)_-$ blocks lead to

$$
\begin{aligned}
Z^{(\text{sing})}_{\text{1-loop}} \quad &\overset{O(p^6)}{=} \quad -\frac{\int dx}{16\pi^2 (d-4)} \frac{N_c \varepsilon^{\mu\nu\alpha\beta}}{96\pi^2 F_0^2} \quad \Big\{ \\
&+ \quad \frac{N_f}{96} \quad i \, \langle [(\chi)_-, (D_\mu U)_-] (D_\nu U)_- (D_\alpha U)_- (D_\beta U)_- \rangle \\
&+ \quad \frac{N_f}{96} \quad i \, \langle [(D_\lambda U)_-, (D^\lambda D_\mu U)^s_-] (D_\nu U)_- (D_\alpha U)_- (D_\beta U)_- \rangle \\
&+ \quad \frac{N_f}{192} \quad \langle [(D_\lambda U)_-, (H^\lambda{}_\mu)_-] (D_\nu U)_- (D_\alpha U)_- (D_\beta U)_- \rangle \\
&- \quad \frac{N_f}{24} \quad \langle (D^\lambda G_{\lambda\mu})_+ (D_\nu U)_- (D_\alpha U)_- (D_\beta U)_- \rangle \\
&- \quad \frac{N_f}{96} \quad \langle [(\chi)_-, (D_\mu U)_-] \{ (G_{\nu\alpha})_+, (D_\beta U)_- \} \rangle \\
&- \quad \frac{N_f}{96} \quad \langle [(D_\lambda U)_-, (D^\lambda D_\mu U)_-] \{ (G_{\nu\alpha})_+, (D_\beta U)_- \} \rangle \\
&+ \quad \ldots \quad \Big\}.
\end{aligned}
\tag{6.42}
$$

Still, the fourth and last line of (6.42) are not yet written in a suitable form. We need to explicitly consider

$$
\begin{aligned}
0 &= \langle (D^\lambda G_{\lambda\mu})_+ (D_\nu U)_- (D_\alpha U)_- (D_\beta U)_- \rangle \varepsilon^{\mu\nu\alpha\beta} \\
&+ \langle (G_{\lambda\mu})_+ \{ (D^\lambda D_\nu U)^s_- (D_\alpha U)_- (D_\beta U)_- - (D_\beta U)_- (D_\alpha U)_- (D^\lambda D_\nu U)^s_- \} \rangle \varepsilon^{\mu\nu\alpha\beta} \\
&+ \langle (G_{\lambda\mu})_+ (D_\nu U)_- (D^\lambda D_\alpha U)^s_- (D_\beta U)_- \rangle \varepsilon^{\mu\nu\alpha\beta} \\
&- \frac{i}{2} \langle (G_{\lambda\mu})_+ \{ (H^\lambda{}_\nu)_+ (D_\alpha U)_- (D_\beta U)_- - (D_\beta U)_- (D_\alpha U)_- (H^\lambda{}_\nu)_+ \} \rangle \varepsilon^{\mu\nu\alpha\beta} \\
&- \frac{i}{2} \langle (G_{\lambda\mu})_+ (D_\nu U)_- (H^\lambda{}_\alpha)_+ (D_\beta U)_- \rangle \varepsilon^{\mu\nu\alpha\beta},
\end{aligned}
$$

$$
\begin{aligned}
&\langle [(D^\lambda U)_-, (D_\lambda D_\mu U)_-] \{ (G_{\nu\alpha})_+, (D_\beta U)_- \} \rangle \varepsilon^{\mu\nu\alpha\beta} \\
= &- \langle (G_{\mu\nu})_+ \{ (D_\lambda D_\alpha U)^s_- (D^\lambda U)_- (D_\beta U)_- - (D_\beta U)_- (D^\lambda U)_- (D_\lambda D_\alpha U)^s_- \} \rangle \varepsilon^{\mu\nu\alpha\beta} \\
&+ \langle (G_{\mu\nu})_+ \{ (D^\lambda U)_- (D_\lambda D_\alpha U)^s_- (D_\beta U)_- - (D_\beta U)_- (D_\lambda D_\alpha U)^s_- (D^\lambda U)_- \} \rangle \varepsilon^{\mu\nu\alpha\beta} \\
&+ \frac{i}{2} \langle (G_{\mu\nu})_+ \{ (H_{\lambda\alpha})_+ (D^\lambda U)_- (D_\beta U)_- - (D_\beta U)_- (D^\lambda U)_- (H_{\lambda\alpha})_+ \} \rangle \varepsilon^{\mu\nu\alpha\beta} \\
&- \frac{i}{2} \langle (G_{\mu\nu})_+ \{ (D^\lambda U)_- (H_{\lambda\alpha})_+ (D_\beta U)_- - (D_\beta U)_- (H_{\lambda\alpha})_+ (D^\lambda U)_- \} \rangle \varepsilon^{\mu\nu\alpha\beta}.
\end{aligned}
$$

While the first auxiliary equation makes use of our total-derivative argument and subsequent symmetrization, the last one only symmetrizes the $(D_\mu D_\nu U)_-$ blocks. Two formulae from Appendix B are needed to finish. Finally, we are able to read off the Γ coefficients belonging to our sets of LECs. For notational convenience, the global factor $N_c/96\pi^2 F_0^2 = 1/32\pi^2 F_0^2$ is omitted in the below Tables.

i	Γ_i	i	Γ_i	i	Γ_i
1	$\frac{4-2N_f^2}{64N_f}$	9	0	17	$-\frac{1}{64}$
2	$-\frac{1}{16}$	10	0	18	$-\frac{1}{64}$
3	$\frac{N_f^2-4}{32N_f}$	11	0	19	$-\frac{N_f}{24}$
4	$\frac{N_f}{48}$	12	$-\frac{N_f}{96}$	20	0
5	$-\frac{N_f}{96}$	13	$\frac{N_f}{24}$	21	0
6	$-\frac{N_f}{24}$	14	$\frac{N_f}{24}$	22	$\frac{N_f}{96}$
7	$-\frac{1}{48}$	15	$-\frac{N_f}{192}$	23	$\frac{N_f}{128}$
8	0	16	0	24	$-\frac{N_f}{16}$

Table 6.1: $\Gamma^{SU(n)}$ coefficients.

i	Γ_i	i	Γ_i	i	Γ_i
1	$-\frac{7}{96}$	9	0	17	$-\frac{1}{128}$
2	$-\frac{1}{16}$	10	0	18	0
3	$\frac{5}{96}$	11	0	19	$-\frac{1}{8}$
4	$\frac{1}{16}$	12	$-\frac{1}{32}$	20	0
5	$-\frac{1}{32}$	13	$\frac{1}{8}$	21	0
6	$-\frac{1}{8}$	14	$\frac{1}{8}$	22	$\frac{1}{32}$
7	$-\frac{1}{48}$	—	—	23	$\frac{3}{128}$
8	0	16	$\frac{1}{64}$	24	$-\frac{3}{16}$

Table 6.2: $\Gamma^{SU(3)}$ coefficients.

Note that each of the five $SU(2)$ monomials, indicated in the last column of Table 3.2, possesses a vanishing Γ coefficient. In other words, those terms are not needed to absorb infinities. As pointed out before, the $SU(2)$ version of Eq. (3.11), i.e., the WZW action with traceless external fields, does not include any contributions to purely strong or e.m. processes. Recall once more that while the former type does not occur in nature, the latter is realized. These reactions can only be described within the extension discussed at the end of Chapter 3.

6.5 Renormalization of the extension

By introducing non-traceless external vector fields, $\tilde{L}_\mu$ and $\tilde{R}_\mu$, into the WZW term, additional contributions which include the building block $\langle \tilde{F}^+_{\alpha\beta} \rangle = \frac{2iN_f}{3} v^{(s)}_{\mu\nu}$ are generated

among the one-loop infinities,

$$
\begin{aligned}
&-\frac{\int dx}{16\pi^2(d-4)}\frac{-iN_c\varepsilon^{\mu\nu\alpha\beta}}{24\pi^2F_0^2}\langle d^\lambda\Gamma_{\lambda\mu}\Delta_\nu\rangle\langle\tilde{F}^+_{\alpha\beta}\rangle \\
&= -\frac{\int dx}{16\pi^2(d-4)}\frac{iN_c\varepsilon^{\mu\nu\alpha\beta}}{24\pi^2F_0^2}\langle\tilde{F}^+_{\alpha\beta}\rangle\times \\
&\quad \Big\{2\langle d^\lambda\Delta_\lambda\Delta_\mu\Delta_\nu\rangle+\langle d^\lambda\Delta_\mu\Delta_\nu\Delta_\lambda\rangle-\langle d^\lambda\Delta_\mu\Delta_\lambda\Delta_\nu\rangle+\frac{i}{4}\langle(D^\lambda G_{\lambda\mu})_+\Delta_\nu\rangle\Big\} \\
&= -\frac{\int dx}{16\pi^2(d-4)}\frac{iN_c\varepsilon^{\mu\nu\alpha\beta}}{24\pi^2F_0^2}\frac{2iN_f}{3}v^{(s)}_{\alpha\beta}\times \\
&\quad \Big\{\frac{1}{32}\langle(D_\lambda D^\lambda U)_-(D_\mu U)_-(D_\nu U)_-\rangle+\frac{1}{64}\langle(D_\lambda D_\mu U)_-(D_\nu U)_-(D^\lambda U)_-\rangle \\
&- \frac{1}{64}\langle(D_\lambda D_\mu U)_-(D^\lambda U)_-(D_\nu U)_-\rangle+\frac{i}{16}\langle(D^\lambda G_{\lambda\mu})_+(D_\nu U)_-\rangle\Big\} \\
&= -\frac{\int dx}{16\pi^2(d-4)}\frac{N_f}{12\pi^2F_0^2}\left\{-\frac{1}{64}(1')-\frac{1}{96}(4')-\frac{1}{16}(5')\right\}. \qquad (6.43)
\end{aligned}
$$

The last line, which has been rewritten in terms of our final structures, enables us to identify the respective non-vanishing Γ coefficients:

$$
\Gamma_{1'}=-\frac{N_f}{768\pi^2F_0}\,,\quad \Gamma_{4'}=-\frac{N_f}{1152\pi^2F_0}\,,\quad \Gamma_{5'}=-\frac{N_f}{192\pi^2F_0}\,. \qquad (6.44)
$$

Let us stress again that although the entire extension program is of particular importance to the $SU(2)$ theory, the above outcome is valid for any flavour number N_f (or n).

Chapter 7

Assignment of LECs to measurable processes

According to Chapter 3, our final $SU(3)$ Lagrangian density $\mathcal{L}_{6,\varepsilon}$ comprises 23 presumably independent monomials and therefore 23 LECs. As mentioned before, the latter play the role of unknown parameters whose (renormalized) values cannot be predicted by ChPT itself but have to be determined (at a certain energy scale μ) via experimental measurements and/or within other theoretical formalisms.[1]

The only thing we can do in ChPT is to follow again Gasser and Leutwyler's example [13] and find out which specific processes are related to which LECs and how the associated contributions, i.e., Feynman rules, do look like. Since our structures are all written in terms of compact building blocks, at first glance we can hardly tell. In what follows this question is answered by expanding our blocks.

When examining exclusive processes theorists and especially experimentalists are primarily interested in reactions with very few particles (as few as possible). Let us therefore concentrate on those.

It would be very nice, if we could readily find a sufficient number of different measurable (or already measured) processes giving access to the values of all 23 LECs. Unfortunately, matters are not that simple. From the experimentalist's point of view, those reactions must not have too tiny differential cross sections. On the other hand, from the theorist's perspective, the calculational effort should not exceed a certain extent. As a first step, the present chapter deals with the formal determination of 13 LECs which are involved in reactions with least particle numbers.

[1] In Chapter 8, a rather simple but commonly used model which additionally includes vector meson degrees of freedom will be discussed in more detail. A related approach can be found in [18]. There, Bijnens *et al.* developed an effective $O(p^6)$ Lagrangian by integrating those vector mesons out. Observe that the problem may also be addressed by considering large N_c arguments [59].

7.1 Electromagnetic external fields

Start out by systematically investigating the leading-order expansion of our building blocks in powers of Goldstone boson fields ϕ, quark masses $\chi = 2B_0 M$, and e.m. fields A_μ. To this end, one must set $L_\mu = R_\mu = -eA_\mu Q$ and $\chi = \chi^\dagger$, where the $SU(3)$ quark mass matrix $M = \mathrm{diag}(m_u, m_d, m_s)$, the electric charge $e > 0$, and the $SU(3)$ quark charge matrix $Q = \mathrm{diag}(\frac{2}{3}, -\frac{1}{3}, -\frac{1}{3})$ have been introduced. Weak interactions are examined afterwards (less systematically). Observe that it is more convenient to work with the $[\cdots]_\pm$ brackets at this point:

$$\begin{aligned}
[\chi]_+ &= \chi - \frac{i}{2F_0}[\chi,\phi] + O(\chi,\phi^2), \\
[\chi]_- &= -\frac{i}{2F_0}\{\chi,\phi\} + O(\chi,\phi^2), \\
[D_\mu U]_- &= \frac{i}{F_0}\partial_\mu\phi - \frac{e}{F_0}A_\mu[Q,\phi] + O(\phi^2), \\
[D_\mu D_\nu U]_-^{(s)} &= \frac{i}{F_0}\partial_\mu\partial_\nu\phi + O(A,\phi), \\
[G_{\mu\nu}]_+ &= -2eF_{\mu\nu}Q + O(A,\phi), \\
[H_{\mu\nu}]_+ &= -\frac{ie}{F_0}F_{\mu\nu}[Q,\phi] + O(A,\phi^2), \\
[D_\alpha G_{\mu\nu}]_+ &= -2e\partial_\alpha F_{\mu\nu}Q + O(A,\phi), \\
[D_\alpha H_{\mu\nu}]_+ &= -\frac{ie}{F_0}\partial_\alpha F_{\mu\nu}[Q,\phi] + O(A,\phi^2).
\end{aligned} \tag{7.1}$$

Respecting the very first (lowest-order) terms of (7.1), we can roughly classify all elements of our monomial set in the following way. Remember that purely e.m. fields do only give rise to odd powers in ϕ.

reaction type	LECs
$\phi + 2\gamma^*$	$3, 8, 9, 19$
$3\phi + \gamma^*$	$1, 2, 5, 6, 7, 13, 14$
$3\phi + 2\gamma^*$	$10, 11, 20, 21, 22, 23, 24$
5ϕ	$4, 12$
$5\phi + \gamma^*$	$16, 17, 18$

Table 7.1: Classification of $SU(3)$ LECs according to their leading-order contribution allowing at most e.m. external fields; the photons may be either virtual or real. This classification defines the ordering scheme in Table 3.2.

Our actual intension is to prepare the determination of some of our LECs. Thus for any envisaged reaction the exact mathematical expressions which originate from the involved monomials need to be worked out. The associated LECs can then be brought

in line with the respective experimental data. Note that $3\phi + 2\gamma^*$ can, in principle, receive non-leading-order contributions from all LECs listed in the first and second line of Table 7.1 (an analogous situation holds for $5\phi + \gamma^*$). Therefore, a restriction to $\phi + 2\gamma^*$, $3\phi + \gamma^*$, and 5ϕ seems to be reasonable in order to render the computations manageable.

7.1.1 The $\phi + 2\gamma^*$ class

As expected, the e.m. reaction type with the least number of Goldstone bosons turns out to be $\phi + 2\gamma^*$:

$$\begin{aligned}
\mathcal{L}_{6,\varepsilon}^{\phi+2\gamma^*} = & - \frac{32ie^2B_0}{F_0}\mathbf{L}_{\mathbf{8}}^{\mathbf{6},\varepsilon}F_{\alpha\beta}F_{\gamma\delta}\langle\{M,\phi\}Q^2\rangle\varepsilon^{\alpha\beta\gamma\delta} \\
& - \frac{32ie^2B_0}{F_0}\mathbf{L}_{\mathbf{9}}^{\mathbf{6},\varepsilon}F_{\alpha\beta}F_{\gamma\delta}\langle\{M,\phi\}\rangle\langle Q^2\rangle\varepsilon^{\alpha\beta\gamma\delta} \\
& + \frac{32ie^2}{F_0}\mathbf{L}_{\mathbf{19}}^{\mathbf{6},\varepsilon}\partial^\mu F_{\mu\alpha}F_{\beta\gamma}\langle\{Q^2,\partial_\delta\phi\}\rangle\varepsilon^{\alpha\beta\gamma\delta}. \qquad (7.2)
\end{aligned}$$

Although, according to its blocks, $\mathbf{L}_{\mathbf{3}}^{\mathbf{6},\varepsilon}$ formally belongs to the same subset as $\mathbf{L}_{\mathbf{8}}^{\mathbf{6},\varepsilon}$, $\mathbf{L}_{\mathbf{9}}^{\mathbf{6},\varepsilon}$, and $\mathbf{L}_{\mathbf{19}}^{\mathbf{6},\varepsilon}$, it happens to give no contribution to this class. With the assumption of isospin invariance ($m := m_u = m_d \neq m_s$) the evaluation of the above traces yields

$$\mathcal{L}_{6,\varepsilon}^{\pi^0+2\gamma^*} = - \frac{64ie^2mB_0}{3F_0}\mathbf{L}_{\mathbf{8}}^{\mathbf{6},\varepsilon}\pi^0F_{\alpha\beta}F_{\gamma\delta}\varepsilon^{\alpha\beta\gamma\delta} + \frac{64ie^2}{3F_0}\mathbf{L}_{\mathbf{19}}^{\mathbf{6},\varepsilon}\partial^\mu F_{\mu\alpha}F_{\beta\gamma}\partial_\delta\pi^0\varepsilon^{\alpha\beta\gamma\delta}, \qquad (7.3)$$

$$\begin{aligned}
\mathcal{L}_{6,\varepsilon}^{\eta_8+2\gamma^*} = & - \frac{64ie^2B_0}{9\sqrt{3}F_0}\{\mathbf{L}_{\mathbf{8}}^{\mathbf{6},\varepsilon}(5m-2m_s) + 12\mathbf{L}_{\mathbf{9}}^{\mathbf{6},\varepsilon}(m-m_s)\}\eta_8F_{\alpha\beta}F_{\gamma\delta}\varepsilon^{\alpha\beta\gamma\delta} \\
& + \frac{64ie^2}{3\sqrt{3}F_0}\mathbf{L}_{\mathbf{19}}^{\mathbf{6},\varepsilon}\partial^\mu F_{\mu\alpha}F_{\beta\gamma}\partial_\delta\eta_8\varepsilon^{\alpha\beta\gamma\delta}. \qquad (7.4)
\end{aligned}$$

As all momenta are meant to flow into the vertex, the corresponding Feynman rules (for details see [60] or [61]) are respectively given by

$$\left(\frac{512e^2}{3F_0}\mathbf{L}_{\mathbf{8}}^{\mathbf{6},\varepsilon}B_0m + \frac{128e^2}{3F_0}\mathbf{L}_{\mathbf{19}}^{\mathbf{6},\varepsilon}(q_1^2+q_2^2)\right)\mathcal{A}, \qquad (7.5)$$

$$\left(\frac{512e^2}{9\sqrt{3}F_0}\{\mathbf{L}_{\mathbf{8}}^{\mathbf{6},\varepsilon}(5m-2m_s) + 12\mathbf{L}_{\mathbf{9}}^{\mathbf{6},\varepsilon}(m-m_s)\}B_0 + \frac{128e^2}{3\sqrt{3}F_0}\mathbf{L}_{\mathbf{19}}^{\mathbf{6},\varepsilon}(q_1^2+q_2^2)\right)\mathcal{A}, \qquad (7.6)$$

where the abbreviation $\mathcal{A} := q_1^\alpha q_2^\beta \varepsilon_1^\gamma \varepsilon_2^\delta \varepsilon_{\alpha\beta\gamma\delta}$ has been introduced; the momenta q_i and the polarization vectors $\varepsilon_i, i \in \{1,2\}$, refer to either of the two photons.

At this point we clearly see that $\pi^0 + 2\gamma^*$ allows the determination of two LECs, namely $\mathbf{L_8^{6,\varepsilon}}$ within the real photon decay and $\mathbf{L_{19}^{6,\varepsilon}}$ when at least one virtual photon is involved. The remaining $\mathbf{L_9^{6,\varepsilon}}$ may then be obtained from the η decay.[2]

7.1.2 The $3\phi + \gamma^*$ class

The next reaction type to be considered is $3\phi + \gamma^*$. Since in the subsequent chapter we will be performing a full one-loop calculation for the 'process' $K^+ + K^- + \pi^0 + \gamma^*$, which evidently belongs to this very class, a careful enquiry of things at the present stage will pay later. The respective Langrangian density reads

$$\begin{aligned}
\mathcal{L}_{6,\varepsilon}^{3\phi+\gamma^*} = & - \frac{32ieB_0}{F_0^3}\mathbf{L_1^{6,\varepsilon}} F_{\alpha\beta}\langle M\{[\phi,Q]\partial_\gamma\phi\partial_\delta\phi + \partial_\gamma\phi\partial_\delta\phi[\phi,Q]\}\rangle\varepsilon^{\alpha\beta\gamma\delta} \\
& - \frac{32ieB_0}{F_0^3}\mathbf{L_2^{6,\varepsilon}} F_{\beta\gamma}\langle M\partial_\alpha\phi\rangle\langle[\phi,Q]\partial_\delta\phi\rangle\varepsilon^{\alpha\beta\gamma\delta} \\
& - \frac{32ieB_0}{F_0^3}\mathbf{L_5^{6,\varepsilon}} F_{\alpha\beta}\langle\{M,\phi\}(Q\partial_\gamma\phi\partial_\delta\phi - \partial_\gamma\phi\partial_\delta\phi Q)\rangle\varepsilon^{\alpha\beta\gamma\delta} \\
& - \frac{32ieB_0}{F_0^3}\mathbf{L_6^{6,\varepsilon}} F_{\alpha\beta}\langle\{M,\phi\}\partial_\gamma\phi Q\partial_\delta\rangle\varepsilon^{\alpha\beta\gamma\delta} \\
& - \frac{32ieB_0}{F_0^3}\mathbf{L_7^{6,\varepsilon}} F_{\alpha\beta}\langle\{M,\phi\}\rangle\langle Q\partial_\gamma\phi\partial_\delta\phi\rangle\varepsilon^{\alpha\beta\gamma\delta} \\
& + \frac{32ie}{F_0^3}\mathbf{L_{13}^{6,\varepsilon}} F_{\mu\alpha}\langle Q(\partial^\mu\partial_\beta\phi\partial_\gamma\phi\partial_\delta\phi - \partial_\gamma\phi\partial_\delta\phi\partial^\mu\partial_\beta\phi)\rangle\varepsilon^{\alpha\beta\gamma\delta} \\
& + \frac{32ie}{F_0^3}\mathbf{L_{14}^{6,\varepsilon}} F_{\alpha\beta}\langle Q(\partial_\mu\partial_\gamma\phi\partial^\mu\phi\partial_\delta\phi - \partial_\delta\phi\partial^\mu\phi\partial_\mu\partial_\gamma\phi)\rangle\varepsilon^{\alpha\beta\gamma\delta}. \qquad (7.7)
\end{aligned}$$

In assuming only incoming momenta, the Mandelstam variables are given by

$$\begin{aligned}
& s = (q+p_1)^2 = (p_2+p_3)^2, \\
& t = (q+p_3)^2 = (p_1+p_2)^2, \\
& u = (q+p_2)^2 = (p_1+p_3)^2, \\
\Rightarrow \quad & s+t+u = m_1^2+m_2^2+m_3^2+q^2, \qquad (7.8)
\end{aligned}$$

where u may be chosen to be dependent. All possible mixed scalar products can then be expressed in terms of the remaining (independent) Mandelstam variables s and t as well as the photon four-momentum squared and the boson masses:

$$q\cdot p_1 = \frac{s-q^2-m_1^2}{2},$$

[2] Since the physical η and η' are mixtures of the octet η_8 and singlet η_1, more (phenomenological) input is needed to relate $\mathbf{L_{19}^{6,\varepsilon}}$ to the η decay.

$$
\begin{aligned}
p_2\cdot p_3 &= \frac{s-m_2^2-m_3^2}{2}\,,\\
q\cdot p_3 &= \frac{s-q^2-m_3^2}{2}\,,\\
p_1\cdot p_2 &= \frac{s-m_1^2-m_2^2}{2}\,,\\
q\cdot p_2 &= \frac{-s-t+m_1^2+m_3^2}{2}\,,\\
p_1\cdot p_3 &= \frac{-s-t+q^2+m_2^2}{2}\,.
\end{aligned}
\tag{7.9}
$$

After carrying out the traces (with the aid of Mathematica or similar software), one finds seven different specific reactions, or to be more precise, reaction subtypes. First of all[3]

$$
\begin{aligned}
\mathcal{L}_{6,\varepsilon}^{\pi^+\pi^-\pi^0\gamma^*} = \quad & \frac{128iemB_0}{3F_0^3}(2\mathbf{L_5^{6,\varepsilon}}+\mathbf{L_6^{6,\varepsilon}})F_{\alpha\beta}\left\{\partial_\gamma\pi^0(\pi^+\partial_\delta\pi^- - \pi^-\partial_\delta\pi^+)\right.\\
& \qquad \left. - \pi^0\partial_\gamma\pi^+\partial_\delta\pi^-\right\}\varepsilon^{\alpha\beta\gamma\delta}\\
+ \quad & \frac{128ie}{3F_0^3}\mathbf{L_{13}^{6,\varepsilon}}F_{\mu\alpha}\{\partial_\beta\pi^0(\partial^\mu\partial_\gamma\pi^+\partial_\delta\pi^- - \partial^\mu\partial_\gamma\pi^-\partial_\delta\pi^+)\\
& \qquad +\partial^\mu\partial_\beta\pi^0\partial_\gamma\pi^+\partial_\delta\pi^-\}\varepsilon^{\alpha\beta\gamma\delta}\\
+ \quad & \frac{64ie}{3F_0^3}\mathbf{L_{14}^{6,\varepsilon}}F_{\alpha\beta}\{\partial_\mu\partial_\gamma\pi^0(\partial^\mu\pi^+\partial_\delta\pi^- - \partial^\mu\pi^-\partial_\delta\pi^+)\\
& \qquad -\partial_\mu\pi^0(\partial^\mu\partial_\gamma\pi^+\partial_\delta\pi^- - \partial^\mu\partial_\gamma\pi^-\partial_\delta\pi^+)\\
& \qquad -\partial_\gamma\pi^0(\partial_\mu\partial_\delta\pi^+\partial^\mu\pi^- - \partial_\mu\partial_\delta\pi^-\partial^\mu\pi^+)\}\varepsilon^{\alpha\beta\gamma\delta},
\end{aligned}
\tag{7.10}
$$

from which one can very easily derive the associated Feynman rule

$$
\left(\frac{256ie}{F_0^3}\{2\mathbf{L_5^{6,\varepsilon}}+\mathbf{L_6^{6,\varepsilon}}+\mathbf{L_{14}^{6,\varepsilon}}\}B_0m - \frac{128ie}{3F_0^3}\{\mathbf{L_{13}^{6,\varepsilon}}+\mathbf{L_{14}^{6,\varepsilon}}\}q^2\right)\mathcal{A}. \tag{7.11}
$$

Note that this time $\mathcal{A} := \varepsilon^\alpha p_1^\beta p_2^\gamma p_3^\delta \varepsilon_{\alpha\beta\gamma\delta}$ has been set for notational convenience. The momenta p_1, p_2, and p_3 refer to the π^+, π^-, and π^0, respectively.

The second process, which will be subject of the next chapter, is provided by the Lagrangian

$$
\mathcal{L}_{6,\varepsilon}^{K^+K^-\pi^0\gamma^*} = \quad - \quad \frac{64ieB_0}{3F_0^3}\{3\mathbf{L_1^{6,\varepsilon}}(m-m_s) - (\mathbf{L_5^{6,\varepsilon}}+2\mathbf{L_6^{6,\varepsilon}})(m+m_s)\}\times
$$

[3]This subtype does, of course, include several distinct physical processes, such as $\gamma^* \to \pi^+ + \pi^- + \pi^0$ or $\gamma^* + \pi^\pm \to \pi^\pm + \pi^0$. The photon may be virtual or real. In the former case it can, e.g., be created through e^+e^- annihilation, $q^2 > 4m_e^2$, or electron scattering, $q^2 < 0$.

$$
\begin{aligned}
& F_{\alpha\beta}\partial_\gamma\pi^0(K^+\partial_\delta K^- - K^-\partial_\delta K^+)\varepsilon^{\alpha\beta\gamma\delta} \\
- \quad & \frac{128iemB_0}{3F_0^3}(4\mathbf{L_5^{6,\varepsilon}} - \mathbf{L_6^{6,\varepsilon}})F_{\alpha\beta}\pi^0\partial_\gamma K^+\partial_\delta K^-\varepsilon^{\alpha\beta\gamma\delta} \\
+ \quad & \frac{64ie}{3F_0^3}\mathbf{L_{13}^{6,\varepsilon}}F_{\mu\alpha}\{\partial_\beta\pi^0(\partial^\mu\partial_\gamma K^+\partial_\delta K^- - \partial^\mu\partial_\gamma K^-\partial_\delta K^+) \\
& \qquad +4\partial^\mu\partial_\beta\pi^0\partial_\gamma K^+\partial_\delta K^-\}\varepsilon^{\alpha\beta\gamma\delta} \\
+ \quad & \frac{64ie}{3F_0^3}\mathbf{L_{14}^{6,\varepsilon}}F_{\alpha\beta}\{2\partial_\mu\partial_\gamma\pi^0(\partial^\mu K^+\partial_\delta K^- - \partial^\mu K^-\partial_\delta K^+) \\
& \qquad +\partial_\mu\pi^0(\partial^\mu\partial_\gamma K^+\partial_\delta K^- - \partial^\mu\partial_\gamma K^-\partial_\delta K^+) \\
& \qquad -2\partial_\gamma\pi^0(\partial_\mu\partial_\delta K^+\partial^\mu K^- - \partial_\mu\partial_\delta K^-\partial^\mu K^+)\}\varepsilon^{\alpha\beta\gamma\delta}
\end{aligned}
\tag{7.12}
$$

and the Feynman rule

$$
\begin{aligned}
& \left(-\frac{256ie}{3F_0^3}\left\{3\mathbf{L_1^{6,\varepsilon}}(m-m_s) - \mathbf{L_5^{6,\varepsilon}}(5m+m_s) - \mathbf{L_6^{6,\varepsilon}}(m+2m_s)\right.\right. \\
& \left.+\frac{3}{4}\mathbf{L_{13}^{6,\varepsilon}}m - \frac{1}{2}\mathbf{L_{14}^{6,\varepsilon}}(5m+4m_s)\right\}B_0 \\
& \left.-\frac{64ie}{3F_0^3}\left\{\frac{5}{2}\mathbf{L_{13}^{6,\varepsilon}} + \mathbf{L_{14}^{6,\varepsilon}}\right\}q^2 + \frac{64ie}{F_0^3}\left\{\frac{1}{2}\mathbf{L_{13}^{6,\varepsilon}} - \mathbf{L_{14}^{6,\varepsilon}}\right\}t\right)\mathcal{A}.
\end{aligned}
\tag{7.13}
$$

The replacement of π^0 by η_8 turns out to yield

$$
\begin{aligned}
\mathcal{L}_{6,\varepsilon}^{\pi^+\pi^-\eta_8\gamma^*} = \quad & \frac{128ieB_0}{\sqrt{3}F_0^3}\{\mathbf{L_2^{6,\varepsilon}}(m-m_s) + \mathbf{L_6^{6,\varepsilon}}m\} \times \\
& F_{\alpha\beta}\partial_\gamma\eta_8(\pi^+\partial_\delta\pi^- - \pi^-\partial_\delta\pi^+)\varepsilon^{\alpha\beta\gamma\delta} \\
- \quad & \frac{128ieB_0}{\sqrt{3}F_0^3}\{(2\mathbf{L_5^{6,\varepsilon}} - \mathbf{L_6^{6,\varepsilon}})m + 2\mathbf{L_7^{6,\varepsilon}}(m-m_s)\} \times \\
& F_{\alpha\beta}\eta_8\partial_\gamma\pi^+\partial_\delta\pi^-\varepsilon^{\alpha\beta\gamma\delta} \\
+ \quad & \frac{128ie}{\sqrt{3}F_0^3}\mathbf{L_{13}^{6,\varepsilon}}F_{\mu\alpha}\partial^\mu\partial_\beta\eta_8\partial_\gamma\pi^+\partial_\delta\pi^-\varepsilon^{\alpha\beta\gamma\delta} \\
+ \quad & \frac{64ie}{\sqrt{3}F_0^3}\mathbf{L_{14}^{6,\varepsilon}}F_{\alpha\beta}\{\partial_\mu\partial_\gamma\eta_8(\partial^\mu\pi^+\partial_\delta\pi^- - \partial^\mu\pi^-\partial_\delta\pi^+) \\
& \qquad +\partial_\mu\eta_8(\partial^\mu\partial_\gamma\pi^+\partial_\delta\pi^- - \partial^\mu\partial_\gamma\pi^-\partial_\delta\pi^+) \\
& \qquad -\partial_\gamma\eta_8(\partial_\mu\partial_\delta\pi^+\partial^\mu\pi^- - \partial_\mu\partial_\delta\pi^-\partial^\mu\pi^+)\}\varepsilon^{\alpha\beta\gamma\delta}
\end{aligned}
\tag{7.14}
$$

with the Feynman rule

$$
\left(\frac{256ie}{\sqrt{3}F_0^3}\left\{2(\mathbf{L_2^{6,\varepsilon}} + \mathbf{L_7^{6,\varepsilon}})(m-m_s) + (2\mathbf{L_5^{6,\varepsilon}} + \mathbf{L_6^{6,\varepsilon}})m\right.\right.
$$

$$-\frac{1}{6}\mathbf{L}_{\mathbf{13}}^{\mathbf{6},\varepsilon}(m+2m_s)+2\mathbf{L}_{\mathbf{14}}^{\mathbf{6},\varepsilon}m\Big\}B_0$$
$$-\frac{64ie}{\sqrt{3}F_0^3}\mathbf{L}_{\mathbf{13}}^{\mathbf{6},\varepsilon}q^2+\frac{64ie}{\sqrt{3}F_0^3}\left\{\mathbf{L}_{\mathbf{13}}^{\mathbf{6},\varepsilon}-2\mathbf{L}_{\mathbf{14}}^{\mathbf{6},\varepsilon}\right\}t\Bigg)\mathcal{A}, \tag{7.15}$$

and

$$\begin{aligned}
\mathcal{L}_{6,\varepsilon}^{K^+K^-\eta_8\gamma^*} = & -\frac{64ieB_0}{\sqrt{3}F_0^3}\{(3\mathbf{L}_{\mathbf{1}}^{\mathbf{6},\varepsilon}-2\mathbf{L}_{\mathbf{2}}^{\mathbf{6},\varepsilon})(m-m_s)-\mathbf{L}_{\mathbf{5}}^{\mathbf{6},\varepsilon}(m+m_s)\}\times \\
& \qquad F_{\alpha\beta}\partial_\gamma\eta_8(K^+\partial_\delta K^- - K^-\partial_\delta K^+)\varepsilon^{\alpha\beta\gamma\delta} \\
& -\frac{128ieB_0}{3\sqrt{3}F_0^3}\{2(2\mathbf{L}_{\mathbf{5}}^{\mathbf{6},\varepsilon}+3\mathbf{L}_{\mathbf{7}}^{\mathbf{6},\varepsilon})(m-m_s)-\mathbf{L}_{\mathbf{6}}^{\mathbf{6},\varepsilon}(m-4m_s)\}\times \\
& \qquad F_{\alpha\beta}\eta_8\partial_\gamma K^+\partial_\delta K^-\varepsilon^{\alpha\beta\gamma\delta} \\
& +\frac{64ie}{\sqrt{3}F_0^3}\mathbf{L}_{\mathbf{13}}^{\mathbf{6},\varepsilon}F_{\mu\alpha}\partial_\beta\eta_8(\partial^\mu\partial_\gamma K^+\partial_\delta K^- - \partial^\mu\partial_\gamma K^-\partial_\delta K^+)\varepsilon^{\alpha\beta\gamma\delta} \\
& -\frac{64ie}{\sqrt{3}F_0^3}\mathbf{L}_{\mathbf{14}}^{\mathbf{6},\varepsilon}F_{\alpha\beta}\partial_\mu\eta_8(\partial^\mu\partial_\gamma K^+\partial_\delta K^- - \partial^\mu\partial_\gamma K^-\partial_\delta K^+)\varepsilon^{\alpha\beta\gamma\delta}
\end{aligned} \tag{7.16}$$

inducing

$$\begin{aligned}
&\Bigg(-\frac{256ie}{3\sqrt{3}F_0^3}\Big\{3[3\mathbf{L}_{\mathbf{1}}^{\mathbf{6},\varepsilon}-2(\mathbf{L}_{\mathbf{2}}^{\mathbf{6},\varepsilon}+\mathbf{L}_{\mathbf{7}}^{\mathbf{6},\varepsilon})](m-m_s)+\mathbf{L}_{\mathbf{5}}^{\mathbf{6},\varepsilon}(m-7m_s) \\
&+\mathbf{L}_{\mathbf{6}}^{\mathbf{6},\varepsilon}(m-4m_s)-\frac{1}{4}\{\mathbf{L}_{\mathbf{13}}^{\mathbf{6},\varepsilon}+2\mathbf{L}_{\mathbf{14}}^{\mathbf{6},\varepsilon}\}(m+2m_s)\Big\}B_0 \\
&-\frac{32ie}{\sqrt{3}F_0^3}\{\mathbf{L}_{\mathbf{13}}^{\mathbf{6},\varepsilon}+2\mathbf{L}_{\mathbf{14}}^{\mathbf{6},\varepsilon}\}q^2-\frac{32ie}{\sqrt{3}F_0^3}\left\{\mathbf{L}_{\mathbf{13}}^{\mathbf{6},\varepsilon}-2\mathbf{L}_{\mathbf{14}}^{\mathbf{6},\varepsilon}\right\}t\Bigg)\mathcal{A}.
\end{aligned} \tag{7.17}$$

The so far collected formulae suffice to formally fix all concerned LECs individually, apart from $\mathbf{L}_{\mathbf{2}}^{\mathbf{6},\varepsilon}$ and $\mathbf{L}_{\mathbf{7}}^{\mathbf{6},\varepsilon}$ where one can only determine the sum. This can be seen from the present discussion and will become even more evident in the final part of the next chapter. As a consequence, the remaining subtypes, which all include neutral kaons, can be numerically predicted.

We have

$$\begin{aligned}
\mathcal{L}_{6,\varepsilon}^{K^0\bar{K}^0\pi^0\gamma^*} = & \quad \frac{64ie(m+m_s)B_0}{3F_0^3}(2\mathbf{L}_{\mathbf{5}}^{\mathbf{6},\varepsilon}+\mathbf{L}_{\mathbf{6}}^{\mathbf{6},\varepsilon})\times \\
& \qquad F_{\alpha\beta}\partial_\gamma\pi^0(K^0\partial_\delta\bar{K}^0-\bar{K}^0\partial_\delta K^0)\varepsilon^{\alpha\beta\gamma\delta} \\
& -\frac{128iemB_0}{3F_0^3}(2\mathbf{L}_{\mathbf{5}}^{\mathbf{6},\varepsilon}+\mathbf{L}_{\mathbf{6}}^{\mathbf{6},\varepsilon})F_{\alpha\beta}\pi^0\partial_\gamma K^0\partial_\delta\bar{K}^0\varepsilon^{\alpha\beta\gamma\delta}
\end{aligned}$$

$$
\begin{aligned}
&+ \quad \frac{128ie}{3F_0^3}\mathbf{L}_{\mathbf{13}}^{\mathbf{6},\varepsilon}F_{\mu\alpha}\{\partial_\beta\pi^0(\partial^\mu\partial_\gamma K^0\partial_\delta\bar{K}^0-\partial^\mu\partial_\gamma\bar{K}^0\partial_\delta K^0)\\
&\qquad\qquad +\partial^\mu\partial_\beta\pi^0\partial_\gamma K^0\partial_\delta\bar{K}^0\}\varepsilon^{\alpha\beta\gamma\delta}\\
&+ \quad \frac{64ie}{3F_0^3}\mathbf{L}_{\mathbf{14}}^{\mathbf{6},\varepsilon}F_{\alpha\beta}\{\partial_\mu\partial_\gamma\pi^0(\partial^\mu K^0\partial_\delta\bar{K}^0-\partial^\mu\bar{K}^0\partial_\delta K^0)\\
&\qquad\qquad -\partial_\mu\pi^0(\partial^\mu\partial_\gamma K^0\partial_\delta\bar{K}^0-\partial^\mu\partial_\gamma\bar{K}^0\partial_\delta K^0)\\
&\qquad\qquad -\partial_\gamma\pi^0(\partial_\mu\partial_\delta K^0\partial^\mu\bar{K}^0-\partial_\mu\partial_\delta\bar{K}^0\partial^\mu K^0)\}\varepsilon^{\alpha\beta\gamma\delta}
\end{aligned}
\tag{7.18}
$$

with the Feynman rule

$$
\left(\frac{256ie}{3F_0^3}\{2\mathbf{L}_{\mathbf{5}}^{\mathbf{6},\varepsilon}+\mathbf{L}_{\mathbf{6}}^{\mathbf{6},\varepsilon}+\mathbf{L}_{\mathbf{14}}^{\mathbf{6},\varepsilon}\}B_0(2m+m_s)-\frac{128ie}{3F_0^3}\{\mathbf{L}_{\mathbf{13}}^{\mathbf{6},\varepsilon}+\mathbf{L}_{\mathbf{14}}^{\mathbf{6},\varepsilon}\}q^2\right)\mathcal{A}, \tag{7.19}
$$

and

$$
\begin{aligned}
\mathcal{L}_{6,\varepsilon}^{K^0+\bar{K}^0+\eta_8+\gamma^*} = &- \quad \frac{64ie(m+m_s)B_0}{\sqrt{3}F_0^3}(2\mathbf{L}_{\mathbf{5}}^{\mathbf{6},\varepsilon}+\mathbf{L}_{\mathbf{6}}^{\mathbf{6},\varepsilon})\times\\
&\qquad\qquad F_{\alpha\beta}\partial_\gamma\eta_8(K^0\partial_\delta\bar{K}^0-\bar{K}^0\partial_\delta K^0)\varepsilon^{\alpha\beta\gamma\delta}\\
&+ \quad \frac{128ieB_0}{3\sqrt{3}F_0^3}\{2\mathbf{L}_{\mathbf{5}}^{\mathbf{6},\varepsilon}(m+2m_s)+\mathbf{L}_{\mathbf{6}}^{\mathbf{6},\varepsilon}(m+2m_s)\}\times\\
&\qquad\qquad F_{\alpha\beta}\eta_8\partial_\gamma K^0\partial_\delta\bar{K}^0\varepsilon^{\alpha\beta\gamma\delta}\\
&- \quad \frac{128ie}{\sqrt{3}F_0^3}\mathbf{L}_{\mathbf{13}}^{\mathbf{6},\varepsilon}F_{\mu\alpha}\{\partial_\beta\eta_8(\partial^\mu\partial_\gamma K^0\partial_\delta\bar{K}^0-\partial^\mu\partial_\gamma\bar{K}^0\partial_\delta K^0)\\
&\qquad\qquad +\partial^\mu\partial_\beta\eta_8\partial_\gamma K^0\partial_\delta\bar{K}^0\}\varepsilon^{\alpha\beta\gamma\delta}\\
&- \quad \frac{64ie}{\sqrt{3}F_0^3}\mathbf{L}_{\mathbf{14}}^{\mathbf{6},\varepsilon}F_{\alpha\beta}\{\partial_\mu\partial_\gamma\eta_8(\partial^\mu K^0\partial_\delta\bar{K}^0-\partial^\mu\bar{K}^0\partial_\delta K^0)\\
&\qquad\qquad -\partial_\mu\eta_8(\partial^\mu\partial_\gamma K^0\partial_\delta\bar{K}^0-\partial^\mu\partial_\gamma\bar{K}^0\partial_\delta K^0)\\
&\qquad\qquad -\partial_\gamma\eta_8(\partial_\mu\partial_\delta K^0\partial^\mu\bar{K}^0-\partial_\mu\partial_\delta\bar{K}^0\partial^\mu K^0)\}\varepsilon^{\alpha\beta\gamma\delta}
\end{aligned}
\tag{7.20}
$$

leading to

$$
\left(-\frac{256ie}{3\sqrt{3}F_0^3}\{2\mathbf{L}_{\mathbf{5}}^{\mathbf{6},\varepsilon}+\mathbf{L}_{\mathbf{6}}^{\mathbf{6},\varepsilon}+\mathbf{L}_{\mathbf{14}}^{\mathbf{6},\varepsilon}\}B_0(4m+5m_s)+\frac{128ie}{\sqrt{3}F_0^3}\{\mathbf{L}_{\mathbf{13}}^{\mathbf{6},\varepsilon}+\mathbf{L}_{\mathbf{14}}^{\mathbf{6},\varepsilon}\}q^2\right)\mathcal{A}. \tag{7.21}
$$

Finally, one finds

$$
\mathcal{L}_{6,\varepsilon}^{\pi^++K^-+K^0+\gamma^*} = \qquad \frac{64\sqrt{2}ieB_0}{3F_0^3}\{3\mathbf{L}_{\mathbf{1}}^{\mathbf{6},\varepsilon}(m-m_s)-(\mathbf{L}_{\mathbf{5}}^{\mathbf{6},\varepsilon}-\mathbf{L}_{\mathbf{6}}^{\mathbf{6},\varepsilon})(m+m_s)\}\times
$$

$$
\begin{aligned}
& F_{\alpha\beta}(K^-\partial_\gamma\pi^+\partial_\delta K^0 - K^+\partial_\gamma\pi^-\partial_\delta\bar{K}^0)\varepsilon^{\alpha\beta\gamma\delta} \\
+ \quad & \frac{128\sqrt{2}iemB_0}{3F_0^3}(\mathbf{L_5^{6,\varepsilon}} - \mathbf{L_6^{6,\varepsilon}}) \times \\
& F_{\alpha\beta}(\pi^+\partial_\gamma K^-\partial_\delta K^0 - \pi^-\partial_\gamma K^+\partial_\delta\bar{K}^0)\varepsilon^{\alpha\beta\gamma\delta} \\
- \quad & \frac{128\sqrt{2}ie(m+m_s)B_0}{3F_0^3}(\mathbf{L_5^{6,\varepsilon}} - \mathbf{L_6^{6,\varepsilon}}) \times \\
& F_{\alpha\beta}(K^0\partial_\gamma\pi^+\partial_\delta K^- - \bar{K}^0\partial_\gamma\pi^-\partial_\delta K^+)\varepsilon^{\alpha\beta\gamma\delta} \\
- \quad & \frac{64\sqrt{2}ie}{3F_0^3}\mathbf{L_{13}^{6,\varepsilon}}F_{\mu\alpha} \times \\
& \big\{\partial^\mu\partial_\beta\pi^+\partial_\gamma K^-\partial_\delta K^0 - \partial^\mu\partial_\beta\pi^-\partial_\gamma K^+\partial_\delta\bar{K}^0 \\
& -\partial^\mu\partial_\beta K^-\partial_\gamma\pi^+\partial_\delta K^0 + \partial^\mu\partial_\beta K^+\partial_\gamma\pi^-\partial_\delta\bar{K}^0 \\
& -2(\partial^\mu\partial_\beta\, K^0\partial_\gamma\pi^+\partial_\delta K^- - \partial^\mu\partial_\beta\bar{K}^0\partial_\gamma\pi^-\partial_\delta K^+)\big\}\varepsilon^{\alpha\beta\gamma\delta} \\
+ \quad & \frac{64\sqrt{2}ie}{3F_0^3}\mathbf{L_{14}^{6,\varepsilon}}F_{\alpha\beta} \times \\
& \big\{2\partial_\mu K^0(\partial^\mu\partial_\gamma\pi^+\partial_\delta K^- - \partial^\mu\partial_\gamma K^-\partial_\delta\pi^+) \\
& -2\partial_\mu\bar{K}^0(\partial^\mu\partial_\gamma\pi^-\partial_\delta K^+ - \partial^\mu\partial_\gamma K^+\partial_\delta\pi^-) \\
& -\partial_\mu\pi^+(\partial^\mu\partial_\gamma K^-\partial_\delta K^0 - \partial^\mu\partial_\gamma K^0\partial_\delta K^-) \\
& +\partial_\mu\pi^-(\partial^\mu\partial_\gamma K^+\partial_\delta\bar{K}^0 - \partial^\mu\partial_\gamma\bar{K}^0\partial_\delta K^+) \\
& +\partial_\mu K^-(\partial^\mu\partial_\gamma\pi^+\partial_\delta K^0 - \partial^\mu\partial_\gamma K^0\partial_\delta\pi^+) \\
& -\partial_\mu K^+(\partial^\mu\partial_\gamma\pi^-\partial_\delta\bar{K}^0 - \partial^\mu\partial_\gamma\bar{K}^0\partial_\delta\pi^-)\big\}\,\varepsilon^{\alpha\beta\gamma\delta}
\end{aligned}
\tag{7.22}
$$

implying the Feynman rule

$$
\begin{aligned}
\Big(\quad & \frac{128\sqrt{2}ie}{3F_0^3}\{3\mathbf{L_1^{6,\varepsilon}} - \mathbf{L_5^{6,\varepsilon}} + \mathbf{L_6^{6,\varepsilon}}\}B_0(m-m_s) \\
- \quad & \frac{32\sqrt{2}ie}{3F_0^3}\mathbf{L_{13}^{6,\varepsilon}}\,B_0(m+m_s) + \frac{64\sqrt{2}ie}{3F_0^3}\mathbf{L_{14}^{6,\varepsilon}}\,B_0(5m+m_s) \\
+ \quad & \frac{32\sqrt{2}ie}{3F_0^3}\{3\mathbf{L_{13}^{6,\varepsilon}} - 4\mathbf{L_{14}^{6,\varepsilon}}\}s - \frac{64\sqrt{2}ie}{3F_0^3}\mathbf{L_{14}^{6,\varepsilon}}\,t + \frac{32\sqrt{2}ie}{3F_0^3}\{\mathbf{L_{13}^{6,\varepsilon}} + 2\mathbf{L_{14}^{6,\varepsilon}}\}q^2\Big)\;\mathcal{A}.
\end{aligned}
\tag{7.23}
$$

7.1.3 The 5ϕ class

So much for e.m. processes. There are only two structures which survive when sending all external fields to zero ($\rightarrow$ pure QCD)

$$\begin{aligned}\mathcal{L}_{6,\varepsilon}^{5\phi} = &- \frac{32iB_0}{F_0^5}\mathbf{L}_{\mathbf{4}}^{\mathbf{6},\varepsilon}\langle\{M,\phi\}\partial_\alpha\phi\partial_\beta\phi\partial_\gamma\phi\partial_\delta\phi\rangle\varepsilon^{\alpha\beta\gamma\delta} \\ &+ \frac{32i}{F_0^5}\mathbf{L}_{\mathbf{12}}^{\mathbf{6},\varepsilon}\langle\partial^\mu\partial_\alpha\phi\{\partial_\mu\phi\partial_\beta\phi\partial_\gamma\phi\partial_\delta\phi+\partial_\delta\phi\partial_\gamma\phi\partial_\beta\partial_\mu\phi\}\rangle\varepsilon^{\alpha\beta\gamma\delta}. \qquad (7.24)\end{aligned}$$

It would be rather tedious to work out all embodied vertices. In order to 'fix' the two concerned LECs, it is sufficient to consider two appropriate processes:[4]

$$\begin{aligned}\mathcal{L}_{6,\varepsilon}^{\pi^+\pi^-\pi^0K^+K^-} = &- \frac{128iB_0}{F_0^5}\mathbf{L}_{\mathbf{4}}^{\mathbf{6},\varepsilon}\{ \\ &+ 6m(\pi^+\partial_\alpha\pi^- - \pi^-\partial_\alpha\pi^+)\partial_\beta\pi^0\partial_\gamma K^+\partial_\delta K^- \\ &+ 6m\,\pi^0\partial_\alpha\pi^+\partial_\beta\pi^-\partial_\gamma K^+\partial_\delta K^- \\ &+ 3(m+m_s)(K^+\partial_\alpha K^- - K^-\partial_\alpha K^+)\partial_\beta\pi^+\partial_\gamma\pi^-\partial_\delta\pi^0\}\,\varepsilon^{\alpha\beta\gamma\delta} \\ &+ \frac{128i}{F_0^5}\mathbf{L}_{\mathbf{12}}^{\mathbf{6},\varepsilon}\{ \\ &\quad 2(\partial^\mu\partial_\alpha\pi^+\partial_\mu\pi^- - \partial^\mu\partial_\alpha\pi^-\partial_\mu\pi^+)\partial_\beta\pi^0\partial_\gamma K^+\partial_\delta K^- \\ &- 2(\partial^\mu\partial_\alpha\pi^+\partial_\mu\pi^0 - \partial^\mu\partial_\alpha\pi^0\partial_\mu\pi^+)\partial_\beta\pi^-\partial_\gamma K^+\partial_\delta K^- \\ &- 2(\partial^\mu\partial_\alpha\pi^+\partial_\mu K^- - \partial^\mu\partial_\alpha K^-\partial_\mu\pi^+)\partial_\beta\pi^-\partial_\gamma\pi^0\partial_\delta K^+ \\ &+ 2(\partial^\mu\partial_\alpha\pi^-\partial_\mu\pi^0 - \partial^\mu\partial_\alpha\pi^0\partial_\mu\pi^-)\partial_\beta\pi^+\partial_\gamma K^+\partial_\delta K^- \\ &- 2(\partial^\mu\partial_\alpha\pi^-\partial_\mu K^+ - \partial^\mu\partial_\alpha K^+\partial_\mu\pi^-)\partial_\beta\pi^+\partial_\gamma\pi^0\partial_\delta K^- \\ &+ (\partial^\mu\partial_\alpha\pi^0\partial_\mu K^+ - \partial^\mu\partial_\alpha K^+\partial_\mu\pi^0)\partial_\beta\pi^+\partial_\gamma\pi^-\partial_\delta K^- \\ &- (\partial^\mu\partial_\alpha\pi^0\partial_\mu K^- - \partial^\mu\partial_\alpha K^-\partial_\mu\pi^0)\partial_\beta\pi^+\partial_\gamma\pi^-\partial_\delta K^+ \\ &+ 3\,(\partial^\mu\partial_\alpha K^+\partial_\mu K^- - \partial^\mu\partial_\alpha K^-\partial_\mu K^+)\partial_\beta\pi^+\partial_\gamma\pi^-\partial_\delta\pi^0\}\,\varepsilon^{\alpha\beta\gamma\delta}, \\ &\qquad (7.25)\end{aligned}$$

$$\mathcal{L}_{6,\varepsilon}^{2\pi^+2\pi^-\eta_8} = \frac{256i}{\sqrt{3}F_0^5}\mathbf{L}_{\mathbf{12}}^{\mathbf{6},\varepsilon}(\partial^\mu\partial_\alpha\pi^+\partial_\mu\pi^- - \partial^\mu\partial_\alpha\pi^-\partial_\mu\pi^+)\partial_\beta\pi^+\partial_\gamma\pi^-\partial_\delta\eta_8\varepsilon^{\alpha\beta\gamma\delta}. \qquad (7.26)$$

With the temporary definition $\mathcal{A} := p_1^\alpha p_2^\beta p_4^\gamma p_5^\delta\varepsilon_{\alpha\beta\gamma\delta}$, where the particles carry the momenta $\pi^+(p_1),\pi^-(p_2),\pi^0(p_3),K^+(p_4)$, and $K^-(p_5)$, the Feynman rule triggered by

[4] N.B.: Purely pionic reactions do not come out due to invariance under G parity [62]; recall that $m_u = m_d$ has been assumed.

Eq. (7.25) becomes

$$\frac{128B_0}{F_0^5} \quad \Big\{ \quad \mathbf{L_4^{6,\varepsilon}} 3(4m+m_s) - \mathbf{L_{12}^{6,\varepsilon}} \Big(p_3\cdot p_4 + p_3\cdot p_5 + 3p_4\cdot p_5 \\ + \quad 2(p_1\cdot p_2 + p_1\cdot p_3 + p_1\cdot p_5 + p_2\cdot p_3 + p_2\cdot p_4) \Big) \quad \Big\} \mathcal{A}. \qquad (7.27)$$

In the second case, we set $\mathcal{A} := p_1^\alpha p_2^\beta p_3^\gamma p_4^\delta \varepsilon_{\alpha\beta\gamma\delta}$ with the particle momenta $\pi^+(p_1)$, $\pi^+(p_2), \pi^-(p_3), \pi^-(p_4)$, and $\eta_8(p_5)$ and find Eq. (7.26) to induce

$$\frac{512}{\sqrt{3}F_0^5} \mathbf{L_{12}^{6,\varepsilon}} (p_1-p_2)\cdot(p_3-p_4)\mathcal{A}. \qquad (7.28)$$

While the latter expression obviously allows the determination of $\mathbf{L_{12}^{6,\varepsilon}}$, the former gives access to $\mathbf{L_4^{6,\varepsilon}}$ afterwards.

7.2 Weak external fields

Going back over Table 7.1, there is one LEC left, $\mathbf{L_3^{6,\varepsilon}}$, that we wish to fix. One possible option to accomplish this consists in allowing the existence of exactly one[5] weak external field $W_\mu^\pm$. However, we have just jumped over to reactions where structures of even intrinsic parity could also be involved. Since it would be far too ambitious to consistently include this sector as well, we only derive the Lagrangian of the odd part. This way the mechanism of including weak external fields (which might be useful for future projects) is elucidated, although $\mathbf{L_3^{6,\varepsilon}}$ is likely to remain undetermined.

The inclusion of weak fields results in setting

$$L_\mu = -eA_\mu Q - \frac{g_W}{\sqrt{2}}(W_\mu^+ T_+ + W_\mu^- T_-), \quad R_\mu = -eA_\mu Q, \\ \text{with} \quad T_+ = \begin{pmatrix} 0 & \cos(\theta_c) & \sin(\theta_c) \\ 0 & 0 & 0 \\ 0 & 0 & 0 \end{pmatrix}, \quad T_- = \begin{pmatrix} 0 & 0 & 0 \\ \cos(\theta_c) & 0 & 0 \\ \sin(\theta_c) & 0 & 0 \end{pmatrix} \qquad (7.29)$$

Here, θ_c is the so-called Cabibbo angle.

We just present the expansion formulae which we actually need

$$\begin{aligned} [\chi]_+ &= \chi - \frac{i}{2F_0}[\chi,\phi] + O(\chi,\phi^2), \\ [\chi]_- &= -\frac{i}{2F_0}\{\chi,\phi\} + O(\chi,\phi^2), \\ [D_\mu U]_- &= iL_\mu + \frac{i}{F_0}\partial_\mu\phi - \frac{1}{F_0}[\phi,L_\mu] + O(\phi^2), \end{aligned}$$

[5] This constraint is necessary to avoid too tiny decay rates.

$$
\begin{aligned}
[G_{\mu\nu}]_+ &= F^L_{\mu\nu} + \frac{i}{F_0}[\phi, F^L_{\mu\nu}] + O(F,\phi^2), \\
[H_{\mu\nu}]_+ &= -F^L_{\mu\nu} - \frac{i}{F_0}[\phi, F^L_{\mu\nu}] + O(F,\phi^2), \\
[D_\alpha G_{\mu\nu}]_+ &= \partial_\alpha F^L_{\mu\nu} + \frac{i}{2F_0}[\partial_\alpha\phi, F^L_{\mu\nu}] + \frac{i}{F_0}[\phi, \partial_\alpha F^L_{\mu\nu}] + O(F,\phi^2). \qquad (7.30)
\end{aligned}
$$

For the first cluster of LECs we get

$$
\begin{aligned}
\mathcal{L}^{\phi+W+\gamma^*}_{6,\varepsilon} = &- \frac{16ieg_W B_0}{\sqrt{2}F_0}\mathbf{L_3^{6,\varepsilon}} F_{\alpha\beta}\langle[M,\phi][Q,W_{\gamma\delta}]\rangle\varepsilon^{\alpha\beta\gamma\delta} \\
&+ \frac{16ieg_W B_0}{\sqrt{2}F_0}\mathbf{L_8^{6,\varepsilon}} F_{\alpha\beta}\langle\{M,\phi\}\{W_{\gamma\delta},Q\}\rangle\varepsilon^{\alpha\beta\gamma\delta} \\
&- \frac{16ieg_W}{\sqrt{2}F_0}\mathbf{L_{19}^{6,\varepsilon}}\left(\partial^\mu F_{\mu\alpha}\langle Q\{W_{\beta\gamma},\partial_\delta\phi\}\rangle + F_{\beta\gamma}\langle\partial^\mu W_{\mu\alpha}\{Q,\partial_\delta\phi\}\rangle\right)\varepsilon^{\alpha\beta\gamma\delta}.
\end{aligned} \qquad (7.31)
$$

Observe the definition $W_{\mu\nu} := W^+_{\mu\nu}T_+ + W^-_{\mu\nu}T_-$ with $W^\pm_{\mu\nu} := \partial_\mu W^\pm_\nu - \partial_\nu W^\pm_\mu$. This time $\mathbf{L_9^{6,\varepsilon}}$ happens to vanish. Computing the traces in (7.31) yields among other contributions (again, $m = m_u = m_d$)

$$
\begin{aligned}
\mathcal{L}^{K+W+\gamma^*}_{6,\varepsilon} = &\quad \frac{16ieg_W B_0\sin(\theta_c)}{3F_0}\{3\mathbf{L_3^{6,\varepsilon}}(m-m_s) + \mathbf{L_8^{6,\varepsilon}}(m+m_s)\}\times \\
&\qquad F_{\alpha\beta}(K^+W^-_{\gamma\delta} + K^-W^+_{\gamma\delta})\varepsilon^{\alpha\beta\gamma\delta} \\
&- \frac{16ieg_W B_0\sin(\theta_c)}{3F_0}\mathbf{L_{19}^{6,\varepsilon}}\left(F_{\beta\gamma}(\partial^\mu W^+_{\mu\alpha}\partial_\delta K^- + \partial^\mu W^-_{\mu\alpha}\partial_\delta K^+)\right. \\
&\qquad \left. + \partial^\mu F_{\mu\alpha}(W^+_{\beta\gamma}\partial_\delta K^- + W^-_{\beta\gamma}\partial_\delta K^+)\right)\varepsilon^{\alpha\beta\gamma\delta}.
\end{aligned} \qquad (7.32)
$$

Chapter 8

Three-pseudoscalar photon interactions in ChPT

8.1 Preliminaries

So far we have primarily dealt with rather formalistic aspects of the odd intrinsic parity sector up to chiral order $O(p^6)$. Now, we want to turn to some application. Our intension is to verify the general results of the previous chapters within a specific example and determine new LECs. Most of the simple processes with a small number of Goldstone bosons (especially pions) have already been computed [63, 18, 64]. A further doable calculation is $\gamma^*(q)+K^\pm(p_1)\to K^\pm(p_2)+\pi^0(p_3)$. Before focussing on this reaction, let us start with the class of processes it belongs to.

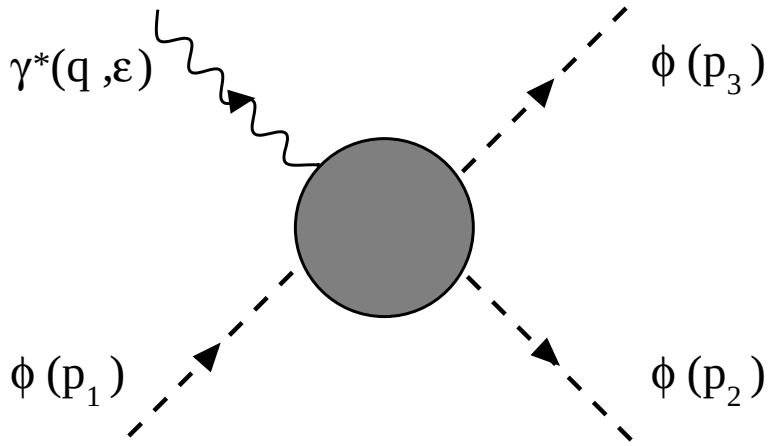

Figure 8.1: General type of reaction : $\gamma^*+3\phi$.

.

Performing a consistent $O(p^6)$ calculation means to consider all (connected) Feynman graphs which have the required external lines and satisfy $D\leq 6$. To stress its

importance, we remind the reader once again of Weinberg's power counting formula

$$D = 2 + \sum_{n=1}^{\infty} 2(n-1)N_{2n} + 2N_L, \tag{8.1}$$

where N_{2n} represents the number of vertices of chiral order $O(p^{2n})$ (at this point we do not distinguish between normal and anomalous vertices) and N_L the number of loops, respectively.

At tree level $(N_L = 0)$, one can have one ε vertex of order $O(p^4)$ $(N_4 = 1)$[1] or $O(p^6)$ $(N_6 = 1)$. At one-loop level $(N_L = 1)$, Eq. (8.1) allows one ε vertex of order $O(p^4)$ and an arbitrary number of vertices from $\mathcal{L}_2$ $(N_2 = 0, 1, 2, \cdots)$.

In expanding the respective Lagrangian densities

$$\begin{aligned} \mathcal{L}_2 &= \mathcal{L}_2^{2\phi+\gamma^*} + \mathcal{L}_2^{4\phi} + \cdots, \\ \mathcal{L}_{WZW} &= \mathcal{L}_{WZW}^{3\phi+\gamma^*} + \mathcal{L}_{WZW}^{5\phi} + \mathcal{L}_{WZW}^{5\phi+\gamma^*} + \cdots, \\ \mathcal{L}_{6,\varepsilon} &= \mathcal{L}_{6,\varepsilon}^{3\phi+\gamma^*} + \cdots, \end{aligned} \tag{8.2}$$

one can extract the relevant parts that generate the needed vertices. Recall that $\mathcal{L}_2$ will only provide vertices with an even number of Goldstone bosons (even power), while the other two Lagrangians will generate odd power vertices.

At tree level there is little danger to miss any of the required contributions. At one-loop level the situation is more subtle. In order to make sure that we include all relevant graphs, let us go ahead in a systematic way using the meanwhile familiar topolocigal relations:

$$\begin{aligned} I - N = N_L - 1 &\overset{N_L=1}{\Longrightarrow} I = N, \\ n_1 + \cdots + n_N &= E + 2I \\ &= 3^* + 2N, \end{aligned} \tag{8.3}$$

where $E(I)$ is again the number of external (internal) Goldstone boson lines, N the total number of vertices, n_i the power of the ith vertex, and N_L the number of loops, respectively. The external photon line has been denoted as a star. We are now able to check out systematically, how many and what kind of vertices are needed for our calculation:

$$\begin{aligned} n_1 &= 5^*, \\ n_1 + n_2 &= 7^* = 2^* + 5 = 4 + 3^*, \\ n_1 + \cdots + n_{N-2} + \underbrace{n_{N-1} + n_N}_{\geq 7^*} &= 3^* + 2N \\ \Rightarrow n_1 + \cdots + n_{N-2} \leq 2(N-2) &\Leftrightarrow n_i \leq 2 \quad \forall i = 1, \cdots, N-2. \end{aligned} \tag{8.4}$$

The latter are no vertices in the proper sense. Therefore, we only have to examine one-loop graphs which involve at most two vertices. The five required types have been noted above and the corresponding Feynman diagrams can be seen below:

[1] Wave function renormalization and corrections to the decay constant must also be included.

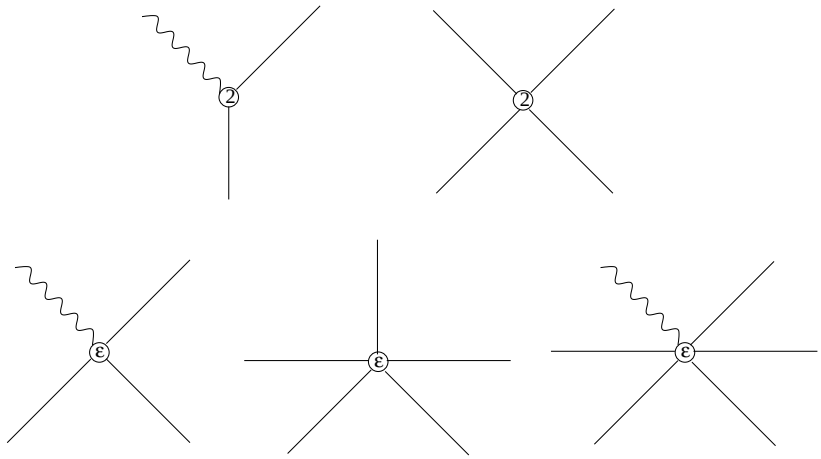

Figure 8.2: Vertices which compose the one-loop graphs. Note that vertices emerging from $\mathcal{L}_2$ are depicted with a 2 in the bubble, while those belonging to $\mathcal{L}_{WZW}$ have got an ε.

8.2 One-loop graphs

Without knowing any functional details of these five elementary vertices, one can still start building up all potential one-loop diagrams by just obeying the topological rules of the game. Differently speaking, we simply need to 'knit' Feynman graphs which have the required four external legs and exactly one loop. Indeed, from a purely topological point of view there are more possible diagrams than actually contribute (compare Fig. 8.3 with Fig. 8.9).

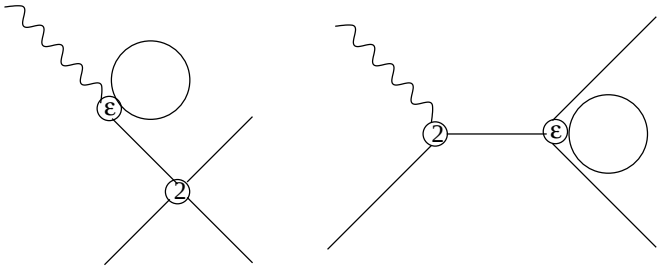

Figure 8.3: Vanishing one-loop graphs.

This is due to the detailed mathematical structure of our five ingredients which we want to carefully work out in the following. To this end, we have to perfom expansions of the kind

$$U \;=\; \exp\left(i\frac{\phi}{F_0}\right) = 1 + \frac{i}{F_0}\phi + \cdots \,,$$

fill in, and collect the needed pieces.

For those diagrams which have an even number of Goldstone bosons (first line in Fig. 8.2) we get

$$\mathcal{L}_2^{2\phi+\gamma^*} = \frac{ie}{2}A_\mu\langle\partial^\mu\phi[Q,\phi]\rangle \tag{8.5}$$

$$\text{and} \qquad \mathcal{L}_2^{4\phi} = \frac{1}{24F_0^2}\langle\partial_\mu\phi[\phi,\partial^\mu\phi]\phi\rangle + \frac{B_0}{24F_0^2}\langle M\phi^4\rangle. \tag{8.6}$$

The second line (depicting the necessary odd power vertices) leads to

$$\mathcal{L}_{WZW}^{3\phi+\gamma^*} = \frac{ieN_c}{24\pi^2F_0^3}A_\alpha\langle Q\partial_\beta\phi\partial_\gamma\phi\partial_\delta\phi\rangle\varepsilon^{\alpha\beta\gamma\delta}, \tag{8.7}$$

$$\mathcal{L}_{WZW}^{5\phi} = \frac{N_c}{240\pi^2F_0^5}\langle\phi\partial_\alpha\phi\partial_\beta\phi\partial_\gamma\phi\partial_\delta\phi\rangle\varepsilon^{\alpha\beta\gamma\delta}, \tag{8.8}$$

and finally

$$\begin{aligned}
\mathcal{L}_{WZW}^{5\phi+\gamma^*} &= -\frac{ieN_c}{288\pi^2F_0^5}A_\alpha\times \\
\Big\langle\ & 3Q([\partial_\beta\phi,\phi][\partial_\gamma\phi,\phi]\partial_\delta\phi + [\partial_\beta\phi,\phi]\partial_\gamma\phi[\partial_\delta\phi,\phi] + \partial_\beta\phi[\partial_\gamma\phi,\phi][\partial_\delta\phi,\phi]) \\
+\ & 2Q(\{\partial_\beta\phi,\phi^2\}\partial_\gamma\phi\partial_\delta\phi + \partial_\beta\phi\{\partial_\gamma\phi,\phi^2\}\partial_\delta\phi + \partial_\beta\phi\partial_\gamma\phi\{\partial_\delta\phi,\phi^2\}) \\
-\ & 4Q(\phi\partial_\beta\phi\phi\partial_\gamma\phi\partial_\delta\phi + \partial_\beta\phi\phi\partial_\gamma\phi\phi\partial_\delta\phi + \partial_\beta\phi\partial_\gamma\phi\phi\partial_\delta\phi\phi)\ \Big\rangle\ \varepsilon^{\alpha\beta\gamma\delta}.
\end{aligned} \tag{8.9}$$

The above Lagrangian densities are not yet written in a suitable form. As we already know, ϕ is a 3×3 matrix collecting the Goldstone boson fields in a compact manner. In order to be able to compute the reaction amplitude, we have to first rewrite ϕ in terms of these fields and some matrices. Actually, there are two different ways to proceed.

One may choose and insert Cartesian (non-physical) fields and conventional Gell-Mann matrices, carry out traces by hand, come to Feynman rules, determine the Cartesian amplitude, and finally go over to the physical one. For pedagogic purposes we illustrate this rather cumbersome method for one very simple vertex.

The second option (which is much more convenient for our computation) consists in using physical fields and 'physical' Gell-Mann matrices from the very beginning and finish up in an analogous way (with the assistance of Mathematica for the traces).

Of course, Mathematica could also simplify our lifes in the former case, but since we want to end up with physical amplitudes, we would always have to perform one additional step, namely the transition from non-physical to physical expressions. Still, one could cross-check our result in that way. Nevertheless, a Cartesian hand-check, which we do at random, seems to be more independent and therefore more reliable.

A more detailed account of the just discussed issues can be found in Appendix D. There, one also encounters the convention that arabic numbers refer to non-physical

and roman to physical objects, respectively. The explicit matrix representation of ϕ,

$$\phi = \sum_{j=1}^{8} \phi_j \lambda_j = \sum_{j=I}^{VIII} \phi_j \lambda_j = \begin{pmatrix} \pi^0 + \frac{1}{\sqrt{3}}\eta_8 & \sqrt{2}\pi^+ & \sqrt{2}K^+ \\ \sqrt{2}\pi^- & -\pi^0 + \frac{1}{\sqrt{3}}\eta_8 & \sqrt{2}K^0 \\ \sqrt{2}K^- & \sqrt{2}\bar{K}^0 & -\frac{2}{\sqrt{3}}\eta_8 \end{pmatrix},$$

obviously contains the physical fields $\phi_I . \cdots, \phi_{VIII}$ being labelled as

$$\begin{aligned} \pi^+ &:= \frac{1}{\sqrt{2}}(\phi_1 - i\phi_2), \\ \pi^- &:= \frac{1}{\sqrt{2}}(\phi_1 + i\phi_2), \\ \pi^0 &:= \phi_3, \end{aligned} \qquad \begin{aligned} K^+ &:= \frac{1}{\sqrt{2}}(\phi_4 - i\phi_5), \\ K^- &:= \frac{1}{\sqrt{2}}(\phi_4 + i\phi_5), \\ K^0 &:= \frac{1}{\sqrt{2}}(\phi_6 - i\phi_7), \\ \bar{K}^0 &:= \frac{1}{\sqrt{2}}(\phi_6 + i\phi_7), \end{aligned} \qquad \eta := \phi_8.$$

Note that, e.g., the π^+ operator destroys an incoming π^+ or creates an outgoing π^- particle. This can best be seen by considering

$$\left\langle 0 \left| \pi^+(x) \right| \pi^+(p) \right\rangle = \frac{e^{-ip\cdot x}}{\sqrt{(2\pi)^3 2E_p}}. \tag{8.10}$$

This equation is only obeyed when choosing $|\pi^+(p)\rangle$ to be

$$|\pi^+(p)\rangle = \frac{1}{\sqrt{2}}\left(a_1^\dagger(p) + i a_2^\dagger(p)\right)|0\rangle. \tag{8.11}$$

Here, $a_1^\dagger(p)$ is the creation operator of a particle of momentum p and Cartesian (non-physical) component 1 while the same holds for $a_2^\dagger(p)$ with the index 2. The physical amplitude comes out to be as follows

$$\begin{aligned} \left\langle \pi^+(p') \left| \hat{\mathcal{M}} \right| \pi^+(p) \right\rangle &= \frac{1}{2}\left\langle 0 \left| \left[a_1(p') - i a_2(p')\right] \hat{\mathcal{M}} \left[a_1^\dagger(p) + i a_2^\dagger(p)\right] \right| 0 \right\rangle \\ &= \frac{1}{2}\left(\mathcal{M}_{11} + i\mathcal{M}_{12} - i\mathcal{M}_{21} + \mathcal{M}_{22}\right). \end{aligned} \tag{8.12}$$

In Eq. (8.12) the first index refers to the final and the second to the initial state, respectively.

Let us briefly point out how to apply the two possible computation methods with the help of our first vertex. At the moment we are requiring all lines, and therefore momenta, to flow into the vertex. For one-loop diagrams we will have to slightly change this strategy.

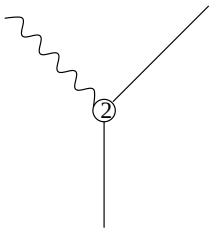

Figure 8.4: $\mathcal{L}_2$ vertex with two incoming Goldstone boson lines (p_1, i_1) and (p_2, i_2) and one incoming photon line (q, ε_μ).

The associated Lagrangian density (8.5) can be rewritten as

$$\mathcal{L}_2^{2\phi+\gamma^*} = -\frac{ie}{2} A_\mu \sum_{j_1,j_2} \partial^\mu \phi_{j_1} \phi_{j_2} \langle Q[\lambda_{j_1}, \lambda_{j_2}] \rangle, \tag{8.13}$$

which is still valid for either of the two options. The crucial point is to get rid of the traces. To this end, we have to specify whether we use the non-physical or the physical objects.

In the former case, we have to deal with the familiar Gell-Mann matrices. Recalling the identity $Q = \frac{1}{2}(\lambda_3 + \frac{1}{\sqrt{3}}\lambda_8)$, we end up with

$$\mathcal{L}_2^{2\phi+\gamma^*} = eA_\mu \sum_{j_1,j_2=1}^{8} \partial^\mu \phi_{j_1} \phi_{j_2} (f_{j_1 j_2 3} + \frac{1}{\sqrt{3}} f_{j_1 j_2 8}), \tag{8.14}$$

which is easily obtained without any computer aid. Its Feynman rule reads

$$e\varepsilon \cdot (p_1 - p_2)(f_{i_1 i_2 3} + \frac{1}{\sqrt{3}} f_{i_1 i_2 8}). \tag{8.15}$$

Since we are interested in physical reactions, we need to know the equivalent expression for physical particles. For charged pions this is to be worked out explicitly in a second. The remaining particle combinations may be treated analogously. Starting from (8.12) and using the anti-symmetry of the f coefficients, we formally get

$$\begin{aligned} \left\langle 0 \left| \hat{\mathcal{M}} \right| \pi^+(p_1), \pi^-(p_2) \right\rangle &= \left\langle \pi^+(-p_2) \left| \hat{\mathcal{M}} \right| \pi^+(p_1) \right\rangle \\ &= -i\mathcal{M}_{21} = -ie\varepsilon \cdot (p_1 - p_2). \end{aligned} \tag{8.16}$$

The second way to go consists in calculating (with the assistance of Mathematica) the traces for non-physical Gell-Mann matrices

$$\mathcal{L}_2^{2\phi+\gamma*} = -ieA_\mu \sum_{j_1,j_2=I}^{VIII} \partial^\mu \phi_{j_1} \phi_{j_2} (\delta_{j_1 I}\delta_{j_2 II} - \delta_{j_1 II}\delta_{j_2 I} + \delta_{j_1 IV}\delta_{j_2 V} - \delta_{j_1 V}\delta_{j_2 IV}), \tag{8.17}$$

which leads to the Feynman rule

$$-ie\varepsilon\cdot(p_1-p_2)(\delta_{i_1I}\delta_{i_2II}-\delta_{i_1II}\delta_{i_2I}+\delta_{i_1IV}\delta_{i_2V}-\delta_{i_1V}\delta_{i_2IV}). \tag{8.18}$$

At first glance we can verify the above calculated pion amplitude to be correctly included in (8.18). Observe that the latter just combines charged fields.

In the remainder of this section, i.e., while deriving the Feynman rules for the other four vertices, we stick to the latter strategy, but we only quote the final results. Let us go ahead according to Figure 8.2.

The second term of $\mathcal{L}_2^{4\phi}$ in (8.6) can be shown to give no contribution to our envisaged loop graphs of Figure 8.9. This stems from the symmetry behaviour of the mentioned term in combination with that of the needed WZW part. Therefore, we can simply omit it in the following. The first part is not worked out in full completeness, i.e., for any combination of Goldstone boson indices. In order to avoid unnecessary work, we restrict ourselves to those combinations which are required for our specific reaction. As we can also see in Fig. 8.9, for all of our one-loop diagrams involving the elementary vertex depicted in Fig. 8.5, two of its Goldstone boson lines are always internal while the other two are external ones. Since we are only allowing incoming external legs at the moment, we may, without loss of generality, fix the pair (i_3,i_4) to the values $(III,IV),(III,V)$, and (IV,V). This way we just drop all the additional information contained in the vertex which we will never need for our specific computation.

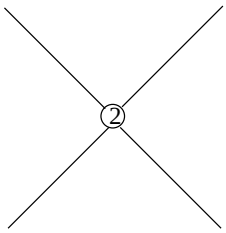

Figure 8.5: $\mathcal{L}_2$ vertex with four incoming Goldstone boson lines (p_1,i_1), $\cdots$, (p_4,i_4).

Before presenting the respective outcome, let us mention that our entire strategy and especially the Mathematica procedures were cross-checked by fully recalculating the reaction $\gamma^*(q)+\pi^\pm(p_1)\to\pi^\pm(p_2)+\pi^0(p_3)$ which had been carried out in [63, 18, 64]. The corresponding results will be shown (in terms of our nomenclature) in sections 8.5.

We must distinguish three different cases. First of all, for $i_3=IV$ and $i_4=V$, we find

$$\frac{i}{6F_0^2}(p_1\cdot p_2+p_3\cdot p_4)\Big(\delta_{i_1I}\delta_{i_2II}+\delta_{i_1II}\delta_{i_2I}+\delta_{i_1III}\delta_{i_2III}$$
$$+\sqrt{3}(\delta_{i_1III}\delta_{i_2VIII}+\delta_{i_1VIII}\delta_{i_2III})+2(\delta_{i_1IV}\delta_{i_2V}+\delta_{i_1V}\delta_{i_2IV})$$

$$
\begin{aligned}
&+\delta_{i_1 VI}\delta_{i_2 VII}+\delta_{i_1 VII}\delta_{i_2 VI}+3\delta_{i_1 VIII}\delta_{i_2 VIII}\Big)\\
&+\frac{i}{12F_0^2}(p_1\cdot p_3+p_2\cdot p_4)\Big(2\delta_{i_1 II}\delta_{i_2 I}-4\delta_{i_1 I}\delta_{i_2 II}-\delta_{i_1 III}\delta_{i_2 III}\\
&-\sqrt{3}(\delta_{i_1 III}\delta_{i_2 VIII}+\delta_{i_1 VIII}\delta_{i_2 III})+4\delta_{i_1 V}\delta_{i_2 IV}-8\delta_{i_1 IV}\delta_{i_2 V}\\
&+2\delta_{i_1 VII}\delta_{i_2 VI}-4\delta_{i_1 VI}\delta_{i_2 VII}-3\delta_{i_1 VIII}\delta_{i_2 VIII}\Big)\\
&+\frac{i}{12F_0^2}(p_1\cdot p_4+p_2\cdot p_3)\Big(2\delta_{i_1 I}\delta_{i_2 II}-4\delta_{i_1 II}\delta_{i_2 I}-\delta_{i_1 III}\delta_{i_2 III}\\
&-\sqrt{3}(\delta_{i_1 III}\delta_{i_2 VIII}+\delta_{i_1 VIII}\delta_{i_2 III})+4\delta_{i_1 IV}\delta_{i_2 V}-8\delta_{i_1 V}\delta_{i_2 IV}\\
&+2\delta_{i_1 VI}\delta_{i_2 VII}-4\delta_{i_1 VII}\delta_{i_2 VI}-3\delta_{i_1 VIII}\delta_{i_2 VIII}\Big),
\end{aligned}
\tag{8.19}
$$

furthermore, for $i_3 = III$ and $i_4 = IV$,

$$
\begin{aligned}
&\frac{i}{12F_0^2}(p_1\cdot p_2+p_3\cdot p_4)\Big(3\sqrt{2}(\delta_{i_1 II}\delta_{i_2 VII}+\delta_{i_1 VII}\delta_{i_2 II})\\
&-(\delta_{i_1 III}\delta_{i_2 V}+\delta_{i_1 V}\delta_{i_2 III})-\sqrt{3}(\delta_{i_1 V}\delta_{i_2 VIII}+\delta_{i_1 VIII}\delta_{i_2 V})\Big)\\
&+\frac{i}{12F_0^2}(p_1\cdot p_3+p_2\cdot p_4)\Big(2\delta_{i_1 III}\delta_{i_2 V}-\delta_{i_1 V}\delta_{i_2 III}\\
&+\sqrt{3}(2\delta_{i_1 VIII}\delta_{i_2 V}-\delta_{i_1 V}\delta_{i_2 VIII})-3\sqrt{2}\delta_{i_1 VII}\delta_{i_2 II}\Big)\\
&+\frac{i}{12F_0^2}(p_1\cdot p_4+p_2\cdot p_3)\Big(2\delta_{i_1 V}\delta_{i_2 III}-\delta_{i_1 III}\delta_{i_2 V}\\
&+\sqrt{3}(2\delta_{i_1 V}\delta_{i_2 VIII}-\delta_{i_1 VIII}\delta_{i_2 V})-3\sqrt{2}\delta_{i_1 II}\delta_{i_2 VII}\Big),
\end{aligned}
\tag{8.20}
$$

and finally, for $i_3 = III$ and $i_4 = V$,

$$
\begin{aligned}
&\frac{i}{12F_0^2}(p_1\cdot p_2+p_3\cdot p_4)\Big(3\sqrt{2}(\delta_{i_1 I}\delta_{i_2 VI}+\delta_{i_1 VI}\delta_{i_2 I})\\
&-(\delta_{i_1 III}\delta_{i_2 IV}+\delta_{i_1 IV}\delta_{i_2 III})-\sqrt{3}(\delta_{i_1 IV}\delta_{i_2 VIII}+\delta_{i_1 VIII}\delta_{i_2 IV})\Big)\\
&+\frac{i}{12F_0^2}(p_1\cdot p_3+p_2\cdot p_4)\Big(2\delta_{i_1 III}\delta_{i_2 IV}-\delta_{i_1 IV}\delta_{i_2 III}\\
&+\sqrt{3}(2\delta_{i_1 VIII}\delta_{i_2 IV}-\delta_{i_1 IV}\delta_{i_2 VIII})-3\sqrt{2}\delta_{i_1 VI}\delta_{i_2 I}\Big)\\
&+\frac{i}{12F_0^2}(p_1\cdot p_4+p_2\cdot p_3)\Big(2\delta_{i_1 IV}\delta_{i_2 III}-\delta_{i_1 III}\delta_{i_2 IV}\\
&+\sqrt{3}(2\delta_{i_1 IV}\delta_{i_2 VIII}-\delta_{i_1 VIII}\delta_{i_2 IV})-3\sqrt{2}\delta_{i_1 I}\delta_{i_2 VI}\Big).
\end{aligned}
\tag{8.21}
$$

So much for the even vertices. Now, we must prepare ourselves to go over to those resulting from $\mathcal{L}_{WZW}$.

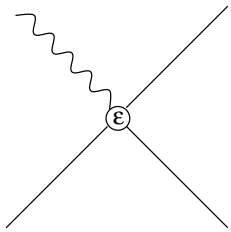

Figure 8.6: $\mathcal{L}_{WZW}$ vertex with three incoming Goldstone boson lines $(p_1,i_1),\cdots,(p_3,i_3)$ and one incoming photon line (q,ε_μ).

Again, we may choose one index, let us say i_1, to take the values III (8.22),IV (8.23), or V (8.24).

$$-\frac{ieN_c}{12\pi^2F_0^3}\quad\Big(\quad \delta_{i_2I}\delta_{i_3II}-\delta_{i_2II}\delta_{i_3I}+\delta_{i_2IV}\delta_{i_3V}-\delta_{i_2V}\delta_{i_3IV}$$
$$+\quad \delta_{i_2VI}\delta_{i_3VII}-\delta_{i_2VII}\delta_{i_3VI}\quad\Big)\quad \underbrace{\varepsilon_{\alpha\beta\gamma\delta}\varepsilon^{\alpha}p_1^{\beta}p_2^{\gamma}p_3^{\delta}}_{=:\mathcal{A}}, \tag{8.22}$$

$$-\frac{ieN_c}{12\pi^2F_0^3}\left(\delta_{i_2V}\delta_{i_3III}-\delta_{i_2III}\delta_{i_3V}+\frac{1}{\sqrt{3}}(\delta_{i_2V}\delta_{i_3VIII}-\delta_{i_2VIII}\delta_{i_3V})\right)\mathcal{A}, \tag{8.23}$$

$$-\frac{ieN_c}{12\pi^2F_0^3}\left(\delta_{i_2III}\delta_{i_3IV}-\delta_{i_2IV}\delta_{i_3III}+\frac{1}{\sqrt{3}}(\delta_{i_2VIII}\delta_{i_3IV}-\delta_{i_2IV}\delta_{i_3VIII})\right)\mathcal{A}. \tag{8.24}$$

The very vertex we have been analysing does not just play an important role at one-loop level but obviously represents the one and only $O(p^4)$ tree contribution.

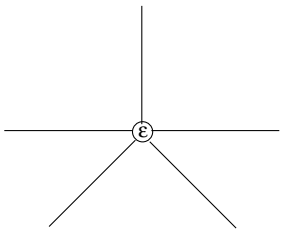

Figure 8.7: $\mathcal{L}_{WZW}$ vertex with five incoming Goldstone boson lines $(p_1,i_1),\cdots,(p_5,i_5)$.

With the assumption of $i_3=III$, $i_4=IV$, and $i_5=V$, the pure QCD vertex in Fig. 8.7 becomes

$$-\frac{iN_c}{4\pi^2F_0^5}\varepsilon_{\alpha\beta\gamma\delta}p_1^{\alpha}p_3^{\beta}p_4^{\gamma}p_5^{\delta}(\delta_{i_1I}\delta_{i_2II}-\delta_{i_1II}\delta_{i_2I}). \tag{8.25}$$

To complete this account, let us turn to the last vertex depicted below. As can be fully understood later, it is absolutely sufficient to concentrate on a special part of the associated Feynman rule, namely the very one where (p_4, i_4) and (p_5, i_5) do not gain any momentum factor $(i_1 = III, i_2 = IV, i_3 = V)$

$$\frac{ieN_c}{72\pi^2 F_0^5}\varepsilon_{\alpha\beta\gamma\delta}\varepsilon^{\alpha}p_1^{\beta}p_2^{\gamma}p_3^{\delta}\Big(9(\delta_{i_4 I}\delta_{i_5 II}+\delta_{i_4 II}\delta_{i_5 I})+\delta_{i_4 III}\delta_{i_5 III} \\ +6(\delta_{i_4 IV}\delta_{i_5 V}+\delta_{i_4 V}\delta_{i_5 IV})+(\delta_{i_4 VI}\delta_{i_5 VII}+\delta_{i_4 VII}\delta_{i_5 VI}) \\ 3\delta_{i_4 VIII}\delta_{i_5 VIII}+\sqrt{3}(\delta_{i_4 III}\delta_{i_5 VIII}+\delta_{i_4 VIII}\delta_{i_5 III})\Big). \tag{8.26}$$

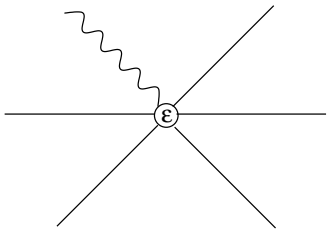

Figure 8.8: $\mathcal{L}_{WZW}$ vertex with five incoming Goldstone boson lines $(p_1, i_1), \cdots, (p_5, i_5)$ and one incoming photon line (q, ε_μ).

In what follows we keep using the momentum assignment $K^+(p_1), K^-(p_2), \pi^0(p_3)$, and $\gamma^*(q)$ where all external momenta do flow into whatever diagram[2] and the abbreviation $\mathcal{A}$ defined above.

[2]N.B.: During the entire calculation we hence consider $\gamma^*(q) + K^+(p_1) + K^-(p_2) + \pi^0(p_3) \to 0$, from which one may easily turn to $\gamma^*(q) + K^\pm(p_1) \to K^\pm(p_2) + \pi^0(p_3)$.

After having carefully collected the required Feynman rules for our elementary vertices, we finally come to consider one-loop graphs. As we have given to understand several times, we need to deal with the below depicted one-loop diagrams which evidently fall into two different groups.

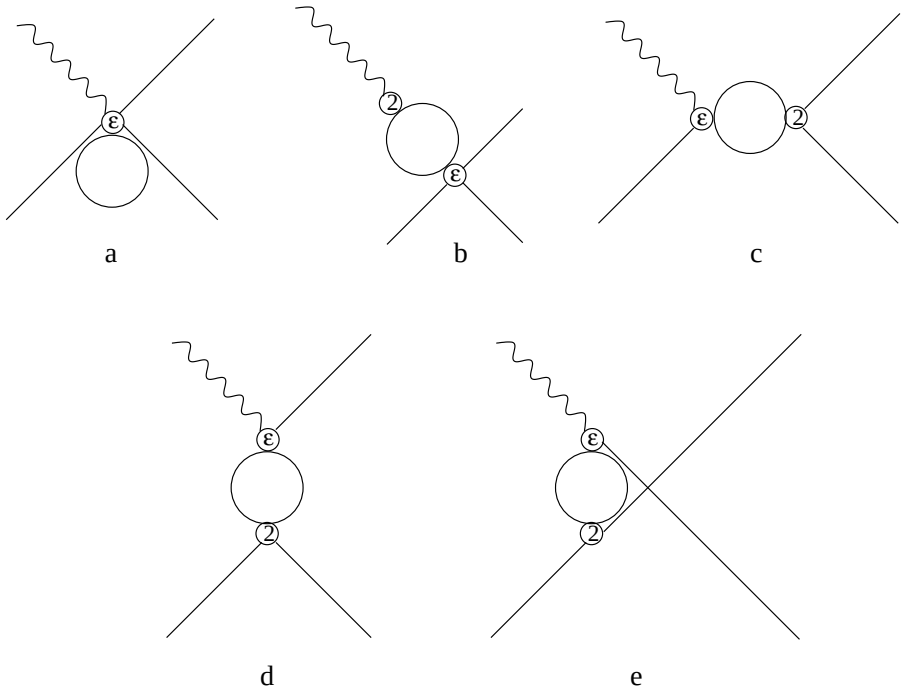

Figure 8.9: Non-vanishing one-loop graphs for three-pseudoscalar photon interactions; in our case $\gamma^*(q) + K^{\pm}(p_1) \to K^{\pm}(p_2) + \pi^0(p_3)$. The assignment of external momenta is in accordance with Fig. 8.1, i.e., time is meant to flow from left to right.

The first category just includes one graph (*a*) whose loop is attached to one single vertex (the loop is composed by one internal line so to speak), while in the second category the loop always binds two different vertices together (the loop is therefore composed by two internal lines). We know for sure from our previous considerations that loops with more than two internal lines do not occur in our special case, although they may for higher chiral power D or other classes of reactions.

We now want to derive the Feynman rules belonging to the above one-loop graphs. In order to construct the very first one, roughly speaking, two of the five boson lines of Figure 8.8 need to be joined together, while the remaining three must be identified as external incoming legs of the interacting bosons. Note that in (8.26), without loss of generality, we had implicitly chosen (p_4, i_4) and (p_5, i_5) to constitute the loop. In mathematical terms all this clearly means that one has to

1. Set $l := p_4 = -p_5$ and $n := i_4 = i_5$. Here, we should emphasize that the boson line carrying (p_5, i_5) has just been turned into an outgoing line, i.e., its momentum has gained a negative sign and the associated Kronecker deltas have been

modified according to the rule $I \leftrightarrow II, IV \leftrightarrow V, VI \leftrightarrow VII$.

2. Introduce a propagator $i(l^2 - m_n^2 + i\varepsilon)^{-1}$.

3. Integrate over the internal momentum l.

4. Multiply with the symmetry factor $1/2$. The origin of this factor can be best understood by first considering Cartesian indices. While for a tree graph there are two possibilities to assign two identical lines to two distinct external momenta, there is only one way to build up a loop out of these lines. When using physical indices this very argument only applies to π^0 and η_8 loops. For the remaining particles our present formalism generates π^+ as well as π^- loops etc., which is a double-counting. Hence the symmetry factor $1/2$ is required from both points of view.

All in all, these steps yield

$$\frac{ieN_c}{144\pi^2 F_0^5}\mathcal{A}\sum_{n,n'=I}^{VIII} a_{n'}\delta_{nn'}\delta_{nn'}\overbrace{\int\frac{d^4l}{(2\pi)^4}\frac{i}{l^2-m_n^2+i\varepsilon}}^{I(m_n^2)}, \tag{8.27}$$

where $a_{n'}$ is supposed to represent the respective coefficients from (8.26). Although we have not yet explained how to exactly handle the integrals, we can insert physical masses and rewrite the above expression as follows

$$\frac{ieN_c}{\pi^2 F_0^5}\left\{\frac{38}{288}I(m_\pi^2)+\frac{28}{288}I(m_K^2)+\frac{6}{288}I(m_\eta^2)\right\}\mathcal{A}. \tag{8.28}$$

Finally, we do also understand why it was sufficient to restrict oneself to that particular part of the Feynman rule shown in (8.26) (the one without explicit p_4 or p_5 occurence). If the internal line was to give rise to any power of the internal momentum l, then the associated integral would completely vanish. The vector integral is inherently zero and the tensor one does not contribute due to its contraction with the totally anti-symmetric ε tensor.

Let us now have a closer look at the second group of graphs $(b,\cdots,e)$. Basically, we have to move on in an absolutely analogous manner. Again, we first need to create the loop. To this end, we must connect two boson lines of the first elementary vertex with two of the second via propagators. Do not forget to turn one line at each vertex into an outgoing one and join it with the remaining incoming one from the other vertex. Afterwards we need to integrate over the two resulting internal lines. Since momentum conservation has to be respected at each vertex, only one of the two integrations survives. Last but not least, the symmetry factor $1/2$ must be taken into account for equivalent reasons. There is no need to explicitly present all the straightforward but tedious details one has to go through to arrive at the final results. Instead, we simply

indicate what kind of different integrals one encounters. After a thorough examination of the relevant ingredients the only necessary type turns out to be

$$\int \frac{d^4l}{(2\pi)^4} \frac{il^\mu l^\mu}{\left[l^2 - m_n^2 + i\varepsilon\right]\left[(l+a)^2 - m_{n'}^2 + i\varepsilon\right]}\,, \tag{8.29}$$

which, nevertheless, comprises two subtypes. While for *b* and *c* of Fig. 8.9 we only need to know the restricted case ($m_n^2 = m_{n'}^2$), *d* and *e* require the more complicated one ($m_n^2 \neq m_{n'}^2$) with two different species of particles running in the loop.

Since our one-loop diagrams suffer from divergences due to singular high-momentum behaviour, we have to provide a mathematical device prescribing how to cope with this particularity. The adequate tool for our purposes is, of course, dimensional regularization (DR). As we have just learned, the different loop graphs lead to different types of integrals according to the number of involved vertices and their individual vertex structures. Putting everything together, we get[3]

$$\begin{aligned}
\frac{ieN_c}{\pi^2 F_0^5} \quad \Big\{ \quad & \frac{38}{288} I(m_\pi^2) + \frac{28}{288} I(m_K^2) + \frac{6}{288} I(m_\eta^2) \\
- \quad & \frac{q^2}{2} B_{22}(m_\pi^2, q^2) \\
- \quad & \frac{(p_1+p_2)^2}{12} \{B_{22}(m_\pi^2, (p_1+p_2)^2) + 3B_{22}(m_K^2, (p_1+p_2)^2)\} \\
- \quad & \frac{(p_1+p_3)^2}{24} \{\tilde{B}_{22}(m_K^2, m_\pi^2, (p_1+p_3)^2) + \tilde{B}_{22}(m_K^2, m_\eta^2, (p_1+p_3)^2)\} \\
- \quad & \frac{(p_2+p_3)^2}{24} \{\tilde{B}_{22}(m_K^2, m_\pi^2, (p_2+p_3)^2) + \tilde{B}_{22}(m_K^2, m_\eta^2, (p_2+p_3)^2)\} \quad \Big\} \mathcal{A}
\end{aligned} \tag{8.30}$$

with the Goldstone boson masses

$$m_\pi^2 = 2B_0 m, \qquad m_K^2 = B_0(m+m_s), \qquad m_\eta^2 = \frac{2}{3} B_0(m+2m_s). \tag{8.31}$$

For details on how to evaluate the integrals within the framework of DR and notational conventions consult Appendix E.

8.3 Tree graphs

Although the present section is dedicated to tree graphs, loops are not yet totally left behind. At $O(p^6)$, in addition to the one-loop diagrams treated so far, there are further

[3]The first line corresponds to diagram *a*, the second to *b*, and so forth.

one-loop contributions which enter as $O(p^2)$ corrections to the WZW tree diagram shown in Fig. 8.6. The latter possesses the Feynman rule

$$-\frac{ieN_c}{12\pi^2 F_0^3}\ \mathcal{A}. \tag{8.32}$$

These corrections arise in

- the mesons' decay constants:

  The relationship between the physical decay constants F_π, F_K and the parameter F_0 is well-known and can be read off from Ref [13]. In contrast to their notation, we express the respective formulae in terms of non-renormalized LECs and our integrals computed in Appendix E:

$$\begin{aligned}\frac{F_\pi}{F_0} &= 1+\frac{4}{F_0^2}(2m_\pi^2-2m_K^2+3m_\eta^2)L_4+\frac{4}{F_0^2}m_\pi^2 L_5 \\ &\quad -\frac{1}{F_0^2}I(m_\pi^2)-\frac{1}{2F_0^2}I(m_K^2)+O(p^4), \qquad (8.33)\\ \frac{F_K}{F_0} &= 1+\frac{4}{F_0^2}(2m_\pi^2-2m_K^2+3m_\eta^2)L_4+\frac{4}{F_0^2}m_K^2 L_5 \\ &\quad -\frac{3}{8F_0^2}I(m_\pi^2)-\frac{3}{4F_0^2}I(m_K^2)-\frac{3}{8F_0^2}I(m_\eta^2)+O(p^4). \qquad (8.34)\end{aligned}$$

- the mesons' wave functions:

  As usual, for each meson field we have to include a factor $\sqrt{Z}$ [61]:

$$\begin{aligned}\sqrt{Z_\pi} &= 1-\frac{4}{F_0^2}(2m_\pi^2-2m_K^2+3m_\eta^2)L_4-\frac{4}{F_0^2}m_\pi^2 L_5 \\ &\quad +\frac{1}{3F_0^2}I(m_\pi^2)+\frac{1}{6F_0^2}I(m_K^2)+O(p^4), \qquad (8.35)\\ \sqrt{Z_K} &= 1-\frac{4}{F_0^2}(2m_\pi^2-2m_K^2+3m_\eta^2)L_4-\frac{4}{F_0^2}m_K^2 L_5 \\ &\quad +\frac{1}{8F_0^2}I(m_\pi^2)+\frac{1}{4F_0^2}I(m_K^2)+\frac{1}{8F_0^2}I(m_\eta^2)+O(p^4). \qquad (8.36)\end{aligned}$$

The combination of both items implies

$$\begin{aligned}\sqrt{Z_\pi}\frac{F_\pi}{F_0} &= 1-\frac{2}{3F_0^2}I(m_\pi^2)-\frac{1}{3F_0^2}I(m_K^2)+O(p^4),\\ \sqrt{Z_K}\frac{F_K}{F_0} &= 1-\frac{1}{4F_0^2}I(m_\pi^2)-\frac{1}{2F_0^2}I(m_K^2)-\frac{1}{4F_0^2}I(m_\eta^2)+O(p^4),\end{aligned}$$

and finally leads to

$$
\begin{aligned}
& -\frac{ieN_c}{12\pi^2 F_\pi F_K^2}\mathcal{A}\left(\sqrt{Z_\pi}\frac{F_\pi}{F_0}\right)\left(\sqrt{Z_K}\frac{F_K}{F_0}\right)^2 \\
= \quad & -\frac{ieN_c}{12\pi^2 F_\pi F_K^2}\mathcal{A}\left(1-\frac{7}{6F_0^2}I(m_\pi^2)-\frac{4}{3F_0^2}I(m_K^2)-\frac{1}{2F_0^2}I(m_\eta^2)\right)+O(p^8),
\end{aligned}
\tag{8.37}
$$

where the integrals I, see Eq. (8.27), represent the mentioned one-loop corrections.

Last but not least, we have to consider tree contributions of order $O(p^6)$. These need to be included for two different reasons. First of all, the concerned parameters (LECs) of $\mathcal{L}_{6,\varepsilon}$ must absorb the one-loop divergences arising at $O(p^4)$. But even if there was no singularity problem, we would have to take those contributions into account in order to be consistent with our requirement of performing a complete p^6 calculation.

The general features of $\mathcal{L}_{6,\varepsilon}$ regarding the reaction type $3\phi+\gamma^*$ were carried out in the previous chapter. Even the reduction to our very process was shown in Eq. (7.12). The corresponding Feynman rule, in its natural form, reads

$$
\begin{aligned}
& \mathcal{F}(\mathbf{L_1^{6,\varepsilon}},\mathbf{L_5^{6,\varepsilon}},\mathbf{L_6^{6,\varepsilon}},\mathbf{L_{13}^{6,\varepsilon}},\mathbf{L_{14}^{6,\varepsilon}}) := \\
& \quad - \frac{256ieB_0}{F_0^3}\Big\{\mathbf{L_1^{6,\varepsilon}}(m-m_s)-\mathbf{L_5^{6,\varepsilon}}(5m+m_s)-\mathbf{L_6^{6,\varepsilon}}(m+2m_s)\Big\}\mathcal{A} \\
& \quad - \frac{64ie}{3F_0^3}\mathbf{L_{13}^{6,\varepsilon}}(p_1^2+p_2^2+4p_3^2+2p_1\cdot p_2+5p_1\cdot p_3+5p_2\cdot p_3)\mathcal{A} \\
& \quad - \frac{128ie}{3F_0^3}\mathbf{L_{14}^{6,\varepsilon}}(4p_1\cdot p_2+p_1\cdot p_3+p_2\cdot p_3)\mathcal{A}.
\end{aligned}
\tag{8.38}
$$

Let us state three remarks at this point:

1. We have introduced the function $\mathcal{F}$ to simplify our notation. We will come to appreciate this in a second.

2. Eq. (8.38) is completely equivalent to Eq. (7.13), but written in terms of other Lorentz invariants.

3. Our assumption of perfect isospin symmetry ($m=m_u=m_d\neq m_s$) makes the contributions belonging to $\mathbf{L_2^{6,\varepsilon}}$ and $\mathbf{L_7^{6,\varepsilon}}$ vanish.

In summary, the total result of our one-loop calculation consists of three pieces, (8.30), (8.37), and (8.38), which have to be added in order to obtain the reaction amplitude. Consistency requires that the decay constants associated to the external Goldstone bosons take their respective physical values, while for those belonging to the loops we globally set $F_0=F_\pi$.

8.4 Renormalization

In applying the concept of Chapter 6, we can get rid of all one-loop singularities by introducing renormalized LECs. Recalling the relation

$$\mathbf{L_i} = \hat{\mathbf{L}}_\mathbf{i} + \Gamma_i \lambda \qquad \left(\lambda = \frac{R}{32\pi^2}\right), \tag{8.39}$$

where we have used the notation $\hat{\mathbf{L}}_\mathbf{i}$ instead of Gasser and Leutwyler's convention $\mathbf{L}_\mathbf{i}^\mathbf{r}$ and where Γ_i has to be read off from Table 6.2, we do immediately get

$$\begin{aligned}
&\mathcal{F}(\mathbf{L_1^{6,\varepsilon}}, \mathbf{L_5^{6,\varepsilon}}, \mathbf{L_6^{6,\varepsilon}}, \mathbf{L_{13}^{6,\varepsilon}}, \mathbf{L_{14}^{6,\varepsilon}}) = \\
&\Big\{ - \frac{256ieB_0}{F_0^3}\left(\hat{\mathbf{L}}_\mathbf{1}^{\mathbf{6},\varepsilon} - \frac{7R}{256\cdot 384\pi^4 F_0^2}\right)(m - m_s) \\
&\quad + \frac{256ieB_0}{3F_0^3}\left(\hat{\mathbf{L}}_\mathbf{5}^{\mathbf{6},\varepsilon} - \frac{R}{256\cdot 128\pi^4 F_0^2}\right)(5m + m_s) \\
&\quad + \frac{256ieB_0}{3F_0^3}\left(\hat{\mathbf{L}}_\mathbf{6}^{\mathbf{6},\varepsilon} - \frac{R}{256\cdot 32\pi^4 F_0^2}\right)(m + 2m_s) \\
&\quad - \frac{64ie}{3F_0^3}\left(\hat{\mathbf{L}}_\mathbf{13}^{\mathbf{6},\varepsilon} + \frac{R}{64\cdot 128\pi^4 F_0^2}\right)(p_1^2 + p_2^2 + 4p_3^2 + 2p_1\cdot p_2 + 5p_1\cdot p_3 + 5p_2\cdot p_3) \\
&\quad - \frac{128ie}{3F_0^3}\left(\hat{\mathbf{L}}_\mathbf{14}^{\mathbf{6},\varepsilon} + \frac{R}{128\cdot 64\pi^4 F_0^2}\right)(4p_1\cdot p_2 + p_1\cdot p_3 + p_2\cdot p_3)\Big\}\mathcal{A} \\
&= \mathcal{F}(\hat{\mathbf{L}}_\mathbf{1}^{\mathbf{6},\varepsilon}, \hat{\mathbf{L}}_\mathbf{5}^{\mathbf{6},\varepsilon}, \hat{\mathbf{L}}_\mathbf{6}^{\mathbf{6},\varepsilon}, \hat{\mathbf{L}}_\mathbf{13}^{\mathbf{6},\varepsilon}, \hat{\mathbf{L}}_\mathbf{14}^{\mathbf{6},\varepsilon}) + \frac{ieR}{128\pi^4 F_0^5}\Big\{\frac{7}{3}B_0(m - m_s) - 3\overbrace{B_0(m + m_s)}^{m_K^2 = \frac{p_1^2+p_2^2}{2}} \\
&\quad - \frac{1}{3}(p_1^2 + p_2^2 + 4p_3^2 + 10p_1\cdot p_2 + 7p_1\cdot p_3 + 7p_2\cdot p_3)\Big\}\mathcal{A}.
\end{aligned} \tag{8.40}$$

The one-loop singularities, i.e., terms proportional to R, being hidden in (8.30) and (8.37) can easily be isolated

$$\begin{aligned}
&\frac{ieR}{128\pi^4 F_0^5} \quad \Big\{q^2 + \frac{2}{3}(p_1+p_2)^2 + \frac{1}{6}(p_1+p_3)^2 + \frac{1}{6}(p_2+p_3)^2 - \frac{7}{3}B_0(m-m_s)\Big\}\mathcal{A} \\
&= \frac{ieR}{128\pi^4 F_0^5} \quad \Big\{\frac{11}{6}(p_1^2 + p_2^2) + \frac{4}{3}p_3^2 \\
&\qquad\qquad + \frac{10}{3}p_1\cdot p_2 + \frac{7}{3}(p_1\cdot p_3 + p_2\cdot p_3) - \frac{7}{3}B_0(m-m_s)\Big\}\mathcal{A}
\end{aligned} \tag{8.41}$$

and are obviously being cancelled, as we have expected, by the singular part of (8.40). Observe that all external particles are assumed to be on the mass shell.

8.5 Pionic reaction

As mentioned before, our computation can be checked by reconsidering the corresponding pionic reaction, i.e., $\gamma^* + \pi^\pm \to \pi^\pm + \pi^0$. We find complete accordance with Bijnens *et al.* [63, 18, 64][4] and want to collect the final results in terms of our nomenclature. The three pieces of information are respectively given by

$$\begin{aligned}
\frac{ieN_c}{6\pi^2 F_0^5} \quad & \Big\{ \quad \frac{1}{2} I(m_\pi^2) + I(m_K^2) - 3q^2 B_{22}(m_K^2, q^2) \\
& - \quad (p_1+p_2)^2 B_{22}(m_\pi^2, (p_1+p_2)^2) \\
& - \quad (p_1+p_3)^2 B_{22}(m_\pi^2, (p_1+p_3)^2) \\
& - \quad (p_2+p_3)^2 B_{22}(m_\pi^2, (p_2+p_3)^2) \quad \Big\}\, \mathcal{A}, \qquad (8.42)
\end{aligned}$$

$$\begin{aligned}
& -\frac{ieN_c}{12\pi^2 F_\pi^3} \mathcal{A} \left(\sqrt{Z_\pi} \frac{F_\pi}{F_0} \right)^3 \\
= \quad & -\frac{ieN_c}{12\pi^2 F_\pi^3} \mathcal{A} \left(1 - \frac{2}{F_0^2} I(m_\pi^2) - \frac{1}{F_0^2} I(m_K^2) \right) + O(p^8), \qquad (8.43)
\end{aligned}$$

$$\begin{aligned}
& \mathcal{G}(\mathbf{L_5^{6,\varepsilon}}, \mathbf{L_6^{6,\varepsilon}}, \mathbf{L_{13}^{6,\varepsilon}}, \mathbf{L_{14}^{6,\varepsilon}}) := \\
& \quad + \quad \frac{256 ieB_0}{F_0^3} \Big(2\mathbf{L_5^{6,\varepsilon}} + \mathbf{L_6^{6,\varepsilon}} \Big) m\, \mathcal{A} \\
& \quad + \quad \frac{128 ie}{3F_0^3} \mathbf{L_{13}^{6,\varepsilon}} q \cdot (p_1+p_2+p_3)\, \mathcal{A} \\
& \quad - \quad \frac{256 ie}{3F_0^3} \mathbf{L_{14}^{6,\varepsilon}} \Big(p_3 \cdot (p_1+p_2) + p_1 \cdot p_2 \Big)\, \mathcal{A}. \qquad (8.44)
\end{aligned}$$

Again, the total result is finite.

[4] Complementary computations have recently been presented: in [65] one finds a $SU(2)$ calculation including e.m. corrections and in [66] a two-loop calculation based on a dispersive method.

8.6 Vector meson contributions to $3\phi + \gamma^*$

We have, up until now in this chapter, carried out everything which is necessary to meet the requirements of a consistent $O(p^6)$ calculation within the framework of mesonic ChPT. However, our final formulae still depend on a couple of unknown parameters, the involved LECs, which prevent us from numerically predicting the squared amplitude. Of course, these LECs can in principle be determined within appropriate experiments. But even without experimental help we are not condemned to idleness. We can actually move on and estimate the LECs' values by using purely theoretical means. These evidently have to go beyond mesonic ChPT.

Let us recall once more the physical meaning of LECs. They are supposed to include whatever QCD information on all particles which do not belong to the Goldstone boson octet. At low energies only the lightest are expected to be significant. The latter are the so-called vector mesons which can, similarly to the pseudoscalar mesons, be compactly collected in a matrix:

$$V_\mu = \begin{pmatrix} \frac{\rho_\mu^0}{2} + \frac{\omega_\mu}{2} & \frac{\rho_\mu^+}{\sqrt{2}} & \frac{K_\mu^{*+}}{\sqrt{2}} \\ \frac{\rho_\mu^-}{\sqrt{2}} & -\frac{\rho_\mu^0}{2} + \frac{\omega_\mu}{2} & \frac{K_\mu^{*0}}{\sqrt{2}} \\ \frac{K_\mu^{*-}}{\sqrt{2}} & \frac{\bar{K}_\mu^{*0}}{\sqrt{2}} & \frac{\phi_\mu}{\sqrt{2}} \end{pmatrix}. \tag{8.45}$$

In what follows we consider tree diagrams which have the usual external lines, i.e., one photon and three Goldstone boson lines, but also comprise explicit internal vector meson lines. The $O(p^6)$ part of these graphs is then to be compared with our previous $O(p^6)$ tree diagrams[5] and this way we are given an estimation of the numerical values of the concerned LECs.

To this end, we first have to find adequate Lagrangian densities satisfying our needs mentioned above.[6] As can be seen in a moment, one must always combine vertices of odd and even intrinsic parity, i.e., ε and non-ε vertices, to obtain the relevant tree graphs. For both sectors Fujiwara *et al.* [68] provided the necessary pieces. In their article the vector mesons are introduced as dynamical gauge boson fields of a hidden local symmetry (for a review on hidden local symmetries, see [69]). In an alternative scheme the vector mesons can be described as massive Yang-Mills bosons [70, 71, 72]. The latter approach and its relation to the hidden-symmetry scheme are extensively discussed in [73].

8.6.1 Even intrinsic parity

In the even intrinsic parity sector, there is just one part giving rise to vector meson fields. Nonetheless, we want to present the complete Lagrangian density at this intro-

[5] This is suggested by their structural similarity.

[6] Pretty much of the general things to follow had been nicely collected in [67].

ductory level:

$$\begin{aligned}
\mathcal{L}^{(2)}_{\text{mass}} &= \frac{F_0^2}{4}\langle \chi^\dagger U + \chi U^\dagger \rangle, && (8.46)\\
\mathcal{L}_A &= -\frac{F_0^2}{4}\langle (D_\mu \xi^\dagger \xi - D_\mu \xi \xi^\dagger)(D^\mu \xi^\dagger \xi - D^\mu \xi \xi^\dagger)\rangle \\
&= \frac{F_0^2}{4}\langle D_\mu U (D^\mu U)^\dagger \rangle, && (8.47)\\
\mathcal{L}_V &= -\frac{F_0^2}{4}\langle (D_\mu \xi^\dagger \xi + D_\mu \xi \xi^\dagger)(D^\mu \xi^\dagger \xi + D^\mu \xi \xi^\dagger)\rangle. && (8.48)
\end{aligned}$$

The 'covariant' derivatives,

$$\begin{aligned}
D_\mu \xi &= (\partial_\mu - igV_\mu)\xi - ieA_\mu \xi Q \\
\text{and} \qquad D_\mu \xi^\dagger &= (\partial_\mu - igV_\mu)\xi^\dagger - ieA_\mu \xi^\dagger Q, && (8.49)
\end{aligned}$$

comprise both the vector meson nonet as well as the e.m. field. One should note that $\xi = \exp(\frac{i}{2}\phi/F_0)$ is the square root of our usual U and $D_\mu U$ our conventional covariant derivative (with e.m. external fields). Symmetry considerations do only fix Eq. (8.48) up to a global coefficient a. In respecting this fact, its leading order reads

$$\begin{aligned}
a\mathcal{L}_V &= m_V^2 \langle V_\mu V^\mu \rangle + 2eg_V A_\mu \langle Q V^\mu \rangle + \left(\frac{eg_V}{m_V}\right)^2 A_\mu A^\mu \langle Q^2 \rangle \\
&- \frac{ig_{V\phi\phi}}{2}\langle V_\mu [\phi, \partial^\mu \phi]\rangle - \frac{aei}{4} A_\mu \langle Q[\phi, \partial^\mu \phi]\rangle + \frac{eg_{V\phi\phi}}{2} A_\mu \langle [[\phi, Q], \phi] V^\mu \rangle. \qquad (8.50)
\end{aligned}$$

Again, we only find even powers in ϕ. Furthermore, observe that the $(V\gamma^*)$ mixing has been introduced into Eq. (8.50) by $g_V = agF_0^2$, the vector meson mass[7] by $m_V^2 = ag^2F_0^2$, and the $(V\phi\phi)$ coupling by $g_{V\phi\phi} = ag/2$. Thus we rediscover the famous KSRF relation [74, 75],

$$\frac{g_V}{g_{V\phi\phi}} = 2F_0^2, \qquad (8.51)$$

to hold for whatever value of a. Moreover, setting the parameter $a = 2$ results in the universality of the vector meson coupling, $g_{V\phi\phi} = g$, as well as in complete vector meson dominance for the e.m. form factor $(\mathcal{L}^{\gamma\phi\phi} = 0)$, both suggested on phenomenological grounds [68].

[7] The assumed $SU(3)$ symmetry ($m_u = m_d = m_s$) just implies one identical mass for all vector mesons ($m_V = m_\rho = \cdots = m_\phi$). Later, we will introduce deviations to this scheme by hand.

8.6.2 Odd intrinsic parity

In the odd intrinsic parity sector, besides our familiar WZW Lagrangian, one encounters four independent structures due to the presence of the vector mesons

$$\begin{aligned}
\mathcal{L}_1 &= \frac{iN_c}{16\pi^2}\varepsilon_{\alpha\beta\gamma\delta}\langle \hat{a}_L^\alpha \hat{a}_L^\beta \hat{a}_L^\gamma \hat{a}_R^\delta - \hat{a}_R^\alpha \hat{a}_R^\beta \hat{a}_R^\gamma \hat{a}_L^\delta \rangle, && (8.52)\\
\mathcal{L}_2 &= \frac{iN_c}{16\pi^2}\varepsilon_{\alpha\beta\gamma\delta}\langle \hat{a}_L^\alpha \hat{a}_R^\beta \hat{a}_L^\gamma \hat{a}_R^\delta \rangle, && (8.53)\\
\mathcal{L}_3 &= -\frac{N_c}{16\pi^2}\varepsilon_{\alpha\beta\gamma\delta}\langle F_V^{\alpha\beta}(\hat{a}_L^\gamma \hat{a}_R^\delta - \hat{a}_R^\gamma \hat{a}_L^\delta)\rangle, && (8.54)\\
\mathcal{L}_4 &= -\frac{N_c}{32\pi^2}\varepsilon_{\alpha\beta\gamma\delta}\langle F_A^{\alpha\beta}(\xi \hat{a}_L^\gamma \hat{a}_R^\delta \xi^\dagger - \xi^\dagger \hat{a}_R^\gamma \hat{a}_L^\delta \xi + \xi^\dagger \hat{a}_L^\gamma \hat{a}_R^\delta \xi - \xi \hat{a}_R^\gamma \hat{a}_L^\delta \xi^\dagger)\rangle, && (8.55)
\end{aligned}$$

with the above building blocks defined as

$$\begin{aligned}
\hat{a}_L^\mu &= \partial^\mu \xi^\dagger \xi - igV^\mu - ieA^\mu \xi^\dagger Q \xi,\\
\hat{a}_R^\mu &= \partial^\mu \xi \xi^\dagger - igV^\mu - ieA^\mu \xi Q \xi^\dagger,\\
F_V^{\mu\nu} &= g\partial^\mu V^\nu - ig^2 V^\mu V^\nu,\\
F_A^{\mu\nu} &= -e\partial^\mu A^\nu Q - ie^2 A^\mu A^\nu Q^2. && (8.56)
\end{aligned}$$

As mentioned in Ref. [72], Fujiwara's original form of $\mathcal{L}_4$ (which is labelled as $\mathcal{L}_6$ in Ref. [68]) is not invariant under charge conjugation transformations C and has to be replaced by its corrected version indicated in Eq. (8.55). However, all calculations concerning $3\pi+\gamma$ presented in [68] do not suffer from this slip since the C invariant $\mathcal{L}_4$ just happens to double the contribution of the non-invariant one.

It is very instructive to analyse what kind of relevant vertices can be generated by the entire odd intrinsic parity Lagrangian

$$\mathcal{L}^\varepsilon = \mathcal{L}_{WZW}^{3\phi+\gamma^*} + \sum_{i=1}^{4} b_i \mathcal{L}_i. \qquad (8.57)$$

In order to keep things transparent, let us summarize the essential facts in the below table. The indicated vertices are meant to represent the formulae

$$\begin{aligned}
(\gamma^*\phi\phi\phi) &= -\frac{ieN_c}{32\pi^2 F_0^3}A_\alpha \langle Q\partial_\beta\phi\partial_\gamma\phi\partial_\delta\phi\rangle \varepsilon^{\alpha\beta\gamma\delta},\\
(V\phi\phi\phi) &= \frac{igN_c}{32\pi^2 F_0^3}\langle V_\alpha\partial_\beta\phi\partial_\gamma\phi\partial_\delta\phi\rangle \varepsilon^{\alpha\beta\gamma\delta},\\
(\gamma^* V\phi) &= -\frac{geN_c}{16\pi^2 F_0}\partial_\alpha A_\beta \langle \{Q, V_\gamma\}\partial_\delta\phi\rangle \varepsilon^{\alpha\beta\gamma\delta},\\
(VV\phi) &= \frac{g^2 N_c}{16\pi^2 F_0}\langle \{\partial_\alpha V_\beta, V_\gamma\}\partial_\delta\phi\rangle \varepsilon^{\alpha\beta\gamma\delta}. && (8.58)
\end{aligned}$$

	$(\gamma^*\phi\phi\phi)$	$(\gamma^*V\phi)$	$(VV\phi)$	$(V\phi\phi\phi)$
$\mathcal{L}_{WZW}^{3\phi+\gamma^*}$	-4/3	—	—	—
$\mathcal{L}_1$	1	—	—	-1
$\mathcal{L}_2$	-1	—	—	1
$\mathcal{L}_3$	—	1	-1	1
$\mathcal{L}_4$	1	-1	—	—

Table 8.1: Relevant vertices and where they come from. The individual pieces are given by the products of the indicated numbers and the respective expressions in (8.58).

Combining odd and even intrinsic parity vertices, one ends up with four different diagrams belonging to the process $3\phi+\gamma^*$ (see Fig. 8.10).

At first sight it might be somewhat confusing to find direct $(\gamma^*\phi\phi\phi)$ pieces to originate from our newly introduced monomials. Since we know for sure from low-energy theorems that in the soft-momentum limit the amplitude of any reaction of the type $3\phi+\gamma^*$ is solely given by the anomaly, i.e., $\mathcal{L}_{WZW}^{3\phi+\gamma^*}$, the other contributions must somehow be wiped out. In fact, one can rather easily show that $\mathcal{L}_1$ induces a contribution of the diagrammatic species *b* (see Fig. 8.10), which exactly cancels its *a* counterpart at low energies. The same is true for $\mathcal{L}_2$. In the $\mathcal{L}_4$ case, it is a diagram of type *c* to do the very job. Everything we have just discussed holds for whatever choice of parameters b_i.

If these parameters remained undetermined, there would be no way at all to numerically estimate our LECs. We could only relate the latter to the former, which would be a rather useless substitution of one set of unknown quantities by another. Therefore (and for general reasons), the b_i must imperatively be fixed. In a first step Fujiwara *et al.* [68] tried to implement exact vector meson dominance by choosing an appropriate set of parameter values. Here, the notion 'exact vector meson dominance' refers to the complete disappearance of direct (1PI) *WZW* like terms, simultaneously for both the $\phi+2\gamma^*$ and the $3\phi+\gamma^*$ case. However, this choice of parameters predicts a rather incompatible amplitude for the precisely measured $\omega\to 3\pi$ decay. To patch up this shortcoming, they took a slightly different parameter set leading to

$$\mathcal{L}^{\varepsilon} \;=\; \mathcal{L}_{WZW}^{3\phi+\gamma^*} + (b_1\mathcal{L}_1 + b_2\mathcal{L}_2)_{b_1-b_2=1} + \mathcal{L}_3 + \mathcal{L}_4, \tag{8.59}$$

which makes the assumption of complete meson vector dominance for our $3\phi+\gamma^*$ reaction type untenable. In addition we want to point out that the first two parameters have not yet been determined separately. Fortunately, in our computations we only encounter the fixed linear combination b_1-b_2.

8.6.3 Estimation

We are finally ready to start the tree calculations. As indicated in Chapter 7, all information we are interested in can exclusively be extracted from the four 'processes':

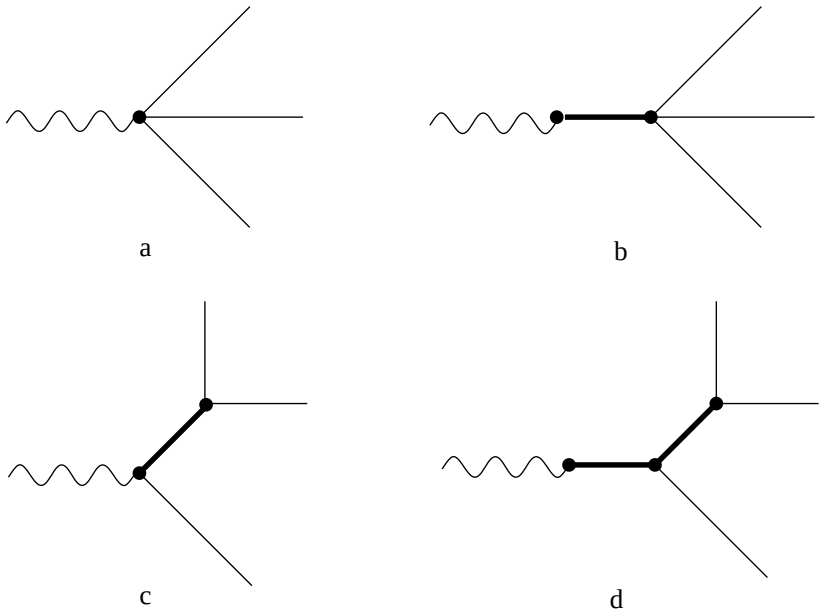

Figure 8.10: Resulting $3\phi+\gamma^*$ tree graphs. The first one, which is 1PI, does not contain vector meson degrees of freedom (bold internal lines). The remaining three, which are 1PR, obviously do. To be consistent with the foregoing chapters, let us assume all external momenta to flow into each diagram.

- $\gamma^* + \pi^+ + \pi^- + \pi^0/\eta_8 \to 0$,
- $\gamma^* + K^+ + K^- + \pi^0/\eta_8 \to 0$.

In departing from the Lagrangian densities (8.50) and (8.59), the only 1PR tree diagrams to be computed are of type *d*. Differently speaking, there are three distinct kinds of vertices which need to be known explicitly. After thoroughly evaluating all traces, we obtain

$$2eg_V A_\mu \langle Q V^\mu \rangle \;=\; eg_V A^\mu \left(\rho^0_\mu + \frac{\omega_\mu}{3} - \frac{\sqrt{2}\phi_\mu}{3} \right) \tag{8.60}$$

for the $(\gamma^* V)$ interaction,

$$\begin{aligned} -\frac{ig_{V\phi\phi}}{2}\langle V_\mu[\phi,\partial^\mu\phi]\rangle = -ig_{V\phi\phi} \;\Big\{\;& \rho^0_\mu(\pi^+\partial^\mu\pi^- - \pi^-\partial^\mu\pi^+) \\ -\;& \rho^-_\mu(\pi^+\partial^\mu\pi^0 - \pi^0\partial^\mu\pi^+) \\ +\;& \rho^+_\mu(\pi^-\partial^\mu\pi^0 - \pi^0\partial^\mu\pi^-) \\ +\;& \frac{1}{2}(\rho^0_\mu + \omega_\mu - \sqrt{2}\phi_\mu)(K^+\partial^\mu K^- - K^-\partial^\mu K^+) \\ -\;& \frac{1}{2}K^{*-}_\mu(K^+\partial^\mu\pi^0 - \pi^0\partial^\mu K^+) \end{aligned}$$

$$
\begin{aligned}
&+ \quad \frac{1}{2} K_\mu^{*+} (K^- \partial^\mu \pi^0 - \pi^0 \partial^\mu K^-) \\
&- \quad \frac{\sqrt{3}}{2} K_\mu^{*-} (K^+ \partial^\mu \eta_8 - \eta_8 \partial^\mu K^+) \\
&+ \quad \frac{\sqrt{3}}{2} K_\mu^{*+} (K^- \partial^\mu \eta_8 - \eta_8 \partial^\mu K^-) \Big\} \qquad (8.61)
\end{aligned}
$$

for the $(V\phi\phi)$ interaction, and

$$
\begin{aligned}
\langle \{\partial_\alpha V_\beta, V_\gamma\} \partial_\delta \phi \rangle \varepsilon^{\alpha\beta\gamma\delta} &= (\partial_\alpha \rho_\beta^0 \omega_\gamma + \partial_\alpha \omega_\beta \rho_\gamma^0) \partial_\delta \pi^0 \varepsilon^{\alpha\beta\gamma\delta} \\
&+ (\partial_\alpha \rho_\beta^- \omega_\gamma + \partial_\alpha \omega_\beta \rho_\gamma^-) \partial_\delta \pi^+ \varepsilon^{\alpha\beta\gamma\delta} \\
&+ (\partial_\alpha \rho_\beta^+ \omega_\gamma + \partial_\alpha \omega_\beta \rho_\gamma^+) \partial_\delta \pi^- \varepsilon^{\alpha\beta\gamma\delta} \\
&+ \frac{1}{2} \Big(\partial_\alpha (\rho_\beta^0 + \omega_\beta + \sqrt{2}\phi_\beta) K_\gamma^{*-} + \partial_\alpha K_\beta^{*-} (\rho_\gamma^0 + \omega_\gamma + \sqrt{2}\phi_\beta) \Big) \partial_\delta K^+ \varepsilon^{\alpha\beta\gamma\delta} \\
&+ \frac{1}{2} \Big(\partial_\alpha (\rho_\beta^0 + \omega_\beta + \sqrt{2}\phi_\beta) K_\gamma^{*+} + \partial_\alpha K_\beta^{*+} (\rho_\gamma^0 + \omega_\gamma + \sqrt{2}\phi_\beta) \Big) \partial_\delta K^- \varepsilon^{\alpha\beta\gamma\delta}
\end{aligned} \qquad (8.62)
$$

for the $(VV\phi)$ interaction, where we have neglected the global factor $\frac{g^2 N_c}{16\pi^2 F_0}$ for simplicity.

To warm up, let us consider the purely pionic 'process' $\gamma^* + \pi^+ + \pi^- + \pi^0 \to 0$. In this case the first internal line of diagram *d* in Fig. 8.10 always has to represent a ω meson while the second one must be a ρ with suitable charge (according to the three possible assignments of pions to the external lines).

In recalling the vector meson propagator to read

$$
i \, \frac{g_{\mu\nu} - p_\mu p_\nu / m_V^2}{m_V^2 - p^2} \, , \qquad (8.63)
$$

one simply has to perform a straightforward tree calculation to obtain the entire contribution of the *d* type diagram[8]

$$
-\frac{ie}{8\pi^2 F_0^3} \left\{ \frac{m_\rho^2}{m_\rho^2 - (p_1+p_2)^2} + \frac{m_\rho^2}{m_\rho^2 - (p_1+p_3)^2} + \frac{m_\rho^2}{m_\rho^2 - (p_2+p_3)^2} \right\} \mathcal{A}. \qquad (8.64)
$$

The latter expression is not of distinct chiral order. We need to expand (the remains of) the propagator, i.e.,

$$
\frac{m_V^2}{m_V^2 - p^2} = \frac{1}{1 - \frac{p^2}{m_V^2}} = 1 + \frac{p^2}{m_V^2} + \cdots \, ,
$$

[8] As the present formalism assumes $SU(3)$ invariance, there is just one universal vector meson mass m_V. Nonetheless, we formally indicate the involved vector mesons by their mass.

to be able to collect the arising $O(p^6)$ pieces

$$-\frac{ie}{4\pi^2 F_0^3}\frac{(p_1+p_2)^2+(p_1+p_3)^2+(p_2+p_3)^2}{2m_\rho^2}\mathcal{A}. \tag{8.65}$$

Let us emphasize once more that the $O(p^4)$ part of (8.64) is being cancelled. The only $O(p^4)$ contribution to survive stems from the WZW Lagrangian itself.

So far the photon has been supposed to be real. In order to extend our computation to the virtual case, the final result has to be slightly modified. Actually, one finds the additional term

$$-\frac{ie}{4\pi^2 F_0^3}\frac{3q^2}{2m_\omega^2}\mathcal{A} \tag{8.66}$$

in case the photon momentum squared is allowed to differ from zero.

Comparison of the conventional ChPT tree graphs at chiral order $O(p^6)$, Eq. (8.44),

$$\left\{256\left(2\hat{\mathbf{L}}_{\mathbf{5}}^{\mathbf{6},\varepsilon}+\hat{\mathbf{L}}_{\mathbf{6}}^{\mathbf{6},\varepsilon}+\hat{\mathbf{L}}_{\mathbf{14}}^{\mathbf{6},\varepsilon}\right)B_0 m-\frac{128}{3}\left(\hat{\mathbf{L}}_{\mathbf{13}}^{\mathbf{6},\varepsilon}+\hat{\mathbf{L}}_{\mathbf{14}}^{\mathbf{6},\varepsilon}\right)q^2\right\}\frac{ie}{F_0^3}\mathcal{A} \tag{8.67}$$

with the corresponding p^6 diagrams including internal vector mesons, Eq. (8.65) plus (8.66),

$$\left\{-\frac{3}{4\pi^2 m_\rho^2}B_0 m-\frac{1}{8\pi^2}\left(\frac{1}{m_\rho^2}+\frac{3}{m_\omega^2}\right)q^2\right\}\frac{ie}{F_0^3}\mathcal{A} \tag{8.68}$$

obviously furnishes two constraints on the concerned LECs without giving access to their individual values.

Next consider $\gamma^*+\pi^++\pi^-+\eta_8\to 0$. Here, just one single diagram of type d, namely the very one possessing the vertex $(\rho^0\rho^0\eta_8)$, is found. After implementing the definition $\Delta m := m_s - m$, the respective analysis of

$$\begin{aligned}\Big\{\quad & \frac{128}{\sqrt{3}}\left(4\hat{\mathbf{L}}_{\mathbf{5}}^{\mathbf{6},\varepsilon}+2\hat{\mathbf{L}}_{\mathbf{6}}^{\mathbf{6},\varepsilon}-\hat{\mathbf{L}}_{\mathbf{13}}^{\mathbf{6},\varepsilon}+4\hat{\mathbf{L}}_{\mathbf{14}}^{\mathbf{6},\varepsilon}\right)B_0 m-\frac{256}{3\sqrt{3}}\left(6\hat{\mathbf{L}}_{\mathbf{2}}^{\mathbf{6},\varepsilon}+6\hat{\mathbf{L}}_{\mathbf{7}}^{\mathbf{6},\varepsilon}+\hat{\mathbf{L}}_{\mathbf{13}}^{\mathbf{6},\varepsilon}\right)B_0\Delta m \\ +\quad & \frac{64}{\sqrt{3}}\left(\hat{\mathbf{L}}_{\mathbf{13}}^{\mathbf{6},\varepsilon}-2\hat{\mathbf{L}}_{\mathbf{14}}^{\mathbf{6},\varepsilon}\right)t-\frac{64}{\sqrt{3}}\hat{\mathbf{L}}_{\mathbf{13}}^{\mathbf{6},\varepsilon}q^2\Big\}\frac{ie}{F_0^3}\mathcal{A}\end{aligned} \tag{8.69}$$

and

$$\left\{-\frac{\sqrt{3}}{8\pi^2 m_\rho^2}t-\frac{\sqrt{3}}{8\pi^2 m_\rho^2}q^2\right\}\frac{ie}{F_0^3}\mathcal{A} \tag{8.70}$$

turns out to yield first veritable pieces of information (which are compatible with the constraints emerging from $\gamma^*+\pi^++\pi^-+\pi^0\to 0$)

$$\hat{\mathbf{L}}_{\mathbf{13}}^{\mathbf{6},\varepsilon}=\hat{\mathbf{L}}_{\mathbf{14}}^{\mathbf{6},\varepsilon} \;=\; \frac{3}{512\pi^2 m_V^2}\,, \tag{8.71}$$

$$2\hat{\mathbf{L}}_{\mathbf{5}}^{\mathbf{6},\varepsilon}+\hat{\mathbf{L}}_{\mathbf{6}}^{\mathbf{6},\varepsilon} = -\frac{9}{1024\pi^2 m_V^2}\,, \tag{8.72}$$

$$\hat{\mathbf{L}}_{\mathbf{2}}^{\mathbf{6},\varepsilon}+\hat{\mathbf{L}}_{\mathbf{7}}^{\mathbf{6},\varepsilon} = -\frac{1}{1024\pi^2 m_V^2}\,, \tag{8.73}$$

In the present context we may set $m_V = m_\rho = m_\omega$.

In complete analogy $\gamma^* + K^+ + K^- + \pi^0 \to 0$ can be addressed. Since this is the very process being under investigation in the present thesis, we do not wish to skip all intermediate steps. The expression

$$-\frac{ie}{4\pi^2 F_0^3}\left\{\frac{(p_1+p_2)^2}{4m_\rho^2}+\frac{3(p_1+p_2)^2}{4m_\omega^2}+\frac{(p_1+p_3)^2}{4m_{K^*}^2}+\frac{(p_2+p_3)^2}{4m_{K^*}^2}\right\}\mathcal{A} \tag{8.74}$$

corresponds to $q^2 = 0$, while a virtual photon gives rise to an extra term

$$-\frac{ie}{4\pi^2 F_0^3}\left\{\frac{1}{2m_\omega^2}+\frac{3}{2m_\rho^2}-\frac{1}{2m_\phi^2}\right\}q^2\,\mathcal{A}. \tag{8.75}$$

All in all, this amounts to

$$\begin{aligned}\Big\{ & -\frac{3}{8\pi^2 m_{K^*}^2}B_0 m-\frac{1}{8\pi^2 m_{K^*}^2}B_0\Delta m-\frac{1}{16\pi^2}\left(\frac{1}{m_\rho^2}+\frac{3}{m_\omega^2}-\frac{1}{m_{K^*}^2}\right)t \\ - & \frac{1}{8\pi^2}\left(\frac{3}{m_\rho^2}+\frac{1}{m_\omega^2}-\frac{1}{m_\phi^2}+\frac{1}{2m_{K^*}^2}\right)q^2\Big\}\frac{ie}{F_0^3}\mathcal{A},\end{aligned} \tag{8.76}$$

which has to be compared with

$$\begin{aligned}\Big\{ & 64\left(8\hat{\mathbf{L}}_{\mathbf{5}}^{\mathbf{6},\varepsilon}+4\hat{\mathbf{L}}_{\mathbf{6}}^{\mathbf{6},\varepsilon}-\hat{\mathbf{L}}_{\mathbf{13}}^{\mathbf{6},\varepsilon}+6\hat{\mathbf{L}}_{\mathbf{14}}^{\mathbf{6},\varepsilon}\right)B_0 m- \\ + & \frac{256}{3}\left(3\hat{\mathbf{L}}_{\mathbf{1}}^{\mathbf{6},\varepsilon}+\hat{\mathbf{L}}_{\mathbf{5}}^{\mathbf{6},\varepsilon}+2\hat{\mathbf{L}}_{\mathbf{6}}^{\mathbf{6},\varepsilon}+2\hat{\mathbf{L}}_{\mathbf{14}}^{\mathbf{6},\varepsilon}\right)B_0\Delta m \\ - & \frac{32}{3}\left(5\hat{\mathbf{L}}_{\mathbf{13}}^{\mathbf{6},\varepsilon}+2\hat{\mathbf{L}}_{\mathbf{14}}^{\mathbf{6},\varepsilon}\right)q^2+32\left(\hat{\mathbf{L}}_{\mathbf{13}}^{\mathbf{6},\varepsilon}-2\hat{\mathbf{L}}_{\mathbf{14}}^{\mathbf{6},\varepsilon}\right)t\Big\}\frac{ie}{F_0^3}\mathcal{A}\end{aligned} \tag{8.77}$$

being taken from the preceding section.

The outcome

$$\hat{\mathbf{L}}_{\mathbf{13}}^{\mathbf{6},\varepsilon} = \frac{1}{768\pi^2}\left(\frac{17}{4m_\rho^2}+\frac{3}{4m_\omega^2}-\frac{3}{2m_\phi^2}+\frac{1}{m_{K^*}^2}\right) \tag{8.78}$$

$$\hat{\mathbf{L}}_{\mathbf{14}}^{\mathbf{6},\varepsilon} = \frac{1}{768\pi^2}\left(\frac{23}{8m_\rho^2}+\frac{21}{8m_\omega^2}-\frac{3}{4m_\phi^2}-\frac{1}{4m_{K^*}^2}\right) \tag{8.79}$$

seems to contradict Eq. (8.71). Note that the higher vector meson masses may be written as m_V plus additional terms in Δm. The latter pieces are obviously not of the chiral order in question. Thus there is no contradiction at all up to our considered level.

Furthermore, we learn that

$$\hat{\mathbf{L}}_{\mathbf{1}}^{\mathbf{6},\varepsilon} - \hat{\mathbf{L}}_{\mathbf{5}}^{\mathbf{6},\varepsilon} = \frac{3}{2048\pi^2 m_V^2} \tag{8.80}$$

must hold.

Finally, let us state the results belonging to $\gamma^* + K^+ + K^- + \eta_8 \to 0$. The expression originating from the vector meson model reads

$$\begin{aligned} \Bigg\{ & -\frac{3\sqrt{3}}{8\pi^2 m_{K^*}^2} B_0 m - \frac{5}{8\sqrt{3}\pi^2 m_{K^*}^2} B_0 \Delta m - \frac{\sqrt{3}}{4\pi^2}\left(\frac{1}{4m_\rho^2} + \frac{1}{12m_\omega^2} - \frac{1}{3m_\phi^2} - \frac{1}{4m_{K^*}^2}\right) t \\ - & \frac{\sqrt{3}}{4\pi^2}\left(\frac{1}{m_\rho^2} + \frac{1}{3m_\omega^2} - \frac{5}{6m_\phi^2} + \frac{1}{4m_{K^*}^2}\right) q^2 \Bigg\} \frac{ie}{F_0^3}\mathcal{A}; \end{aligned} \tag{8.81}$$

the conventional ChPT Feynman rule

$$\begin{aligned} \Bigg\{ & \frac{64}{\sqrt{3}}\left(8\hat{\mathbf{L}}_{\mathbf{5}}^{\mathbf{6},\varepsilon} + 4\hat{\mathbf{L}}_{\mathbf{6}}^{\mathbf{6},\varepsilon} + \hat{\mathbf{L}}_{\mathbf{13}}^{\mathbf{6},\varepsilon} + 2\hat{\mathbf{L}}_{\mathbf{14}}^{\mathbf{6},\varepsilon}\right) B_0 m \\ + & \frac{128}{3\sqrt{3}}\left(18\hat{\mathbf{L}}_{\mathbf{1}}^{\mathbf{6},\varepsilon} - 12\hat{\mathbf{L}}_{\mathbf{2}}^{\mathbf{6},\varepsilon} + 14\hat{\mathbf{L}}_{\mathbf{5}}^{\mathbf{6},\varepsilon} + 8\hat{\mathbf{L}}_{\mathbf{6}}^{\mathbf{6},\varepsilon} - 12\hat{\mathbf{L}}_{\mathbf{7}}^{\mathbf{6},\varepsilon} + \hat{\mathbf{L}}_{\mathbf{13}}^{\mathbf{6},\varepsilon} + 2\hat{\mathbf{L}}_{\mathbf{14}}^{\mathbf{6},\varepsilon}\right) B_0 \Delta m \\ - & \frac{32}{\sqrt{3}}\left(\hat{\mathbf{L}}_{\mathbf{13}}^{\mathbf{6},\varepsilon} + 2\hat{\mathbf{L}}_{\mathbf{14}}^{\mathbf{6},\varepsilon}\right) q^2 - \frac{32}{\sqrt{3}}\left(\hat{\mathbf{L}}_{\mathbf{13}}^{\mathbf{6},\varepsilon} - 2\hat{\mathbf{L}}_{\mathbf{14}}^{\mathbf{6},\varepsilon}\right) t \Bigg\} \frac{ie}{F_0^3}\mathcal{A} \end{aligned} \tag{8.82}$$

is taken from the foregoing chapter. All in all, this yields

$$\hat{\mathbf{L}}_{\mathbf{1}}^{\mathbf{6},\varepsilon} = \frac{3}{2048\pi^2 m_V^2}\ ,\ \hat{\mathbf{L}}_{\mathbf{5}}^{\mathbf{6},\varepsilon} = 0\ ,\ \text{and}\ \hat{\mathbf{L}}_{\mathbf{6}}^{\mathbf{6},\varepsilon} = -\frac{9}{1024\pi^2 m_V^2}\ . \tag{8.83}$$

Before closing this chapter, let us summarize the results in the below table.

LECs	estimated value
$\hat{\mathbf{L}}_{\mathbf{1}}^{\mathbf{6},\varepsilon}$	$\frac{3}{2048\pi^2 m_V^2}$
$\hat{\mathbf{L}}_{\mathbf{2}}^{\mathbf{6},\varepsilon} + \hat{\mathbf{L}}_{\mathbf{7}}^{\mathbf{6},\varepsilon}$	$-\frac{1}{1024\pi^2 m_V^2}$
$\hat{\mathbf{L}}_{\mathbf{5}}^{\mathbf{6},\varepsilon}$	0
$\hat{\mathbf{L}}_{\mathbf{6}}^{\mathbf{6},\varepsilon}$	$-\frac{9}{1024\pi^2 m_V^2}$
$\hat{\mathbf{L}}_{\mathbf{13}}^{\mathbf{6},\varepsilon}$	$\frac{3}{512\pi^2 m_V^2}$
$\hat{\mathbf{L}}_{\mathbf{14}}^{\mathbf{6},\varepsilon}$	$\frac{3}{512\pi^2 m_V^2}$

Table 8.2: Estimation of LECs belonging to the class $3\phi + \gamma^*$ (compare with Table 7.1). Within the vector meson model discussed in the present chapter, five LECs can be estimated individually; for the remaining two we can only determine their sum.

Chapter 9

Experiments

9.1 Differential cross section of the reaction $K^{\pm} + e^{-} \to K^{\pm} + e^{-} + \pi^{0}$

In order to calculate the differential cross section of a physical process, one basically has to square the corresponding amplitude. Let us carry on considering the reaction $\gamma^*(q) + K^{\pm}(p_1) \to K^{\pm}(p_2) + \pi^0(p_3)$, where the photon is now meant to be virtual. Within the standard one-photon-exchange approximation this is equivalent to $K^{\pm}(p_1) + e^{-}(k_1) \to K^{\pm}(p_2) + e^{-}(k_2) + \pi^0(p_3)$ with $q = k_1 - k_2$. While in the two-to-two-particle case the kinematics is fully described by three independent Lorentz invariants, e.g., s, t, and q^2 (see Chapter 7), the two-to-three-particle situation requires five such variables. A common set is given by

$$\begin{aligned} &s = (p_2 + p_3)^2,\ t = (p_1 - p_2)^2,\ q^2 = (k_1 - k_2)^2, \\ &S = (k_1 + p_1)^2,\ s_1 = (k_2 + p_3)^2, \end{aligned} \tag{9.1}$$

which obviously extends the one belonging to the hadronic subreaction. Note that S equals the squared total energy in the c.m. frame.

As always in electro-hadronic reactions, the entire amplitude can be split into a leptonic and a hadronic part

$$\mathcal{M} = \underbrace{e\bar{u}(k_2)\gamma^{\alpha}u(k_1)}_{\text{leptonic part}} \quad q^{-2} \underbrace{\varepsilon_{\alpha\beta\gamma\delta}p_1^{\beta}p_2^{\gamma}p_3^{\delta}F}_{\text{hadronic part}}. \tag{9.2}$$

The former, which is described by QED alone, is a well-understood and therefore rather uninteresting object. Only the latter (more precisely, the complex function F) contains valuable information on the hadronic system in question and provides the possibility to compare our ChPT predictions with experimental data.

Let us turn to the squared amplitude $|\mathcal{M}|^2$. If the incident electrons are completely unpolarized and we further ignore the polarization of the final electron states, then the

squaring of the leptonic part will actually yield

$$\begin{aligned}\mathcal{L}^{\alpha\alpha'} &= \frac{e^2}{2}\sum_{s_1,s_2}\bar{u}(k_2)\gamma^{\alpha}u(k_1)\bar{u}(k_1)\gamma^{\alpha'}u(k_2)\\ &= \frac{e^2}{8m_e^2}\Big\langle\gamma^{\alpha}(\gamma_\mu k_1^\mu+m_e)\gamma^{\alpha'}(\gamma_\nu k_2^\nu+m_e)\Big\rangle\\ &= \frac{e^2}{2m_e^2}\Big(k_1^\alpha k_2^{\alpha'}+k_2^\alpha k_1^{\alpha'}+g^{\alpha\alpha'}(m_e^2-k_1\cdot k_2)\Big).\end{aligned}\tag{9.3}$$

For the hadronic part one needs to carry out

$$\mathcal{H}_{\alpha\alpha'}=\varepsilon_{\alpha\beta\gamma\delta}\varepsilon_{\alpha'\beta'\gamma'\delta'}p_1^\beta p_2^\gamma p_3^\delta p_1^{\beta'}p_2^{\gamma'}p_3^{\delta'}|F|^2.\tag{9.4}$$

The double-epsilon expression can be found in the appendix of [76]

$$\begin{aligned}&\varepsilon_{\alpha\beta\gamma\delta}\varepsilon_{\alpha'\beta'\gamma'\delta'}=\\ &-\ g_{\alpha\alpha'}\Big(g_{\beta\beta'}(g_{\gamma\gamma'}g_{\delta\delta'}-g_{\gamma\delta'}g_{\delta\gamma'})-g_{\beta\gamma'}(g_{\gamma\beta'}g_{\delta\delta'}-g_{\gamma\delta'}g_{\delta\beta'})+g_{\beta\delta'}(g_{\gamma\beta'}g_{\delta\gamma'}-g_{\gamma\gamma'}g_{\delta\beta'})\Big)\\ &+\ g_{\alpha\beta'}\Big(g_{\beta\alpha'}(g_{\gamma\gamma'}g_{\delta\delta'}-g_{\gamma\delta'}g_{\delta\gamma'})-g_{\beta\gamma'}(g_{\gamma\alpha'}g_{\delta\delta'}-g_{\gamma\delta'}g_{\delta\alpha'})+g_{\beta\delta'}(g_{\gamma\alpha'}g_{\delta\gamma'}-g_{\gamma\gamma'}g_{\delta\alpha'})\Big)\\ &-\ g_{\alpha\gamma'}\Big(g_{\beta\alpha'}(g_{\gamma\beta'}g_{\delta\delta'}-g_{\gamma\delta'}g_{\delta\beta'})-g_{\beta\beta'}(g_{\gamma\alpha'}g_{\delta\delta'}-g_{\gamma\delta'}g_{\delta\alpha'})+g_{\beta\delta'}(g_{\gamma\alpha'}g_{\delta\gamma'}-g_{\gamma\beta'}g_{\delta\alpha'})\Big)\\ &+\ g_{\alpha\delta'}\Big(g_{\beta\alpha'}(g_{\gamma\beta'}g_{\delta\gamma'}-g_{\delta\beta'}g_{\gamma\gamma'})-g_{\beta\beta'}(g_{\gamma\alpha'}g_{\delta\gamma'}-g_{\gamma\gamma'}g_{\delta\alpha'})+g_{\beta\gamma'}(g_{\gamma\alpha'}g_{\delta\gamma'}-g_{\gamma\beta'}g_{\delta\alpha'})\Big),\end{aligned}\tag{9.5}$$

and leads to

$$\begin{aligned}&\varepsilon_{\alpha\beta\gamma\delta}\varepsilon_{\alpha'\beta'\gamma'\delta'}p_1^\beta p_2^\gamma p_3^\delta p_1^{\beta'}p_2^{\gamma'}p_3^{\delta'}=\\ &\quad-\ g_{\alpha\alpha'}\Big(p_1^2\,p_2^2\,p_3^2+2\,p_1\cdot p_2\,p_1\cdot p_3\,p_2\cdot p_3\\ &\quad-\ p_1^2(p_2\cdot p_3)^2-p_2^2(p_1\cdot p_3)^2-p_3^2(p_1\cdot p_2)^2\Big)\\ &\quad-\ p_{1\alpha}p_{1\alpha'}\Big((p_2\cdot p_3)^2-p_2^2\,p_3^2\Big)\\ &\quad-\ p_{2\alpha}p_{2\alpha'}\Big((p_1\cdot p_3)^2-p_1^2\,p_3^2\Big)\\ &\quad-\ p_{3\alpha}p_{3\alpha'}\Big((p_1\cdot p_2)^2-p_1^2\,p_2^2\Big)\\ &\quad-\ (p_{1\alpha}p_{2\alpha'}+p_{2\alpha}p_{1\alpha'})(p_3^2\,p_1\cdot p_2-p_1\cdot p_3\,p_2\cdot p_3)\\ &\quad-\ (p_{1\alpha}p_{3\alpha'}+p_{3\alpha}p_{1\alpha'})(p_2^2\,p_1\cdot p_3-p_1\cdot p_2\,p_2\cdot p_3)\\ &\quad-\ (p_{2\alpha}p_{3\alpha'}+p_{3\alpha}p_{2\alpha'})(p_1^2\,p_2\cdot p_3-p_1\cdot p_2\,p_1\cdot p_3).\end{aligned}\tag{9.6}$$

Although $|F|^2$ is the very object we are interested in, let us, for the sake of completeness, mention the formula for the associated differential cross section. Observe

that the Lorentz invariant S is usually fixed. The standard expression [60] reads

$$\frac{d\sigma}{ds_1\, ds\, dq^2\, dt} = \frac{m_e^2\pi |\mathcal{M}|^2}{8(2\pi)^5\lambda(s,m_e^2,m_K^2)(-\Delta_4)^{1/2}} \tag{9.7}$$

with

$$\lambda(s,m_e^2,m_K^2) = \Big(s-(m_e+m_K)^2\Big)\Big(s-(m_e-m_K)^2\Big) \tag{9.8}$$

and the Gram determinant

$$\Delta_4 = \frac{1}{8}\begin{vmatrix} k_1\cdot k_1 & p_1\cdot k_1 & k_2\cdot k_1 & p_2\cdot k_1 \\ k_1\cdot p_1 & p_1\cdot p_1 & k_2\cdot p_1 & p_2\cdot p_1 \\ k_1\cdot k_2 & p_1\cdot k_2 & k_2\cdot k_2 & p_2\cdot k_2 \\ k_1\cdot p_2 & p_1\cdot p_2 & k_2\cdot p_2 & p_2\cdot p_2 \end{vmatrix}. \tag{9.9}$$

9.2 Numerical results

The previously treated process

$$K^\pm + e^- \to K^\pm + e^- + \pi^0 \tag{9.10}$$

has not yet been experimentally investigated. However, experiments of this kind (for both pions and kaons) are about to be taken up [77]. In order to determine the physical range of the Mandelstam variables corresponding to phase space regions which are sensitive to F, one would need to perform Monte-Carlo simulations which are beyond the scope of this thesis. Nevertheless, recall that all mathematical input regarding (9.10) has been provided in the foregoing and present chapter.

Our final formulae, presented in Chapter 8, enter other experiments as well. A different set-up makes use of a $K^\pm$ beam to be scattered off a nuclear Coulomb field via the Primakoff reaction

$$K^\pm + N(Z,A) \to K^\pm + N(Z,A) + \pi^0. \tag{9.11}$$

Pionic Primakoff experiments (though with limited accuracy of the data) were carried out by Antipov *et al.* [78]. Therefore, let us compute $|F^{3\pi}(s,t,q^2)|$ for the kinematical regions indicated in their article: $4\ m_\pi^2 \le s \le 10\ m_\pi^2, |t| \le 3.5\ m_\pi^2, Q^2 = -q^2 \le 2\times 10^3 \mathrm{MeV}^2$. Since

$$F^{3\pi}(s,t,q^2) = -\frac{ie}{4F_\pi^3\pi^2}\Big(1+O(p^2)\Big) \tag{9.12}$$

holds, it is natural to omit the global factor and investigate the remaining part in order to systematically study the effects of $O(p^6)$ corrections to the leading-order $O(p^4)$ contribution. Before presenting our results, we need to specify the involved masses and constants: $m_\pi = 135\,\mathrm{MeV}, m_K = 496\,\mathrm{MeV}, m_\rho = m_\omega = 770\,\mathrm{MeV}$, and $F_0 = 92.4\,\mathrm{MeV}$.

As can be seen in Fig. 9.1 the tree graphs of order $O(p^4)$ and $O(p^6)$ do not possess any dependence on the Mandelstam variables s,t, and u. Therefore, kinematical variations can only be seen in the loop part. It is very interesting to note that the latter and the $O(p^6)$ tree contributions are of comparable size. A change of t from $-0.7\ m_\pi^2$ to $-3.5\ m_\pi^2$ implies a very slight decrease of the average slope of the full line. Recall that the entire amplitude is completely symmetric in s,t, and u. All in all, one can conclude that the experimental value of $|F^{3\pi}| = 12.9 \pm 0.9 \pm 0.5$ GeV^{-3} [78] is significantly above the ChPT prediction. However, $O(p^6)$ corrections go in the right direction.[1]

Up until now the virtual photon has been almost real. Of course, it is also worth studying the Q^2 behaviour of the pionic process. As can clearly be seen in Fig. 9.2, the main Q^2 dependence stems from the $O(p^6)$ tree graphs. The loop contribution diminishes when decreasing s towards its threshold value $4\ m_\pi^2$.

Although there is no data available for the kaonic reaction, we still want to explore the behaviour of $|F^{KK\pi}|$ in comparable kinematical regions. The additionally needed mass parameters are chosen as $m_\eta = 547$ MeV (which occurs in the respective loops), $m_{K^*} = 892$ MeV, $m_\phi = 1019$ MeV. This time the $O(p^6)$ tree graphs exhibit an explicit dependence on t. Therefore, the dashed horizontal line in Fig. 9.3 is lowered by making the t values more and more negative. Actually, if we went on like this, we would end up below the $O(p^4)$ level ($= 1$). Remember that the loop graphs are totally symmetric in s and u. Taking the same $s - s_0$ range as in the pionic example, we find a very small positive slope of the full line. Furthermore, the loop contribution gets more important when changing t from -0.7 to $-3.5\ m_\pi^2$.

Finally, consider Fig. 9.4. Since t is fixed and the $O(p^6)$ tree graphs are independent of s or u, the dashed line is identical in both subfigures. The full line shows a very slight variation due to the decrease of s towards threshold. Actually, for kaons the two chosen s values represent almost the same scenarios.

[1] In disaccordance with the discussion shown in [63] the variable t must be negative in the physical region. By using positive t values, we can reproduce their results within an uncertainty of $< 1\%$. This is due to non-specified mass parameters in [63].

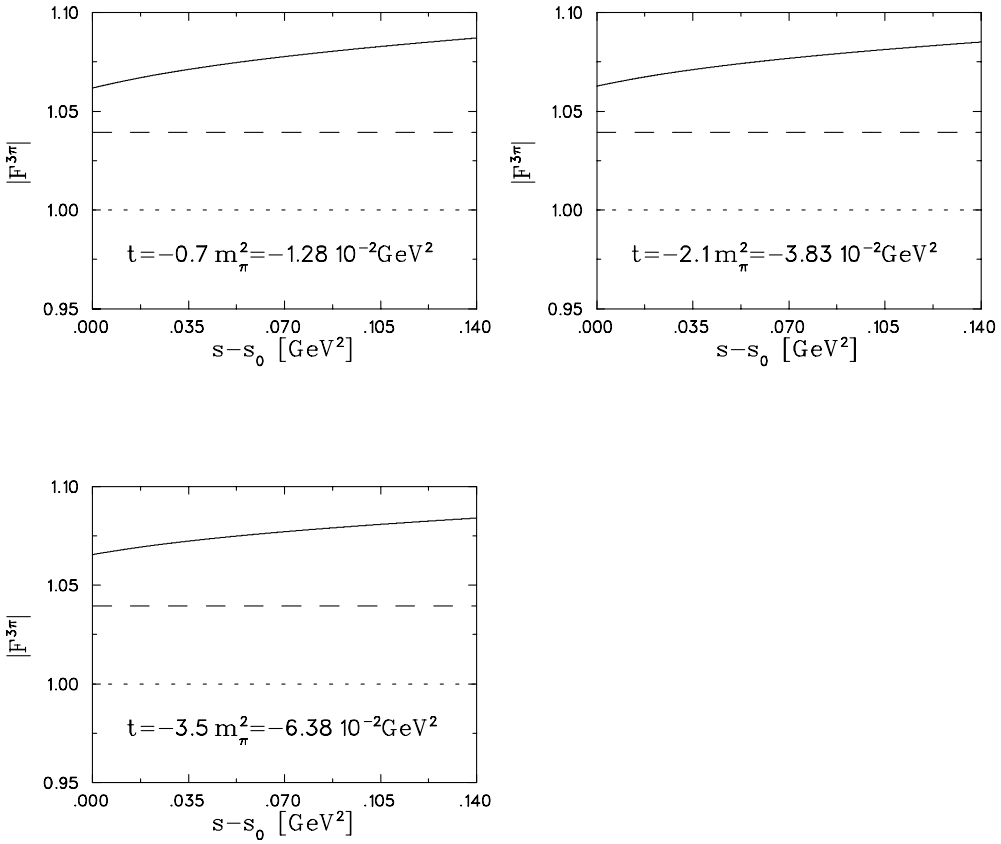

Figure 9.1: Numerical investigation of $|F^{3\pi}|$ (global factor 9.72 GeV^{-3} omitted) at fixed $Q^2 = -q^2 = 2 \times 10^3 \text{MeV}^2$ and three different t values. The full line includes all (tree and loop) contributions up to $O(p^6)$; the dashed line only comprises tree graphs up to $O(p^6)$; the dotted line just represents the leading-order $O(p^4)$ part.

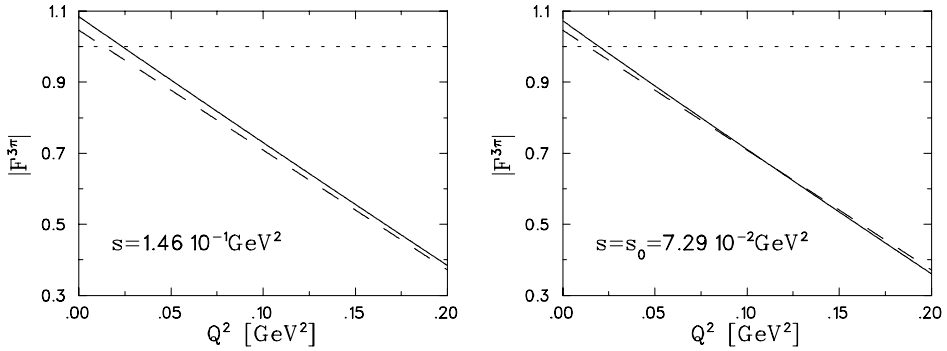

Figure 9.2: Q^2 dependence of $|F^{3\pi}|$ at fixed $t = -6.38 \times 10^{-2}\text{GeV}^2$. While in the first case s lies $7.29 \times 10^{-2}\text{GeV}^2$ above the threshold value $s_0 = 4\ m_\pi^2$, the second figure describes threshold production.

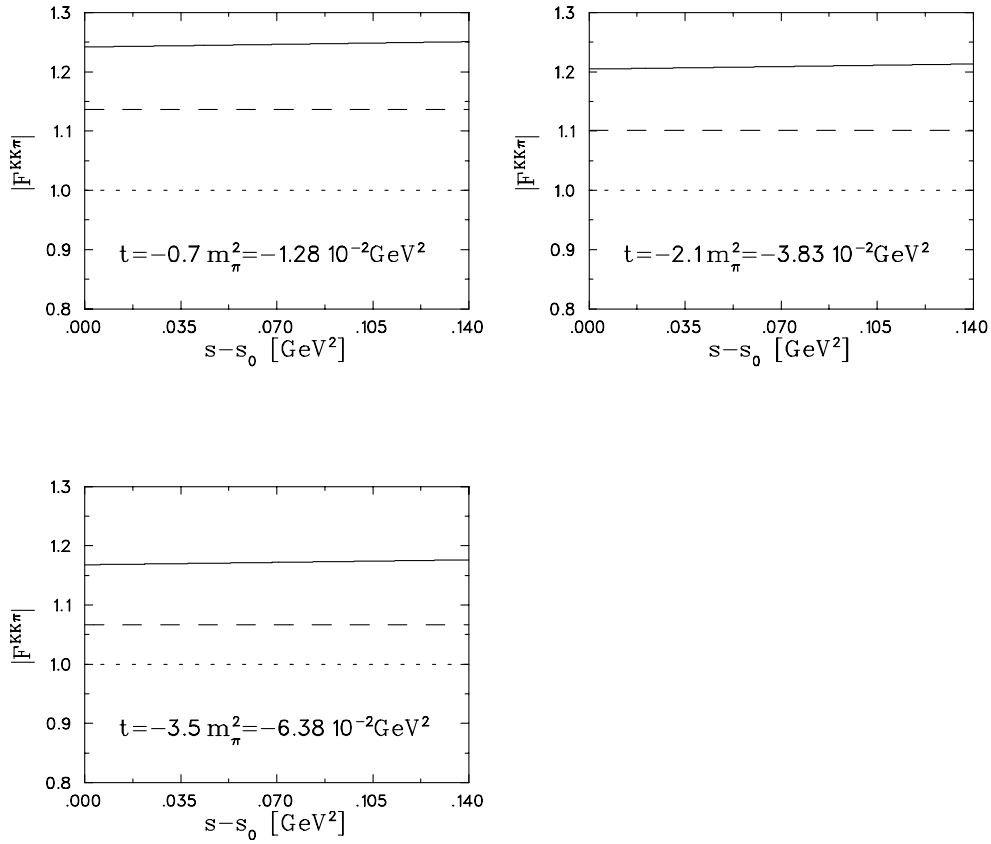

Figure 9.3: $|F^{KK\pi}|$ at fixed $Q^2 = -q^2 = 2 \times 10^3 \text{MeV}^2$ and three different t values.

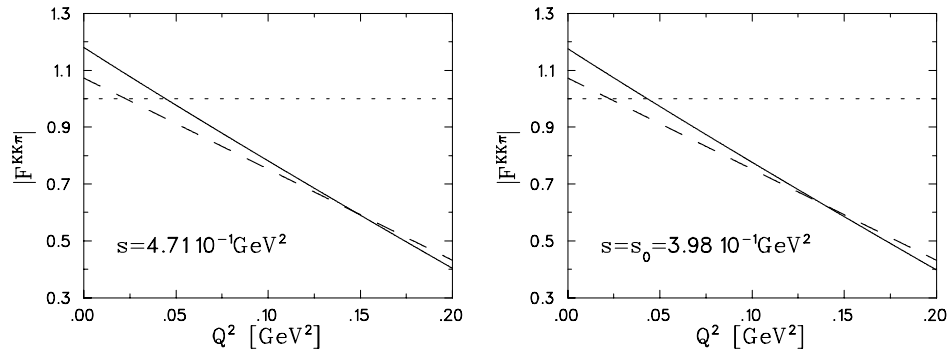

Figure 9.4: $|F^{KK\pi}|$ at fixed $t = -6.38 \times 10^{-2}\text{GeV}^2$; the s value is chosen to be $7.29 \times 10^{-2}\text{GeV}^2$ above and at threshold ($s_0 = (m_K + m_\pi)^2$).

Chapter 10

Summary and outlook

In the present Ph.D. thesis we have investigated two fairly different, though related, aspects of the odd intrinsic parity sector of mesonic ChPT up to next-to-leading order, $O(p^6)$.

The first part has been devoted to the one-loop renormalization of the leading-order term, the so-called Wess-Zumino-Witten action. As every renormalization project of a (non-renormalizable) effective field theory, this formalistic procedure has been carried out within three major steps:

1. Extraction of the respective one-loop contribution.

2. Compact isolation of arising one-loop singularities.

3. Absorption of the isolated infinite structures.

Before addressing those items, a monomial $SU(n)$ set constituting the most general anomalous chiral Lagrangian density at $O(p^6)$, $\mathcal{L}_{6,\varepsilon}$, has been systematically developed. Following the strategy of Fearing and Scherer [21], their final list could be modified and reduced by slightly changing the form (and therefore the transformation rules) of the basic building blocks. This way, the use of the so-called partial-integration argument becomes more transparent and efficient. In addition to that, the implementation of Bianchi identities and new trace relations have led to further reductions. All in all, we have derived 24 $SU(n)$, 23 $SU(3)$, and 5 $SU(2)$ elements.

It is worth noting the following points. First, within our approach (which was, e.g., also used in [15, 79]) there is little danger of incompleteness, i.e., we should not have missed any element. Nevertheless, one should ask whether additional structures might be built up from basic building blocks which are not individually invariant. Second, although we have very carefully pursued the strategy mentioned above, our final set may still include further redundancies. According to our knowledge, there is no general algorithm to decide if a set of monomials is linearly independent or not. Therefore, our resulting list might get modified in the future. New substantial ideas

and/or more refined mathematical procedures could help to further reduce the number of terms. Clearly, the smaller the number, the better for the determination of the respective LECs and for the practical applicability of ChPT in general.

In order to fully include e.m. processes into the $SU(2)$ framework, the chiral group has been enlarged to $SU(n)_L \times SU(n)_R \times U(1)_V$, which naturally implies the rise of additional monomials. We have presented a set of 8 elements which is valid for any flavour number n.

As far as we can see, the present study provides the most systematic and complete account on anomalous p^6 terms in mesonic ChPT. In particular, the numbers are considerably smaller than those given in [19, 20, 21].

Items 1. and 2. require sophisticated theoretical tools, namely specific topics of the path-integral formalism, such as the saddle-point evaluation, and the heat kernel technique, which have been introduced and discussed. We have spent a great deal of effort on collecting and illustrating the fundamental ideas and notions of either of these methods. In other words, the presented material is intended to supply a compact and helpful summary to be assisted by whatever modern textbook on quantum field theory.

After successfully checking 1. and 2., which had already been worked out by several groups [17, 18, 19, 20], point 3. has been addressed. The infinite parts of the LECs have been derived for all of our final sets (also for the extension). Note that the exact number of LECs to receive an infinite part depends on the chosen final set and is therefore of secondary interest.

As long as LECs remain undetermined, the associated Lagrangian density does not have any predictive power. For this reason, one needs a numerical estimation, which may stem from experimental data or from complementary theoretical models. In the present thesis, Feynman rules have been thoroughly worked out, covering a subset of 13 LECs, by considering pure QCD and e.m. processes. In other words, those couplings have at least formally been fixed. Fits to experimental data (if available) require, of course, the passage from Feynman rules to respective cross sections. A comparison with adequate theroretical models can already be achieved on the level of reaction amplitudes. While some of our LECs have been estimated via theoretical means (within a model including vector mesons as additional internal degrees of freedom), the adjustment with experimental data has to be done in the future. More space for further work consists in considering the remaining LECs as well as those belonging to the extension (analysis of $SU(2)$ processes). However, the entire set might not be completely determined within the next decade.

The second part, which might be more interesting for experimentalists, deals with some application. A consistent one-loop, i.e., $O(p^6)$, calculation has been carried out for the anomalous process $\gamma^*(q) + K^\pm(p_1) \to K^\pm(p_2) + \pi^0(p_3)$. Besides the leading-order tree term, which is of $O(p^4)$, loop and further tree graphs enter as $O(p^6)$ corrections. Loops emerge from two different sources:

- So-called regular loops.
- Loops due to wave function renormalization and corrections to the decay con-

stants.

By allowing internal vector meson degrees of freedom the involved $O(p^6)$ LECs have been estimated. Our entire method and its outcome has been cross-checked by recomputing the reaction $\gamma^*(q)+\pi^\pm(p_1)\to\pi^\pm(p_2)+\pi^0(p_3)$ and comparing with [63, 64].

The pionic process had already been investigated within a Primakoff experiment, $\pi^\pm+N(Z,A)\to\pi^\pm+N(Z,A)+\pi^0$ [78]. The associated ChPT structure function has been numerically evaluated and discussed for the kinematics proposed in [78]. In addition, we have studied its Q^2 dependence. The same has been done for kaons.

Both, the kaonic and the pionic reaction, are subject of experiments of the type $K^\pm+e^-\to K^\pm+e^-+\pi^0$ to be done in the near future. The entire theoretical framework which is necessary to compute the corresponding differential cross section has been presented. As soon as the kinematical areas of the experiments are known, one can start calculating numerical ChPT predictions. The results must then be implemented in an event generation to identify regions of phase space which are sensitive to $F^{KK\pi}$ or $F^{3\pi}$, respectively.

Appendix A

Initial structures

#	initial structures
1	$i\,\langle (D_\lambda D^\lambda U)_-(D_\mu U)_-(D_\nu U)_-(D_\alpha U)_-(D_\beta U)_-\rangle \varepsilon^{\mu\nu\alpha\beta}$
2	$i\,\langle (D_\lambda D_\mu U)_-\{(D^\lambda U)_-(D_\nu U)_-(D_\alpha U)_-(D_\beta U)_- + (D_\beta U)_-(D_\alpha U)_-(D_\nu U)_-(D^\lambda U)_-\}\rangle \varepsilon^{\mu\nu\alpha\beta}$
3	$i\,\langle (D_\lambda D_\mu U)_-\{(D_\nu U)_-(D^\lambda U)_-(D_\alpha U)_-(D_\beta U)_- + (D_\beta U)_-(D_\alpha U)_-(D^\lambda U)_-(D_\nu U)_-\}\rangle \varepsilon^{\mu\nu\alpha\beta}$
4	$i\,\langle (\chi)_-(D_\mu U)_-(D_\nu U)_-(D_\alpha U)_-(D_\beta U)_-\rangle \varepsilon^{\mu\nu\alpha\beta}$
5	$\langle (D^\lambda G_{\lambda\mu})_+(D_\nu U)_-(D_\alpha U)_-(D_\beta U)_-\rangle \varepsilon^{\mu\nu\alpha\beta}$
6	$\langle (D_\lambda G_{\mu\nu})_+\{(D^\lambda U)_-(D_\alpha U)_-(D_\beta U)_- - (D_\beta U)_-(D_\alpha U)_-(D^\lambda U)_-\}\rangle \varepsilon^{\mu\nu\alpha\beta}$
7	$\langle (D_\lambda G_{\mu\nu})_+(D_\alpha U)_-(D^\lambda U)_-(D_\beta U)_-\rangle \varepsilon^{\mu\nu\alpha\beta}$
8	$\langle (D_\mu G_{\lambda\nu})_+\{(D^\lambda U)_-(D_\alpha U)_-(D_\beta U)_- - (D_\beta U)_-(D_\alpha U)_-(D^\lambda U)_-\}\rangle \varepsilon^{\mu\nu\alpha\beta}$
9	$\langle (D_\mu G_{\lambda\nu})_+(D_\alpha U)_-(D^\lambda U)_-(D_\beta U)_-\rangle \varepsilon^{\mu\nu\alpha\beta}$
10	$\langle (D_\mu G_{\nu\alpha})_+\{(D_\lambda U)_-(D^\lambda U)_-(D_\beta U)_- - (D_\beta U)_-(D^\lambda U)_-(D_\lambda U)_-\}\rangle \varepsilon^{\mu\nu\alpha\beta}$
11	$\langle (G_{\mu\nu})_+\{(D_\lambda D^\lambda U)_-(D_\alpha U)_-(D_\beta U)_- - (D_\beta U)_-(D_\alpha U)_-(D_\lambda D^\lambda U)_-\}\rangle \varepsilon^{\mu\nu\alpha\beta}$
12	$\langle (G_{\lambda\mu})_+\{(D^\lambda D_\nu U)_-(D_\alpha U)_-(D_\beta U)_- - (D_\beta U)_-(D_\alpha U)_-(D^\lambda D_\nu U)_-\}\rangle \varepsilon^{\mu\nu\alpha\beta}$
13	$\langle (G_{\mu\nu})_+\{(D_\lambda D_\alpha U)_-(D^\lambda U)_-(D_\beta U)_- - (D_\beta U)_-(D^\lambda U)_-(D_\lambda D_\alpha U)_-\}\rangle \varepsilon^{\mu\nu\alpha\beta}$
14	$\langle (G_{\mu\nu})_+\{(D_\lambda D_\alpha U)_-(D_\beta U)_-(D^\lambda U)_- - (D^\lambda U)_-(D_\beta U)_-(D_\lambda D_\alpha U)_-\}\rangle \varepsilon^{\mu\nu\alpha\beta}$
15	$\langle (G_{\mu\nu})_+(D_\alpha U)_-(D_\lambda D^\lambda U)_-(D_\beta U)_-\rangle \varepsilon^{\mu\nu\alpha\beta}$
16	$\langle (G_{\lambda\mu})_+(D_\nu U)_-(D^\lambda D_\alpha U)_-(D_\beta U)_-\rangle \varepsilon^{\mu\nu\alpha\beta}$
17	$\langle (G_{\mu\nu})_+\{(D_\lambda U)_-(D^\lambda D_\alpha U)_-(D_\beta U)_- - (D_\beta U)_-(D^\lambda D_\alpha U)_-(D_\lambda U)_-\}\rangle \varepsilon^{\mu\nu\alpha\beta}$
18	$\langle (D_\lambda D_\mu H_{\nu\alpha})_+\{(D^\lambda U)_-(D_\beta U)_- + (D_\beta U)_-(D^\lambda U)_-\}\rangle \varepsilon^{\mu\nu\alpha\beta}$
19	$\langle (D_\lambda H_{\mu\nu})_+\{(D^\lambda D_\alpha U)_-(D_\beta U)_- + (D_\beta U)_-(D^\lambda D_\alpha U)_-\}\rangle \varepsilon^{\mu\nu\alpha\beta}$
20	$\langle (D_\mu H_{\lambda\nu})_+\{(D^\lambda D_\alpha U)_-(D_\beta U)_- + (D_\beta U)_-(D^\lambda D_\alpha U)_-\}\rangle \varepsilon^{\mu\nu\alpha\beta}$
21	$\langle (D_\mu H_{\nu\alpha})_+\{(D_\lambda D^\lambda U)_-(D_\beta U)_- + (D_\beta U)_-(D_\lambda D^\lambda U)_-\}\rangle \varepsilon^{\mu\nu\alpha\beta}$
22	$\langle (D_\mu H_{\nu\alpha})_+\{(D_\lambda D_\beta U)_-(D^\lambda U)_- + (D^\lambda U)_-(D_\lambda D_\beta U)_-\}\rangle \varepsilon^{\mu\nu\alpha\beta}$
23	$\langle (H_{\mu\nu})_+\{(D_\lambda D^\lambda D_\alpha U)_-(D_\beta U)_- + (D_\beta U)_-(D_\lambda D^\lambda D_\alpha U)_-\}\rangle \varepsilon^{\mu\nu\alpha\beta}$
24	$\langle (H_{\lambda\mu})_+\{(D^\lambda U)_-(D_\nu U)_-(D_\alpha U)_-(D_\beta U)_- + (D_\beta U)_-(D_\alpha U)_-(D_\nu U)_-(D^\lambda U)_-\}\rangle \varepsilon^{\mu\nu\alpha\beta}$
25	$\langle (H_{\lambda\mu})_+\{(D_\nu U)_-(D^\lambda U)_-(D_\alpha U)_-(D_\beta U)_- + (D_\beta U)_-(D_\alpha U)_-(D^\lambda U)_-(D_\nu U)_-\}\rangle \varepsilon^{\mu\nu\alpha\beta}$
26	$\langle (H_{\mu\nu})_+\{(D_\lambda U)_-(D^\lambda U)_-(D_\alpha U)_-(D_\beta U)_- + (D_\beta U)_-(D_\alpha U)_-(D^\lambda U)_-(D_\lambda U)_-\}\rangle \varepsilon^{\mu\nu\alpha\beta}$

#	continuation
27	$\langle (H_{\mu\nu})_+ \{ (D_\lambda U)_- (D_\alpha U)_- (D^\lambda U)_- (D_\beta U)_- + (D_\beta U)_- (D^\lambda U)_- (D_\alpha U)_- (D_\lambda U)_- \} \rangle \varepsilon^{\mu\nu\alpha\beta}$
28	$\langle (D_\lambda D_\mu H_{\nu\alpha})_+ \rangle \langle (D^\lambda U)_- (D_\beta U)_- \rangle \varepsilon^{\mu\nu\alpha\beta}$
29	$\langle (D_\lambda D^\lambda D_\mu U)_- \rangle \langle (H_{\nu\alpha})_+ (D_\beta U)_- \rangle \varepsilon^{\mu\nu\alpha\beta}$
30	$\langle (H_{\mu\nu})_+ (D_\alpha U)_- \rangle \langle (D_\beta U)_- (D_\lambda U)_- (D^\lambda U)_- \rangle \varepsilon^{\mu\nu\alpha\beta}$
31	$\langle (H_{\mu\nu})_+ \{ (D_\lambda U)_- (D_\alpha U)_- + (D_\alpha U)_- (D_\lambda U)_- \} \rangle \langle (D^\lambda U)_- (D_\beta U)_- \rangle \varepsilon^{\mu\nu\alpha\beta}$
32	$\langle (D_\mu \chi)_+ (D_\nu H_{\alpha\beta})_+ \rangle \varepsilon^{\mu\nu\alpha\beta}$
33	$\langle (D_\mu \chi)_+ \{ (G_{\nu\alpha})_+ (D_\beta U)_- - (D_\beta U)_- (G_{\nu\alpha})_+ \} \rangle \varepsilon^{\mu\nu\alpha\beta}$
34	$\langle (D_\mu \chi)_- \{ (H_{\nu\alpha})_+ (D_\beta U)_- + (D_\beta U)_- (H_{\nu\alpha})_+ \} \rangle \varepsilon^{\mu\nu\alpha\beta}$
35	$\langle (D_\mu G_{\nu\alpha})_+ \{ (\chi)_+ (D_\beta U)_- - (D_\beta U)_- (\chi)_+ \} \rangle \varepsilon^{\mu\nu\alpha\beta}$
36	$\langle (D_\mu H_{\nu\alpha})_+ \{ (\chi)_- (D_\beta U)_- + (D_\beta U)_- (\chi)_- \} \rangle \varepsilon^{\mu\nu\alpha\beta}$
37	$i \langle (D^\lambda G_{\lambda\mu})_+ \{ (G_{\nu\alpha})_+ (D_\beta U)_- + (D_\beta U)_- (G_{\nu\alpha})_+ \} \rangle \varepsilon^{\mu\nu\alpha\beta}$
38	$i \langle (D^\lambda G_{\mu\nu})_+ \{ (G_{\lambda\alpha})_+ (D_\beta U)_- + (D_\beta U)_- (G_{\lambda\alpha})_+ \} \rangle \varepsilon^{\mu\nu\alpha\beta}$
39	$i \langle (D_\lambda G_{\mu\nu})_+ \{ (G_{\alpha\beta})_+ (D^\lambda U)_- + (D^\lambda U)_- (G_{\alpha\beta})_+ \} \rangle \varepsilon^{\mu\nu\alpha\beta}$
40	$i \langle (D_\mu G_{\lambda\nu})_+ \{ (G^\lambda{}_\alpha)_+ (D_\beta U)_- + (D_\beta U)_- (G^\lambda{}_\alpha)_+ \} \rangle \varepsilon^{\mu\nu\alpha\beta}$
41	$i \langle (D_\mu G_{\lambda\nu})_+ \{ (G_{\alpha\beta})_+ (D^\lambda U)_- + (D^\lambda U)_- (G_{\alpha\beta})_+ \} \rangle \varepsilon^{\mu\nu\alpha\beta}$
42	$i \langle (D_\mu G_{\nu\alpha})_+ \{ (G_{\lambda\beta})_+ (D^\lambda U)_- + (D^\lambda U)_- (G_{\lambda\beta})_+ \} \rangle \varepsilon^{\mu\nu\alpha\beta}$
43	$i \langle (D^\lambda H_{\lambda\mu})_+ \{ (H_{\nu\alpha})_+ (D_\beta U)_- + (D_\beta U)_- (H_{\nu\alpha})_+ \} \rangle \varepsilon^{\mu\nu\alpha\beta}$
44	$i \langle (D^\lambda H_{\mu\nu})_+ \{ (H_{\lambda\alpha})_+ (D_\beta U)_- + (D_\beta U)_- (H_{\lambda\alpha})_+ \} \rangle \varepsilon^{\mu\nu\alpha\beta}$
45	$i \langle (D_\lambda H_{\mu\nu})_+ \{ (H_{\alpha\beta})_+ (D^\lambda U)_- + (D^\lambda U)_- (H_{\alpha\beta})_+ \} \rangle \varepsilon^{\mu\nu\alpha\beta}$
46	$i \langle (D_\mu H_{\lambda\nu})_+ \{ (H^\lambda{}_\alpha)_+ (D_\beta U)_- + (D_\beta U)_- (H^\lambda{}_\alpha)_+ \} \rangle \varepsilon^{\mu\nu\alpha\beta}$
47	$i \langle (D_\mu H_{\lambda\nu})_+ \{ (H_{\alpha\beta})_+ (D^\lambda U)_- + (D^\lambda U)_- (H_{\alpha\beta})_+ \} \rangle \varepsilon^{\mu\nu\alpha\beta}$
48	$i \langle (D_\mu H_{\nu\alpha})_+ \{ (H_{\lambda\beta})_+ (D^\lambda U)_- + (D^\lambda U)_- (H_{\lambda\beta})_+ \} \rangle \varepsilon^{\mu\nu\alpha\beta}$
49	$i \langle (D_\lambda D^\lambda U)_- (G_{\mu\nu})_+ (G_{\alpha\beta})_+ \rangle \varepsilon^{\mu\nu\alpha\beta}$
50	$i \langle (D^\lambda D_\mu U)_- \{ (G_{\lambda\nu})_+ (G_{\alpha\beta})_+ + (G_{\alpha\beta})_+ (G_{\lambda\nu})_+ \} \rangle \varepsilon^{\mu\nu\alpha\beta}$
51	$i \langle (D_\lambda D^\lambda U)_- (H_{\mu\nu})_+ (H_{\alpha\beta})_+ \rangle \varepsilon^{\mu\nu\alpha\beta}$
52	$i \langle (D^\lambda D_\mu U)_- \{ (H_{\lambda\nu})_+ (H_{\alpha\beta})_+ + (H_{\alpha\beta})_+ (H_{\lambda\nu})_+ \} \rangle \varepsilon^{\mu\nu\alpha\beta}$
53	$\langle (\chi)_- \{ (G_{\mu\nu})_+ (D_\alpha U)_- (D_\beta U)_- - (D_\beta U)_- (D_\alpha U)_- (G_{\mu\nu})_+ \} \rangle \varepsilon^{\mu\nu\alpha\beta}$
54	$\langle (\chi)_+ \{ (H_{\mu\nu})_+ (D_\alpha U)_- (D_\beta U)_- + (D_\beta U)_- (D_\alpha U)_- (H_{\mu\nu})_+ \} \rangle \varepsilon^{\mu\nu\alpha\beta}$
55	$i \langle (G_{\lambda\mu})_+ \{ (H^\lambda{}_\nu)_+ (D_\alpha U)_- (D_\beta U)_- - (D_\beta U)_- (D_\alpha U)_- (H^\lambda{}_\nu)_+ \} \rangle \varepsilon^{\mu\nu\alpha\beta}$
56	$i \langle (G_{\lambda\mu})_+ \{ (H_{\nu\alpha})_+ (D^\lambda U)_- (D_\beta U)_- - (D_\beta U)_- (D^\lambda U)_- (H_{\nu\alpha})_+ \} \rangle \varepsilon^{\mu\nu\alpha\beta}$
57	$i \langle (G_{\lambda\mu})_+ \{ (H_{\nu\alpha})_+ (D_\beta U)_- (D^\lambda U)_- - (D^\lambda U)_- (D_\beta U)_- (H_{\nu\alpha})_+ \} \rangle \varepsilon^{\mu\nu\alpha\beta}$
58	$i \langle (G_{\mu\nu})_+ \{ (H_{\lambda\alpha})_+ (D^\lambda U)_- (D_\beta U)_- - (D_\beta U)_- (D^\lambda U)_- (H_{\lambda\alpha})_+ \} \rangle \varepsilon^{\mu\nu\alpha\beta}$
59	$i \langle (G_{\mu\nu})_+ \{ (H_{\lambda\alpha})_+ (D_\beta U)_- (D^\lambda U)_- - (D^\lambda U)_- (D_\beta U)_- (H_{\lambda\alpha})_+ \} \rangle \varepsilon^{\mu\nu\alpha\beta}$
60	$i \langle (G_{\mu\nu})_+ \{ (H_{\alpha\beta})_+ (D_\lambda U)_- (D^\lambda U)_- - (D^\lambda U)_- (D_\lambda U)_- (H_{\alpha\beta})_+ \} \rangle \varepsilon^{\mu\nu\alpha\beta}$
61	$\langle (\chi)_- (D_\mu U)_- (G_{\nu\alpha})_+ (D_\beta U)_- \rangle \varepsilon^{\mu\nu\alpha\beta}$
62	$i \langle (G_{\lambda\mu})_+ \{ (D^\lambda U)_- (H_{\nu\alpha})_+ (D_\beta U)_- - (D_\beta U)_- (H_{\nu\alpha})_+ (D^\lambda U)_- \} \rangle \varepsilon^{\mu\nu\alpha\beta}$
63	$i \langle (G_{\lambda\mu})_+ (D_\nu U)_- (H^\lambda{}_\alpha)_+ (D_\beta U)_- \rangle \varepsilon^{\mu\nu\alpha\beta}$
64	$i \langle (G_{\mu\nu})_+ \{ (D^\lambda U)_- (H_{\lambda\alpha})_+ (D_\beta U)_- - (D_\beta U)_- (H_{\lambda\alpha})_+ (D^\lambda U)_- \} \rangle \varepsilon^{\mu\nu\alpha\beta}$

#	continuation
65	$\langle (D_\mu \chi)_- \rangle \langle (H_{\nu\alpha})_+ (D_\beta U)_- \rangle \varepsilon^{\mu\nu\alpha\beta}$
66	$\langle (\chi)_- \rangle \langle (D_\mu H_{\nu\alpha})_+ (D_\beta U)_- \rangle \varepsilon^{\mu\nu\alpha\beta}$
67	$\langle (\chi)_- \rangle \langle (G_{\mu\nu})_+ (D_\alpha U)_- (D_\beta U)_- \rangle \varepsilon^{\mu\nu\alpha\beta}$
68	$\langle (\chi)_+ (D_\mu U)_- \rangle \langle (H_{\nu\alpha})_+ (D_\beta U)_- \rangle \varepsilon^{\mu\nu\alpha\beta}$
69	$i \langle (\chi)_+ \{ (G_{\mu\nu})_+ (H_{\alpha\beta})_+ - (H_{\alpha\beta})_+ (G_{\mu\nu})_+ \} \rangle \varepsilon^{\mu\nu\alpha\beta}$
70	$i \langle (\chi)_- (G_{\mu\nu})_+ (G_{\alpha\beta})_+ \rangle \varepsilon^{\mu\nu\alpha\beta}$
71	$i \langle (\chi)_- (H_{\mu\nu})_+ (H_{\alpha\beta})_+ \rangle \varepsilon^{\mu\nu\alpha\beta}$
72	$\langle (G_{\mu\nu})_+ \{ (G_{\lambda\alpha})_+ (H^\lambda{}_\beta)_+ + (H^\lambda{}_\beta)_+ (G_{\lambda\alpha})_+ \} \rangle \varepsilon^{\mu\nu\alpha\beta}$
73	$i \langle (\chi)_- \rangle \langle (G_{\mu\nu})_+ (G_{\alpha\beta})_+ \rangle \varepsilon^{\mu\nu\alpha\beta}$
74	$i \langle (\chi)_- \rangle \langle (H_{\mu\nu})_+ (H_{\alpha\beta})_+ \rangle \varepsilon^{\mu\nu\alpha\beta}$

Table A.1: List of 74 anomalous $SU(n)$ structures of order $O(p^6)$ we start with. Besides the hierarchy argument discussed in the text (the four different categories are separated by triple lines), our ordering scheme is supposed to respect the rule: single traces $>$ multiple traces.

#	initial structures
$1'$	$\partial^\lambda v^{(s)}_{\lambda\mu}\langle (D_\nu U)_-(D_\alpha U)_-(D_\beta U)_-\rangle \varepsilon^{\mu\nu\alpha\beta}$
$2'$	$\partial_\lambda v^{(s)}_{\mu\nu}\langle (D^\lambda U)_-(D_\alpha U)_-(D_\beta U)_-\rangle \varepsilon^{\mu\nu\alpha\beta}$
$3'$	$\partial_\mu v^{(s)}_{\lambda\nu}\langle (D^\lambda U)_-(D_\alpha U)_-(D_\beta U)_-\rangle \varepsilon^{\mu\nu\alpha\beta}$
$4'$	$v^{(s)}_{\lambda\mu}\langle (D^\lambda D_\nu U)_-(D_\alpha U)_-(D_\beta U)_-\rangle \varepsilon^{\mu\nu\alpha\beta}$
$5'$	$v^{(s)}_{\mu\nu}\langle (D_\lambda D^\lambda U)_-(D_\alpha U)_-(D_\beta U)_-\rangle \varepsilon^{\mu\nu\alpha\beta}$
$6'$	$v^{(s)}_{\mu\nu}\langle (D_\lambda D_\alpha U)_-\{(D^\lambda U)_-(D_\beta U)_- - (D_\beta U)_-(D^\lambda U)_-\}\rangle \varepsilon^{\mu\nu\alpha\beta}$
$7'$	$i\,\partial^\lambda v^{(s)}_{\lambda\mu}\langle (G_{\nu\alpha})_+(D_\beta U)_-\rangle \varepsilon^{\mu\nu\alpha\beta}$
$8'$	$i\,\partial^\lambda v^{(s)}_{\mu\nu}\langle (G_{\lambda\alpha})_+(D_\beta U)_-\rangle \varepsilon^{\mu\nu\alpha\beta}$
$9'$	$i\,\partial_\lambda v^{(s)}_{\mu\nu}\langle (G_{\alpha\beta})_+(D^\lambda U)_-\rangle \varepsilon^{\mu\nu\alpha\beta}$
$10'$	$i\,\partial_\mu v^{(s)}_{\lambda\nu}\langle (G^\lambda{}_\alpha)_+(D_\beta U)_-\rangle \varepsilon^{\mu\nu\alpha\beta}$
$11'$	$i\,\partial_\mu v^{(s)}_{\lambda\nu}\langle (G_{\alpha\beta})_+(D^\lambda U)_-\rangle \varepsilon^{\mu\nu\alpha\beta}$
$12'$	$i\,\partial_\mu v^{(s)}_{\nu\alpha}\langle (G_{\lambda\beta})_+(D^\lambda U)_-\rangle \varepsilon^{\mu\nu\alpha\beta}$
$13'$	$i\,v^{(s)}_{\mu\nu}\langle (D^\lambda G_{\lambda\alpha})_+(D_\beta U)_-\rangle \varepsilon^{\mu\nu\alpha\beta}$
$14'$	$i\,v^{(s)}_{\lambda\mu}\langle (D^\lambda G_{\nu\alpha})_+(D_\beta U)_-\rangle \varepsilon^{\mu\nu\alpha\beta}$
$15'$	$i\,v^{(s)}_{\mu\nu}\langle (D_\lambda G_{\alpha\beta})_+(D^\lambda U)_-\rangle \varepsilon^{\mu\nu\alpha\beta}$
$16'$	$i\,v^{(s)}_{\lambda\mu}\langle (D_\nu G^\lambda{}_\alpha)_+(D_\beta U)_-\rangle \varepsilon^{\mu\nu\alpha\beta}$
$17'$	$i\,v^{(s)}_{\mu\nu}\langle (D_\alpha G_{\lambda\beta})_+(D^\lambda U)_-\rangle \varepsilon^{\mu\nu\alpha\beta}$
$18'$	$i\,v^{(s)}_{\lambda\mu}\langle (D_\nu G_{\alpha\beta})_+(D^\lambda U)_-\rangle \varepsilon^{\mu\nu\alpha\beta}$
$19'$	$i\,v^{(s)}_{\mu\nu}\langle (G_{\alpha\beta})_+(D_\lambda D^\lambda U)_-\rangle \varepsilon^{\mu\nu\alpha\beta}$
$20'$	$i\,v^{(s)}_{\lambda\mu}\langle (G_{\nu\alpha})_+(D^\lambda D_\beta U)_-\rangle \varepsilon^{\mu\nu\alpha\beta}$
$21'$	$i\,v^{(s)}_{\mu\nu}\langle (G_{\lambda\alpha})_+(D^\lambda D_\beta U)_-\rangle \varepsilon^{\mu\nu\alpha\beta}$
$22'$	$i\,v^{(s)}_{\lambda\mu}\langle (H^\lambda{}_\nu)_+(D_\alpha U)_-(D_\beta U)_-\rangle \varepsilon^{\mu\nu\alpha\beta}$
$23'$	$i\,v^{(s)}_{\lambda\mu}\langle (H_{\nu\alpha})_+\{(D^\lambda U)_-(D_\beta U)_- - (D_\beta U)_-(D^\lambda U)_-\}\rangle \varepsilon^{\mu\nu\alpha\beta}$
$24'$	$i\,v^{(s)}_{\mu\nu}\langle (H_{\lambda\alpha})_+\{(D^\lambda U)_-(D_\beta U)_- - (D_\beta U)_-(D^\lambda U)_-\}\rangle \varepsilon^{\mu\nu\alpha\beta}$
$25'$	$v^{(s)}_{\mu\nu}\langle (\chi)_-(D_\alpha U)_-(D_\beta U)_-\rangle \varepsilon^{\mu\nu\alpha\beta}$
$26'$	$i\,v^{(s)}_{\mu\nu}\langle (\chi)_-(G_{\alpha\beta})_+\rangle \varepsilon^{\mu\nu\alpha\beta}$
$27'$	$v^{(s)}_{\lambda\mu}\langle (G^\lambda{}_\nu)_+(H_{\alpha\beta})_+\rangle \varepsilon^{\mu\nu\alpha\beta}$
$28'$	$v^{(s)}_{\lambda\mu}\langle (G_{\nu\alpha})_+(H^\lambda{}_\beta)_+\rangle \varepsilon^{\mu\nu\alpha\beta}$
$29'$	$v^{(s)}_{\mu\nu}\langle (G_{\lambda\alpha})_+(H^\lambda{}_\beta)_+\rangle \varepsilon^{\mu\nu\alpha\beta}$
$30'$	$i\,v^{(s)}_{\mu\nu}v^{(s)}_{\alpha\beta}\langle (\chi)_-\rangle \varepsilon^{\mu\nu\alpha\beta}$

Table A.2: List of 30 additional anomalous p^6 structures due to the extension of the chiral group.

Appendix B

Eliminating relations

B.1 Relations induced by partial integration

$$
\begin{aligned}
(1) - (2) + (3) &= 0, \\
(5) + (12) + (16) &= 0, \\
(6) + (11) + (14) + (17) &= 0, \\
(7) + (13) + (15) &= 0, \\
(8) - (12) &= 0, \\
(9) + (16) &= 0, \\
(10) + (13) + (17) &= 0, \\
(18) + (21) + (22) + \frac{1}{16}(26) + \frac{1}{8}(27) &= 0, \\
(20) - \frac{1}{16}(24) - \frac{1}{16}(25) &= 0, \\
(22) + \frac{1}{16}(26) &= 0, \\
(19) + (23) - \frac{1}{16}(26) - \frac{1}{8}(27) &= 0, \\
(21) + (23) - \frac{1}{8}(26) &= 0, \\
(28) - \frac{1}{8}(31) &= 0, \\
(29) + \frac{1}{4}(30) &= 0, \\
(32) + \frac{1}{4}(36) + \frac{1}{16}(54) &= 0, \\
(32) - \frac{1}{4}(34) &= 0, \\
(37) + (38) - (50) &= 0,
\end{aligned}
$$

$$
\begin{aligned}
(39)+(49) &= 0,\\
(41)+(42)+(50) &= 0,\\
(43)+(44)-(52) &= 0,\\
(45)+(51) &= 0,\\
(47)+(48)+(52) &= 0,\\
(65)+(66)-\frac{1}{2}(68) &= 0;
\end{aligned}
\tag{B.1}
$$

$$
\begin{aligned}
(1')+3(4') &= 0,\\
(2')+(5')-(6') &= 0,\\
(7')+(14')+(20') &= 0,\\
(8')+(13')+(21') &= 0,\\
(9')+(15')+(19') &= 0,\\
(10')-(16') &= 0.
\end{aligned}
\tag{B.2}
$$

B.2 Relations induced by EOM

$$
\begin{aligned}
(1) &= (4),\\
(11) &= (53)-\frac{2}{N_f}(67),\\
(15) &= -(61)-\frac{1}{N_f}(67),\\
(21) &= (36)-\frac{2}{N_f}(66),\\
(49) &= (70)-\frac{1}{N_f}(73),\\
(51) &= (71)-\frac{1}{N_f}(74);
\end{aligned}
\tag{B.3}
$$

$$
\begin{aligned}
(5') &= (25'),\\
(19') &= (26').
\end{aligned}
\tag{B.4}
$$

B.3 Epsilon relations

$$
\begin{aligned}
(11)+2(12)-(13)+(14) &= 0,\\
(15)-2(16)-(17) &= 0,\\
(24)-(25) &= 0,
\end{aligned}
$$

$$
\begin{aligned}
2(24)+(26)-(27) &= 0,\\
(38)-2(40)+(42) &= 0,\\
(44)-2(46)+(48) &= 0,\\
(49)-2(50) &= 0,\\
(51)-2(52) &= 0,\\
2(55)+(56)-(57) &= 0,\\
2(55)-(58)+(59) &= 0,\\
2(56)+2(58)+(60) &= 0,\\
(62)-2(63) &= 0,\\
(62)+(64) &= 0,\\
(72) &= 0;
\end{aligned}
\tag{B.5}
$$

$$
\begin{aligned}
2(1')+3(2') &= 0,\\
(1')+3(3') &= 0,\\
2(7')+2(8')+(9') &= 0,\\
2(13')+2(14')+(15') &= 0,\\
(13')+2(16')+(17') &= 0,\\
(14')-2(16')-(18') &= 0,\\
2(22')+(23') &= 0,\\
2(22')-(24') &= 0,\\
(27')-(29') &= 0,\\
(28')+(29') &= 0.
\end{aligned}
\tag{B.6}
$$

B.4 Relations induced by Bianchi identities

$$
\begin{aligned}
(10)-\frac{1}{4}(26) &= 0,\\
(32)-\frac{1}{4}(33) &= 0,\\
(35)+\frac{1}{4}(54) &= 0,\\
(36)-\frac{1}{4}(53)+\frac{1}{2}(61) &= 0,\\
(42)+\frac{1}{4}(57)+\frac{1}{4}(62) &= 0,\\
(48)-\frac{1}{4}(58)-\frac{1}{4}(64) &= 0,
\end{aligned}
$$

$$(66) - \frac{1}{2}(67) = 0; \tag{B.7}$$

$$\begin{aligned} (8') - 2(10') &= 0, \\ (9') - 2(11') &= 0, \\ (12') &= 0, \\ (18') + \frac{1}{4}(23') &= 0. \end{aligned} \tag{B.8}$$

B.5 Trace relations

$SU(2)$:

$$\begin{aligned} (2) &= 0, \\ (4) &= 0, \\ (12) &= 0, \\ (13) &= 0, \\ (24) &= 0, \\ (26) &= 0, \\ (30) &= 0, \\ (31) &= 0, \\ (37) &= 0, \\ (43) &= 0, \\ (53) + 2(61) &= 0, \\ (53) - (67) &= 0, \\ (54) + 2(68) &= 0, \\ (58) &= 0, \\ (59) &= 0, \\ (60) &= 0, \\ (63) &= 0, \\ 2(70) - (73) &= 0, \\ 2(71) - (74) &= 0; \end{aligned} \tag{B.9}$$

$SU(3)$:

$$(26) + (27) + 2(30) + (31) = 0. \tag{B.10}$$

Appendix C

Functional calculus

For our purposes, functional analysis (and especially the functional derivative) can be seen as the ∞-dimensional generalization of finite-dimensional analysis. We first repeat some fundamental notions of the finite-dimensional case and state their infinite-dimensional counterparts afterwards. For a more rigorous introduction one may consult any textbook on the field.

- **finite-dimensional mapping**:

$$f \;:\; \mathbf{R^m} \to \mathbf{R^n},\; x \mapsto (f_1(x), \cdots, f_n(x))^T \quad \text{with } x = (x_1, \cdots, x_m)^T \tag{C.1}$$

- **(total) derivative**:

$$\lim_{\|h\|_m \to 0} \frac{\|f(x+h) - f(x) - L(x)h\|_n}{\|h\|_m} = 0 \tag{C.2}$$

with $L(x) = \left(\dfrac{\partial f_i(x)}{\partial x_j}\right)$ (Jacobian)

N.B.: if f linear mapping $\Rightarrow L(x) = L = f$

special case:

$$f : \mathbf{R^m} \to \mathbf{R} \;\Rightarrow\; L(x) = \left(\frac{\partial f(x)}{\partial x_j}\right) = \operatorname{grad} f(x) \tag{C.3}$$

  - **partial derivative**:

$$\frac{\partial f(x)}{\partial x_i} = \lim_{\varepsilon \to 0} \frac{f(x + \varepsilon e_i) - f(x)}{\varepsilon}, \qquad \text{N.B.: } \frac{\partial x_j}{\partial x_i} = \delta_{ij}$$

– **directional derivative**:

$$\langle L(x)|h\rangle = L(x)^T \cdot h = \sum_i \frac{\partial f(x)}{\partial x_i} h_i$$

– **extrema**:

$$\text{grad} f(x) = 0 \;\Leftrightarrow\; \frac{\partial f(x)}{\partial x_i} = 0 \;\forall i$$

- **∞-dimensional mapping**:

$$F \;:\; \mathbf{M} \to \mathbf{N},\; f \mapsto F[f] \qquad \text{(C.4)}$$
with $\mathbf{M}, \mathbf{N}$ ∞-dimensional Banach spaces

- **(total) derivative**:

$$\lim_{\|h\|_{\mathbf{M}} \to 0} \frac{\|F[f+h] - F[f] - \frac{\delta F}{\delta f}[h]\|_{\mathbf{N}}}{\|h\|_{\mathbf{M}}} = 0 \qquad \text{(C.5)}$$

special case:

$$F : \mathbf{M} \to \mathbf{R} \text{ (functional)} \;\Rightarrow\; \frac{\delta F}{\delta f} \text{ (distribution)} \qquad \text{(C.6)}$$

$$\text{N.B.: if } F \text{ distribution} \Rightarrow \frac{\delta F}{\delta f} = F$$

– **partial derivative**:

$$\frac{\delta F}{\delta f(x)} = \lim_{\varepsilon \to 0} \frac{F[f + \varepsilon\delta(\cdot - x)] - F[f]}{\varepsilon}, \qquad \text{N.B.: } \frac{\delta f(y)}{\delta f(x)} = \delta(x-y)$$

– **directional derivative**:

$$\frac{\delta F}{\delta f}[h] = \left\langle \frac{\delta F}{\delta f} \middle| h \right\rangle = \int dx \frac{\delta F}{\delta f(x)} h(x)$$

– **extrema**:

$$\delta F = 0 \;\Leftrightarrow\; \int dx \frac{\delta F}{\delta f(x)} h(x) = 0 \;\forall\; h(x)$$

Appendix D

Gell-Mann matrices

In QCD and related topics ($\rightarrow$ ChPT) one cannot help dealing with the Lie group $SU(3)$. Therefore, let us have a closer look at its generators $\frac{\lambda_i}{2}$, where $i \in \{1,\cdots,8\}$. The λ_i obey the following commutation and anti-commutation relations:

$$[\lambda_a,\lambda_b] = 2i f_{abc}\lambda_c, \qquad \{\lambda_a,\lambda_b\} = \frac{4}{3}\delta_{ab} + 2d_{abc}\lambda_c. \tag{D.1}$$

The combination of both yields a helpful identity:

$$\lambda_a\lambda_b = i f_{abc}\lambda_c + \frac{2}{3}\delta_{ab} + d_{abc}\lambda_c. \tag{D.2}$$

abc	123	147	156	246	257	345	367	458	678
f_{abc}	1	$\frac{1}{2}$	$-\frac{1}{2}$	$\frac{1}{2}$	$\frac{1}{2}$	$\frac{1}{2}$	$-\frac{1}{2}$	$\frac{1}{2}\sqrt{3}$	$\frac{1}{2}\sqrt{3}$
abc	118	146	157	228	247	256	338	344	
d_{abc}	$\sqrt{\frac{1}{3}}$	$\frac{1}{2}$	$\frac{1}{2}$	$\sqrt{\frac{1}{3}}$	$-\frac{1}{2}$	$\frac{1}{2}$	$\sqrt{\frac{1}{3}}$	$\frac{1}{2}$	
abc	355	366	377	448	558	668	778	888	
d_{abc}	$\frac{1}{2}$	$-\frac{1}{2}$	$-\frac{1}{2}$	$-\frac{1}{2\sqrt{3}}$	$-\frac{1}{2\sqrt{3}}$	$-\frac{1}{2\sqrt{3}}$	$-\frac{1}{2\sqrt{3}}$	$-\sqrt{\frac{1}{3}}$	

Table D.1: Non-vanishing f (totally anti-symmetric) and d coefficients (totally symmetric).

The following standard ('non-physical') representation is almost always found in physical literature:

$$\lambda_1 = \begin{pmatrix} 0 & 1 & 0 \\ 1 & 0 & 0 \\ 0 & 0 & 0 \end{pmatrix}, \quad \lambda_2 = \begin{pmatrix} 0 & -i & 0 \\ i & 0 & 0 \\ 0 & 0 & 0 \end{pmatrix}, \quad \lambda_3 = \begin{pmatrix} 1 & 0 & 0 \\ 0 & -1 & 0 \\ 0 & 0 & 0 \end{pmatrix},$$

$$
\begin{aligned}
\lambda_4 &= \begin{pmatrix} 0 & 0 & 1 \\ 0 & 0 & 0 \\ 1 & 0 & 0 \end{pmatrix}, \quad \lambda_5 = \begin{pmatrix} 0 & 0 & -i \\ 0 & 0 & 0 \\ i & 0 & 0 \end{pmatrix}, \quad \lambda_6 = \begin{pmatrix} 0 & 0 & 0 \\ 0 & 0 & 1 \\ 0 & 1 & 0 \end{pmatrix}, \\
\lambda_7 &= \begin{pmatrix} 0 & 0 & 0 \\ 0 & 0 & -i \\ 0 & i & 0 \end{pmatrix}, \quad \lambda_8 = \sqrt{\frac{1}{3}} \begin{pmatrix} 1 & 0 & 0 \\ 0 & 1 & 0 \\ 0 & 0 & -2 \end{pmatrix}.
\end{aligned} \tag{D.3}
$$

Nevertheless, for our needs it turns out to be more convenient to use so-called 'physical' Gell-Mann matrices, which are just linear combination of the former ones:

$$
\begin{aligned}
\lambda_I := \frac{1}{\sqrt{2}}(\lambda_1 + i\lambda_2), \qquad \lambda_{II} &:= \frac{1}{\sqrt{2}}(\lambda_1 - i\lambda_2), \\
\lambda_{III} &:= \lambda_3, \\
&\vdots
\end{aligned} \tag{D.4}
$$

They explicitly read

$$
\begin{aligned}
\lambda_I &= \begin{pmatrix} 0 & \sqrt{2} & 0 \\ 0 & 0 & 0 \\ 0 & 0 & 0 \end{pmatrix}, \quad \lambda_{II} = \begin{pmatrix} 0 & 0 & 0 \\ \sqrt{2} & 0 & 0 \\ 0 & 0 & 0 \end{pmatrix}, \quad \lambda_{III} = \begin{pmatrix} 1 & 0 & 0 \\ 0 & -1 & 0 \\ 0 & 0 & 0 \end{pmatrix}, \\
\lambda_{IV} &= \begin{pmatrix} 0 & 0 & \sqrt{2} \\ 0 & 0 & 0 \\ 0 & 0 & 0 \end{pmatrix}, \quad \lambda_V = \begin{pmatrix} 0 & 0 & 0 \\ 0 & 0 & 0 \\ \sqrt{2} & 0 & 0 \end{pmatrix}, \quad \lambda_{VI} = \begin{pmatrix} 0 & 0 & 0 \\ 0 & 0 & \sqrt{2} \\ 0 & 0 & 0 \end{pmatrix}, \\
\lambda_{VII} &= \begin{pmatrix} 0 & 0 & 0 \\ 0 & 0 & 0 \\ 0 & \sqrt{2} & 0 \end{pmatrix}, \quad \lambda_{VIII} = \sqrt{\frac{1}{3}} \begin{pmatrix} 1 & 0 & 0 \\ 0 & 1 & 0 \\ 0 & 0 & -2 \end{pmatrix}.
\end{aligned} \tag{D.5}
$$

Appendix E

Loop integrals

For our specific needs we have to distinguish between two general types of integrals according to their number of internal (loop) lines. Before roughly explaining how to evaluate these integrals, let us have a word on dimensional regularization. For more calculational details consult [80, 81, 10, 61].

E.1 Dimensional regularization

As the powerful technique of dimensional regularization has become quite popular over the last 30 years, a rather short description of its main ideas seems to be sufficient. In other words, this appendix is not meant to provide a mathematically detailed proof but a compact reference of the results to be presented.

The crucial point is to consider integrals in n (non-integer!) space-time dimenions which do coincide with ours for $n = 4$. After having carried out the relevant computations in n dimensions, the results are continued back to usual Minkowski space isolating the singular parts as poles in $\varepsilon = 4 - n$. This way one gets an explicit control over singularities, i.e., one can absorb them by judiciously choosing the renormalization constants.[1]

E.2 Integrals with one internal line

First of all, note that we always include the factor μ^{4-n} in order to render the integral's dimensionality independent of n. The parameter μ is an arbitrary auxiliary quantity which has the dimension of a mass. It appears in the intermediate parts of our calculations, but cannot ultimately influence relations between physical observables.

[1] As always in QCD the so-called modified minimal substraction scheme will be applied in which renormalization constants are chosen to subtract off not only the ε poles but also the omnipresent $(\ln(4\pi) + \Gamma'(1) + 1)/32\pi^2$ term.

The associated master integral can be shown to yield

$$\begin{aligned} I(m^2) &= \int \frac{d^n l}{(2\pi)^n} \frac{\mu^{4-n}\, i}{l^2 - m^2 + i\varepsilon} \\ &= \frac{m^2}{16\pi^2} \left[\underbrace{-\frac{2}{\varepsilon} + \gamma_E - 1 - \ln(4\pi)}_{R} + \ln\left(\frac{m^2}{\mu^2}\right) + O(\varepsilon) \right]. \end{aligned} \tag{E.1}$$

Although being standard, the above notation might be slightly confusing. The ε symbol in the last line is supposed to substitute $4-n$ and has nothing to do with the one in the first line indicating how to evaluate the integral. Furthermore, note that Euler's constant γ_E equals $-\Gamma'(1)$.

E.3 Integrals with two internal lines

Next, we want to examine integrals involving two internal lines. Since the two propagating particles do not need to have the same mass, we must consider a general ($m_1^2 \neq m_2^2$) and a special case ($m^2 = m_1^2 = m_2^2$). Let us start with the latter one whose solution is, of course, less complicated and therefore more instructive.

E.3.1 Special case

Essentially using the so-called Feynman trick

$$\frac{1}{ab} = \int_0^1 dz \frac{1}{[az + b(1-z)]^2}\,, \tag{E.2}$$

the master integral turns out to be

$$\begin{aligned} B_0(m^2, a^2) &= \int \frac{d^n l}{(2\pi)^n} \frac{\mu^{4-n}\, i}{[l^2 - m^2 + i\varepsilon]\,[(l+a)^2 - m^2 + i\varepsilon]} \\ &= \frac{1}{16\pi^2} \left[R + 1 + \ln\left(\frac{m^2}{\mu^2}\right) + J^{(0)}\left(\frac{a^2}{m^2}\right) \right], \end{aligned} \tag{E.3}$$

with the definition

$$J^{(k)}(x) := \int_0^1 dy y^k \ln\left[1 + x(y^2 - y) - i\varepsilon\right]. \tag{E.4}$$

For $k = 0$ the above function becomes

$$J^{(0)}(x) = \begin{cases} -2 - \sigma \ln\left(\frac{\sigma-1}{\sigma+1}\right) & (x < 0) \\ -2 + 2\sqrt{\frac{4}{x} - 1}\,\operatorname{arccot}\left(\sqrt{\frac{4}{x} - 1}\right) & (0 \leq x < 4)\,, \\ -2 - \sigma \ln\left(\frac{1-\sigma}{1+\sigma}\right) - i\pi\sigma & (x > 4) \end{cases}$$

(E.5)

$$\text{where} \qquad \sigma(x) \;=\; \sqrt{1-\frac{4}{x}}, \qquad x \notin [0,4].$$

At this stage, we need to point out that the tensor integrals

$$a^\mu B_1(m^2,q^2) \;=\; \int \frac{d^n l}{(2\pi)^n} \frac{\mu^{n-4}\; i l^\mu}{[l^2-m^2+i\varepsilon][(l+a)^2-m^2+i\varepsilon]} \tag{E.6}$$

and

$$\begin{aligned} &a^\mu a^\nu B_{21}(m^2,a^2) + a^2 g^{\mu\nu} B_{22}(m^2,a^2) \\ &\qquad = \int \frac{d^n l}{(2\pi)^n} \frac{\mu^{4-n}\; i l^\mu l^\nu}{[l^2-m^2+i\varepsilon]\,[(l+a)^2-m^2+i\varepsilon]} \end{aligned} \tag{E.7}$$

can be expressed in terms of (E.1) and (E.3). Observe that there is no other way to write the left-hand side of (E.6) and (E.7) due to Lorentz covariance and the available variables. First, let us consider the auxiliary integral $B_1(m^2,a^2)$ by contracting (E.6) with a_μ

$$a^2 B_1(m^2,a^2) = \int \frac{d^n l}{(2\pi)^n} \frac{\mu^{n-4}\; i a\cdot l}{[l^2-m^2+i\varepsilon][(l+a)^2-m^2+i\varepsilon]}\,. \tag{E.8}$$

Respecting the identity

$$a\cdot l = \frac{1}{2}[(l+a)^2-m^2-(l^2+a^2-m^2)], \tag{E.9}$$

one finds

$$\begin{aligned} a^2 B_1(m^2,a^2) \;&=\; \frac{i}{2}\int \frac{d^n l}{(2\pi)^n} \mu^{n-4} \frac{[(l+a)^2-m^2]-[l^2-m^2]-a^2}{[l^2-m^2+i\varepsilon][(l+a)^2-m^2+i\varepsilon]} \\ &=\; \frac{i}{2}\int \frac{d^n l}{(2\pi)^n} \mu^{n-4} \left\{ \frac{1}{l^2-m^2+i\varepsilon} - \frac{1}{(l+a)^2-m^2+i\varepsilon} \right. \\ &\quad \left. - \frac{a^2}{[l^2-m^2+i\varepsilon][(l+a)^2-m^2+i\varepsilon]} \right\} \\ &=\; -\frac{1}{2} a^2 B_0(m^2,a^2). \end{aligned} \tag{E.10}$$

Next, we determine the function $B_{22}(m^2,a^2)$ which is the only one to occur in our calculation. To this end, multiply (E.7) by $g_{\mu\nu}$ and use $g_{\mu\nu}g^{\mu\nu} = n$:

$$\begin{aligned} &a^2 B_{21}(m^2,a^2) + n a^2 B_{22}(m^2,a^2) \\ &\qquad = \int \frac{d^n l}{(2\pi)^n} \frac{\mu^{n-4}\; i l^2}{[l^2-m^2+i\varepsilon]\,[(l+a)^2-m^2+i\varepsilon]} \\ &\qquad = \int \frac{d^n l}{(2\pi)^n} \frac{\mu^{n-4}\; i(l^2-m^2+m^2)}{[l^2-m^2+i\varepsilon]\,[(l+a)^2-m^2+i\varepsilon]} \\ &\qquad = I(m^2) + m^2 B_0(m^2,a^2). \end{aligned} \tag{E.11}$$

On the other hand, contracting (E.7) with a_μ yields:

$$\begin{aligned}
& a^2 a^\nu \left(B_{21}(m^2,a^2) + B_{22}(m^2,a^2)\right) \\
&\quad = \int \frac{d^n l}{(2\pi)^n} \frac{\mu^{n-4}\, i a\cdot l\, l^\nu}{[l^2-m^2+i\varepsilon]\,[(l+a)^2-m^2+i\varepsilon]} \\
&\quad = \frac{\mu^{n-4}\, i}{2} \int \frac{d^n l}{(2\pi)^n} \frac{l^\nu}{l^2-m^2+i\varepsilon} \\
&\quad - \frac{\mu^{n-4}\, i}{2} \int \frac{d^n l}{(2\pi)^n} \frac{l^\nu}{(l+a)^2-m^2+i\varepsilon} \\
&\quad - \frac{\mu^{n-4}\, i a^2}{2} \int \frac{d^n l}{(2\pi)^n} \frac{l^\nu}{[l^2-m^2+i\varepsilon]\,[(l+a)^2-m^2+i\varepsilon]} \\
&\quad = \frac{a^\nu}{2} I(m^2) + \frac{a^2 a^\nu}{4} B_0(m^2,a^2). \qquad \text{(E.12)}
\end{aligned}$$

Taking advantage of (E.11) and (E.12), B_{22} reads:

$$B_{22}(m^2,a^2) = \frac{1}{(n-1)a^2}\left[\frac{1}{2} I(m^2) + \frac{4m^2-a^2}{4} B_0(m^2,a^2)\right]. \qquad \text{(E.13)}$$

Our basic integrals $I(m^2)$ and $B_0(m^2,a^2)$ both contain the quantity R which diverges for $n=4$. That is the reason why we have to work out the Taylor expansion for $(n-4) \ll 1$. With

$$\begin{aligned}
\frac{1}{n-1} &= \frac{1}{3} - \frac{n-4}{9} + O\Big((n-4)^2\Big), \\
(n-4) B_0(m^2,a^2) &= \frac{1}{8\pi^2} + O(n-4), \\
(n-4) I(m^2) &= \frac{m^2}{8\pi^2} + O(n-4), \qquad \text{(E.14)}
\end{aligned}$$

we finally obtain

$$a^2 B_{22}(m^2,a^2) = \frac{I(m^2)}{6} + \frac{\left(4m^2-a^2\right) B_0(m^2,a^2)}{12} - \frac{m^2}{48\pi^2} + \frac{a^2}{288\pi^2}. \qquad \text{(E.15)}$$

E.3.2 General case

For the general (and more complicated) case one clearly has to proceed analogously. Here, we simply quote those results which enter our calculations:

$$\begin{aligned}
\tilde{B}_0(m_1^2,m_2^2,a^2) &= \int \frac{d^n l}{(2\pi)^n} \frac{\mu^{4-n}\, i}{[l^2-m_1^2+i\varepsilon][(l+a)^2-m_2^2+i\varepsilon]} \\
&= \mu^{4-n}\, i \int_0^1 dz \int \frac{d^n l}{(2\pi)^n} (l^2 - A^2(z) + i\varepsilon)^{-2}
\end{aligned}$$

$$
\begin{aligned}
&= \frac{1}{(4\pi)^2}\left\{R+1+\int_0^1 dz \ln\left(\frac{A^2(z)-i\varepsilon}{\mu^2}\right)\right\} \\
\text{with}\quad A^2(z) &= sz^2+(m_2^2-m_1^2-s)z+m_1^2, \quad \text{where} \quad s:=a^2. \qquad \text{(E.16)}
\end{aligned}
$$

The remaining integral leads to the real part

$$
\begin{aligned}
&\int_0^1 dz \ln\left(\frac{|sz^2+(m_2^2-m_1^2-s)z+m_1^2|}{\mu^2}\right) \\
&= -2+\frac{1}{2}\left\{\ln\left(\frac{m_1^2}{\mu^2}\right)+\ln\left(\frac{m_2^2}{\mu^2}\right)\right\}+\frac{m_1^2-m_2^2}{2s}\ln\left(\frac{m_1^2}{m_2^2}\right)+F,
\end{aligned}
$$

with

$$
F = \begin{cases}
\frac{\Lambda}{s}\ln\left(\frac{|s-(m_1^2+m_2^2)+\Lambda|}{2m_1m_2}\right) & \text{for} \quad s\le(m_1-m_2)^2 \quad \text{or} \quad s\ge(m_1+m_2)^2 \\
-\frac{\Lambda}{s}\arctan\left(\frac{\Lambda}{s-(m_1^2+m_2^2)}\right) & \text{for} \quad (m_1-m_2)^2\le s\le m_1^2+m_2^2 \\
-\frac{\Lambda}{s}\left\{\arctan\left(\frac{\Lambda}{s-(m_1^2+m_2^2)}\right)-\pi\right\} & \text{for} \quad m_1^2+m_2^2\le s\le(m_1+m_2)^2
\end{cases}
$$

and

$$
\begin{aligned}
\Lambda &= \sqrt{|(s-(m_1^2+m_2^2))^2-4m_1^2m_2^2|} \\
&= \begin{cases}
\sqrt{4m_1^2m_2^2-(s-(m_1^2+m_2^2))^2} & \text{for} \quad (m_1-m_2)^2<s<(m_1+m_2)^2\,. \\
\sqrt{(s-(m_1^2+m_2^2))^2-4m_1^2m_2^2} & \text{otherwise}
\end{cases}
\end{aligned}
\qquad \text{(E.17)}
$$

The corresponding imaginary part reads

$$
-i\frac{\pi}{s}\Theta(s-(m_1+m_2)^2)\sqrt{(s-(m_1^2+m_2^2))^2-4m_1^2m_2^2}. \qquad \text{(E.18)}
$$

Again, we need to know the second constituent of the following sum

$$
\begin{aligned}
&a^\mu a^\nu \tilde{B}_{21}(m_1^2,m_2^2,a^2)+a^2g^{\mu\nu}\tilde{B}_{22}(m_1^2,m_2^2,a^2) \\
&\qquad = \int\frac{d^nl}{(2\pi)^n}\frac{\mu^{4-n}\,il^\mu l^\nu}{[l^2-m_1^2+i\varepsilon][(l+a)^2-m_2^2+i\varepsilon]}\,. \qquad \text{(E.19)}
\end{aligned}
$$

One finds

$$
\begin{aligned}
\tilde{B}_{22}(m_1^2,m_2^2,a^2) &= \frac{I(m_1^2)+I(m_2^2)}{12a^2}+\frac{(m_1^2-m_2^2)\left(I(m_1^2)-I(m_2^2)\right)}{12a^4} \\
&- \left(\frac{1}{12}-\frac{1}{6a^2}(m_1^2+m_2^2)+\frac{1}{12a^4}(m_1^2-m_2^2)^2\right)\tilde{B}_0(m_1^2,m_2^2,a^2) \\
&- \frac{m_1^2+m_2^2}{96\pi^2a^2}+\frac{1}{288\pi^2}\,. \qquad \text{(E.20)}
\end{aligned}
$$

One can easily check that $\tilde{B}_0(m_1^2,m_2^2,a^2)$ and $\tilde{B}_{22}(m_1^2,m_2^2,a^2)$ are both invariant under mass exchange ($m_1^2\leftrightarrow m_2^2$). When setting $m_1^2=m_2^2$ we rediscover our former results.

Bibliography

[1] J. F. Donoghue, E. Golowich, and B. R. Holstein, *Dynamics of the Standard Model* (University Press, Cambridge, 1992).

[2] M. Creutz, *Quarks, Gluons, and Lattices* (University Press, Cambridge, 1983).

[3] H. J. Rothe, *Lattice Gauge Theories: An Introduction* (World Scientific, Singapore, 1997).

[4] I. Zahed and G. E. Brown, Phys. Rev. **142**, 1 (1986).

[5] R. K. Bhaduri, *Models of the Nucleon: from Quarks to Solitons* (Addison-Wesley, New York, 1988).

[6] A. W. Thomas and W. Weise, *The Structure of the Nucleon* (WILEY-VCH Verlag, Berlin, 2001).

[7] G. 't Hooft, Nucl. Phys. **B72**, 461 (1974).

[8] E. Witten, Nucl. Phys. **B160**, 57 (1979).

[9] R. Kaiser and H. Leutwyler, Eur. Phys. J. C **17**, 623 (2000).

[10] S. Scherer, lecture notes: *Einführung in die chirale Störungstheorie*, 1999, http://www.kph.uni-mainz.de/T/lecture.html.

[11] J. Gasser, lecture notes: *QCD at low energies*, 1988, (unpublished).

[12] J. Gasser and H. Leutwyler, Ann. Phys. **158**, 142 (1984).

[13] J. Gasser and H. Leutwyler, Nucl. Phys. **B250**, 465 (1985).

[14] J. Bijnens, G. Colangelo, and G. Ecker, Phys. Lett. B **441**, 437 (1998).

[15] J. Bijnens, G. Colangelo, and G. Ecker, JHEP **9902**, 20 (1999).

[16] J. Bijnens, G. Colangelo, and G. Ecker, Ann. Phys. **280**, 100 (2000).

[17] J. F. Donoghue and D. Wyler, Nucl. Phys. **B316**, 289 (1989).

[18] J. Bijnens, A. Bramon, and F. Cornet, Z. Phys. **C46**, 599 (1990).

[19] D. Issler, SLAC-PUB-4943 (unpublished).

[20] R. Akhoury and A. Alfakih, Ann. Phys. **210**, 81 (1991).

[21] H. W. Fearing and S. Scherer, Phys. Rev. D **53**, 315 (1996).

[22] A. M. Bernstein, D. Drechsel, and T. Walcher, in *Chiral Dynamics: Theory and Experiment* (Springer, Berlin, 1998).

[23] H. Fritzsch, M. Gell-Mann, and H. Leutwyler, Phys. Lett. B **47**, 365 (1973).

[24] D. J. Gross and F. Wilczek, Phys. Rev. D **8**, 3633 (1973).

[25] S. Weinberg, Phys. Rev. Lett. **31**, 494 (1973).

[26] Y. Nambu, Phys. Rev. Lett. **4**, 380 (1960).

[27] J. Goldstone, Nuovo Cim. **19**, 154 (1961).

[28] J. Goldstone, A. Salam, and S. Weinberg, Phys. Rev. **127**, 965 (1962).

[29] S. Weinberg, Physica **96A**, 327 (1979).

[30] D. G. Sutherland, Phys. Lett. **23**, 384 (1966).

[31] D. G. Sutherland, Nucl. Phys. **B2**, 433 (1967).

[32] M. Veltman, Proc. R. Soc. London **301**, 107 (1967).

[33] S. L. Adler, Phys. Rev. **177**, 2476 (1969).

[34] W. A. Bardeen, Phys. Rev. **184**, 1848 (1969).

[35] J. S. Bell and R. Jackiw, Nuovo Cim. **60A**, 147 (1969).

[36] J. Wess and B. Zumino, Phys. Lett. B **37**, 95 (1971).

[37] E. Witten, Nucl. Phys. **B223**, 422 (1983).

[38] K. Chou, Phys. Lett. B **134**, 67 (1984).

[39] H. Kawai and S. Tye, Phys. Lett. B **140**, 403 (1984).

[40] J. L. Mañes, Nucl. Phys. **B250**, 369 (1985).

[41] A. P. Balachandran, G. Marmo, B. S. Skagerstam, and A. Stern, *Classical Topology and Quantum States* (World Scientific, Singapore, 1991).

[42] H. W. Fearing and S. Scherer, Phys. Rev. D **52**, 6445 (1995).

[43] R. Haag, Phys. Rev. **112**, 669 (1958).

[44] L. H. Ryder, *Quantum Field Theory, Second Edition* (University Press, Cambridge, 1996).

[45] S. Weinberg, *The Quantum Theory of Fields* (University Press, Cambridge, 1996), Vol. I and II.

[46] R. P. Feynman, Ph.D. thesis, Princeton Universtity, 1942.

[47] L. D. Faddeev and V. N. Popov, Phys. Lett. B **25**, 29 (1967).

[48] B. D. Witt, Phys. Rev. D **7**, 742 (1964).

[49] G. 't Hooft, Nucl. Phys. **B35**, 167 (1971).

[50] R. D. Ball, Phys. Rev. **182**, 3 (1989).

[51] S. Coleman and E. Weinberg, Phys. Rev. Lett. **12**, 1888 (1973).

[52] W. Greiner, *Feldquantisierung* (Harry Deutsch Verlag, Frankfurt am Main, 1993).

[53] T. Kugo, *Eichtheorie* (Springer, Berlin, 1997).

[54] P. Ramond, *Field Theory: A Modern Primer, Second Edition* (Addison-Wesley Publishing Company, New York, 1992).

[55] R. J. Rivers, *Path integral methods in quantum field theory* (University Press, Cambridge, 1987).

[56] J. Zinn-Justin, *Quantum Field Theory and Critical Phenomena, Second Edition* (Clarendon Press, Oxford, 1993).

[57] P. Ramond and S. W. Hawking, Commun. in Math. Phys. **55**, 149 (1977).

[58] J. Bijnens, Int. J. of Mod. Phys. A **8**, 3045 (1993).

[59] M. Knecht and A. Nyffeler, hep-ph/0106034.

[60] J. D. Bjorken and S. D. Drell, *Relativistische Quantenmechanik* (Bibliographisches Institut, Mannheim, 1966).

[61] T. Fuchs, diploma thesis, Johannes Gutenberg-Universität Mainz, 1999.

[62] J. J. Sakurai, *Invariance Principles and Elementary Particles* (University Press, Princeton, 1964).

[63] J. Bijnens, A. Bramon, and F. Cornet, Phys. Lett. B **237**, 488 (1990).

[64] A. Bramon, E. Pallante, and R. Petronzio, Phys. Lett. B **271**, 237 (1991).

[65] L. Ametller, hep-ph/0107127.

[66] T. Hannah, Nucl. Phys. **B593**, 577 (2001).

[67] G. Knöchlein, private communication.

[68] T. Fujiwara, Prog. Theor. Phys. **73**, 926 (1985).

[69] M. Bando, T. Kugo, and K. Yamawaki, Phys. Rep. **164**, 217 (1988).

[70] O. Kaymakcalan, S. Rajeev, and J. Schlechter, Phys. Rev. D **30**, 594 (1984).

[71] O. Kaymakcalan and J. Schlechter, Phys. Rev. D **31**, 1101 (1985).

[72] P. Jain, Phys. Rev. D **37**, 3252 (1988).

[73] U. G. Meißner, Phys. Rep **161**, 213 (1988).

[74] K. Kawarabayashi and M. Suzuki, Phys. Rev. Lett. **16**, 255 (1966).

[75] A. Riazuddin and A. Fayyazuddin, Phys. Rev. **147**, 1071 (1966).

[76] C. Itzykson and J. B. Zuber, *Quantum Field Theory* (McGraw-Hill, New York, 1985).

[77] M. A. Moinester and V. Steiner, hep-ex/9801011.

[78] Y. M. Antipov *et al.*, Phys. Rev. D **36**, 21 (1987).

[79] N. Fettes, U. G. Meißner, M. Mojžiš, and S. Steininger, Ann. Phys. **283**, 273 (2000).

[80] G. Leibbrandt, Rev. Mod. Phys. **47**, 849 (1975).

[81] M. Veltman, *Diagrammatica* (University Press, Cambridge, 1994).

Thomas Ebertshäuser

Chirale Störungstheorie für Mesonen – Sektor ungerader innerer Parität

In der vorliegenden Dissertation wurden zwei verschiedene Aspekte des Sektors ungerader innerer Parität der mesonischen chiralen Störungstheorie, welcher auch als anomal bezeichnet wird, untersucht.

Der erste, eher formale Komplex der Arbeit befaßte sich mit der Ein-Schleifen-Renormierung des führenden anomalen Terms (der chiralen Ordnung $O(p^4)$), der sog. Wess-Zumino-Witten-Wirkung. Wie jedes Renormierungsprojekt einer (nicht renormierbaren) effektiven Wirkung, ließ sich dieses Vorhaben in drei Teilschritte untergliedern. Zunächst mußte der gesamte Ein-Schleifen-Anteil der Theorie mittels der Sattelpunkt-Methode, die auf dem Pfadintegral-Formalis- mus fußt, extrahiert werden. Im Anschluß konnten alle singulären Ein-Schleifen-Strukturen im Rahmen der Heat-Kernel-Technik isoliert werden. Zu guter Letzt mußten diese divergenten Anteile der Ordnung $O(p^6)$ absorbiert werden. Zur Absorption benötigte man daher eine allgemeinste anomale Lagrange-Dichte der Ordnung $O(p^6)$, welche aufbauend auf der Arbeit von Fearing und Scherer systematisch entwickelt wurde. Erweitert man die chirale Gruppe $SU(n)_L \times SU(n)_R$ auf $SU(n)_L \times SU(n)_R \times U(1)_V$, so kommen zusätzliche Monome ins Spiel, welche ebenfalls bestimmt wurden. Die renormierten Koeffizienten dieser allgemeinsten Lagrange-Dichte, die Niederenergiekonstanten, waren zunächst als freie Parameter zu betrachten. Um die Theorie mit physikalischer Vorhersagekraft auszustatten, mußten diese Koeffizienten individuell fixiert werden. Unter Betrachtung eines komplementären Modells, das zusätzliche vektormesonische Freiheitsgrade vorsah, konnten die Amplituden geeigneter Prozesse bestimmt und durch strukturellen Vergleich mit den Ergebnissen der mesonischen chiralen Störungstheorie eine numerische Abschätzung einiger Niederenergiekonstanten vorgenommen werden.

Der angewandte Teil hatte eine konsistente Ein-Schleifen-Rechnung für den anomalen Prozeß $\gamma^* + K^\pm \to K^\pm + \pi^0$ zum Inhalt. Neben dem Baum-Graphen der Ordnung $O(p^4)$ mußten Schleifen- und Baum-Diagramme der Ordnung $O(p^6)$ einbezogen werden. Die entstandenen Divergenzen wurden erwartungsgemäß von den zuvor renormierten Niederenergiekonstanten weggehoben. Zur Kontrolle unserer Resultate wurde eine bereits vorhandene Rechnung zum Prozeß $\gamma^* + \pi^\pm \to \pi^\pm + \pi^0$ reproduziert. Unter Einbeziehung der abgeschätzten Werte der jeweiligen Niederenergiekonstanten konnten die zugehörigen hadronischen Strukturfunktionen numerisch bestimmt und diskutiert werden.